JESCEE
Journal of Emerging Supply Chain, Clean Energy, and Process Engineering

p-ISSN 2963-8577
e-ISSN 2964-3511

Vol 2. No 2. 2023

JESCEE | Vol. 2 | No. 2 | pp. 85-186 | JAKARTA 2023 | ISSN 2963-8577

Faculty of
Industrial Technology
Universitas Pertamina

Universitas Pertamina

Journal of

Emerging Supply Chain, Clean Energy, and Process Engineering

Vol 2, No 2, 2023

Journal of
Emerging Supply Chain, Clean Energy, and Process Engineering
Vol 2, No 2, 2023

Journal of

Emerging Supply Chain, Clean Energy, and Process Engineering

Vol 2, No 2, 2023

Reviewers

1. Dr. Eng. Imam Wahyudi Farid, S.T., M.T. (Institut Teknologi Sepuluh Nopember, Indonesia)
2. Dr. Eng. R.B. Seno Wulung, S.T., M.T. (Politeknik ATK Kementerian Perindustrian, Indonesia)
3. Dr. Eng. Muhammad Abdillah, S.T., M.T. (Universitas Pertamina, Indonesia)
4. Eduardus Budi Nursanto, S.T., M.Eng., Ph.D (Universitas Pertamina, Indonesia)
5. Dr. Eng. Iwan Sukarno, ST., M.Eng., CLIP (Universitas Pertamina, Indonesia)
6. Agung Nugroho, S.T., Ph.D (Universitas Pertamina, Indonesia)

Imprint

JESCEE is published by Faculty of Industrial Technology, Universitas Pertamina, Jakarta Selatan, Indonesia.

Postal Address

JESCEE Secretariat:

Universitas Pertamina

Jl. Teuku Nyak Arief, Simprug, Kebayoran Lama, Jakarta Selatan, 12220

Indonesias

Business hour: Monday to Friday

07:00 to 17:00 GMT+7

e-mail: jescee@universitaspertamina.ac.id

Journal of

Emerging Supply Chain, Clean Energy, and Process Engineering

Vol 2, No 2, 2023

PREFACE

The Journal of Emerging Supply Chain, Clean Energy and Process Engineering (JESCEE) is a journal of the Faculty of Industrial Technology, Universitas Pertamina that promotes communication between researchers, dissemination of research results, development of academic culture, and development of new ideas in the fields of mechanical, electrical, chemical, and logistics. This journal's volume 2, issue no. 2 has captivated the attention of numerous researchers interested in publishing their work.

On behalf of the Editor-in-Chief, I would like to thank the people who support this journal, especially the Dean of the Faculty of Industrial Technology Industrial for their direct and indirect assistance, the editors who work well and are dedicated, the reviewers who provide suggestions and constructive criticism for each paper collected, and the authors who entrust JESCEE with the publication of their research results.

We hope that this publication will continue to expand and present the most recent information in the fields of mechanical, electrical, chemical, and logistical. We also welcome collaboration from parties who are pleased with the existence of this journal and wish for its further growth.

Jakarta, October 2023
Editor-in-Chief

Dr. Eng. Muhammad Abdillah

Journal of

Emerging Supply Chain, Clean Energy, and Process Engineering

Vol 2, No 2, 2023

List of Contents

Vol. 2, No. 2, October 2023, pp. 85-97
p-ISSN: 2963-8577
e-ISSN: 2964-3511
DOI: 10.57102/jescee.v2i2.65

JESCEE
Journal of Emerging Supply Chain, Clean Energy, and Process Engineering

INVENTORY MANAGEMENT WITH DEMAND FORECAST FOR EYEGLASS LENSES USING THE TIME SERIES METHOD AT AN OPTICAL STORE

Thobias Adriel Silaen[1], Yelita Anggiane Iskandar[1*]
[1]Department of Logistics Engineering, Faculty of Industrial Engineering, Universitas Pertamina

Abstract
In the healthcare sector, supply chain management is one of the most important elements since in the logistics of medical devices and pharmaceutical products, patient satisfaction is the main focus in efforts to improve service quality. One of the problems that often occurs in the optical supply chain is inventory control. The optical store is one of the microenterprises engaged in optometric health services. The enclosed supply chain is a three-echelon model, where the store is at the second level. The process of ordering lenses at the store from suppliers is not carried out based on predicted demand. The determination of the safety stock amount and the reorder point also still has a fairly low accuracy there. This is indicated by overstock and stock-out situations that still occur frequently in this company. Overstock causes the product to be damaged because it has been stored for too long and stock out causes lost sales. To solve the problem in this research, the prediction of future demand is overcome by using several time series methods, such as cyclical models, cyclical trend models, and ARIMA models. Forecasting result validation is implemented by calculating the calculation of errors using MAPE, MAD, and MSE then it was found that the forecasting model chosen to predict the demand for the lenses is a cyclical trend model. The result of the demand forecasting and safety stock size calculation with 3 service levels are used as input to determine the reorder point. After observing the condition of the company and the targets set by the company, the calculation results with a service level of 90% is the most possible to be implemented.

Keywords:
Healthcare; inventory control; demand forecasting; safety stock; reorder point

Article History:
Received: July 24th, 2023
Revised: October 12th, 2023
Accepted: October 22th, 2023
Published: October 31st, 2023

Corresponding Author:
Yelita Anggiane Iskandar
Department of Logistics Engineering, Universitas Pertamina, Indonesia
Email:
yelita.ai@universitaspertamina.ac.id

1. Introduction

In the health sector, supply chain management is an important element because, in the logistics of pharmaceutical products, patient satisfaction is the main focus in efforts to improve service quality [1]. Improving the quality of healthcare services depends directly on the efficiency of its supply chain management [1]. Health care supply chain covering the supply and demand management of drugs and medical products. Medicines, or healthcare equipment like syringes are some of the most discussed research objects related to their requirements or demand forecasting in the future while those focusing on optical products were hardly found. One of the health services under the optical supply chain is an optometry service company or an optical company/shop/store. Like any other business, optical stores need innovative and operational models to stay competitive in the market. The optical supply chain has its own special models and challenges to meet the needs of patients who have different requirements for their eye health. One of the problems that often occur in the optical supply chain is related to inventory control [2]. Inventory is a factor that is important because it greatly influences the continuity of sales activities [2]. Some important activities in inventory control are demand forecasting, determining the amount of safety stock and reorder points, and several other issues in order to improve the quality of service to customers. Even though [2] discussed inventory management, they did not consider the calculation lies under the information system that they designed while we know that applications without strong formulation in the backend will provide a bare impact on the operational processes in the optical stores.

Inventory is a number of materials in process available in the company for the production process, as well as goods provided to meet demand from customers at any time [3]. Inventory planning has the challenge of serving production needs by minimizing existing inventory stocks to make the costs more efficient which are usually a burden to the company. In the early stages of inventory planning, demand forecasting is required. Forecasting sales of eyeglass lens products is needed to find out the amount of safety stock needed and also the reorder point [4]. Demand forecasting is an important activity in the industrial sector that aims to estimate the amount of product or service to be produced to meet end demand [4]. This is because demand forecasting can affect other work processes, such as purchasing raw materials and production planning [4]. So, we need a forecasting technique that has a high level of accuracy. Forecasting accuracy can be assessed as high if the error calculation is carried out with several selected methods which shows that the error obtained is very small [5]. Forecasting results with the lowest error become input in the calculation of safety stock and reorder point. Safety stock is the minimum amount of inventory that must be owned in each period by a company to overcome the risk of delays in the arrival of materials and possible fluctuations in demand. The calculation of safety stock is based on the service level (probability of fulfilling needs) that has been determined by the company [6]. Service level is a value set by a company that aims to meet customer needs [7]. The reorder point is the inventory level that has been set as the time to reorder to balance the inventory [8]. Reorder point is determined by three factors, namely lead time, safety stock, and average demand (obtained from demand forecasting results [6].

The observed optical store or we can say Store X is one of the micro businesses engaged in optometric health services. This company sells various health eyewear products (lenses and frames) as well as visual inspection services (examination of patient vision) and tinting color services (lens tinting). Single-vision lenses are lenses that have one focus point and function to correct one type of visual impairment, namely nearsightedness or farsightedness [9]. A bifocal lens is a lens that has two focus points and functions to correct two types of visual impairment in one lens, namely nearsightedness (myopia) and old eyes (presbyopia) [10]. The difference between the two lenses is in the number of focus points. Bifocal lenses have two focal points, namely the spherical (SPH) and addition (ADD), while single vision lenses only have one focal point, namely the spherical (SPH). Spheris is a unit of measurement used to indicate the strength of spectacle lenses in correcting vision so that vision is clear again and addition is a measure of correction needed for people with nearsightedness or presbyopia [11].

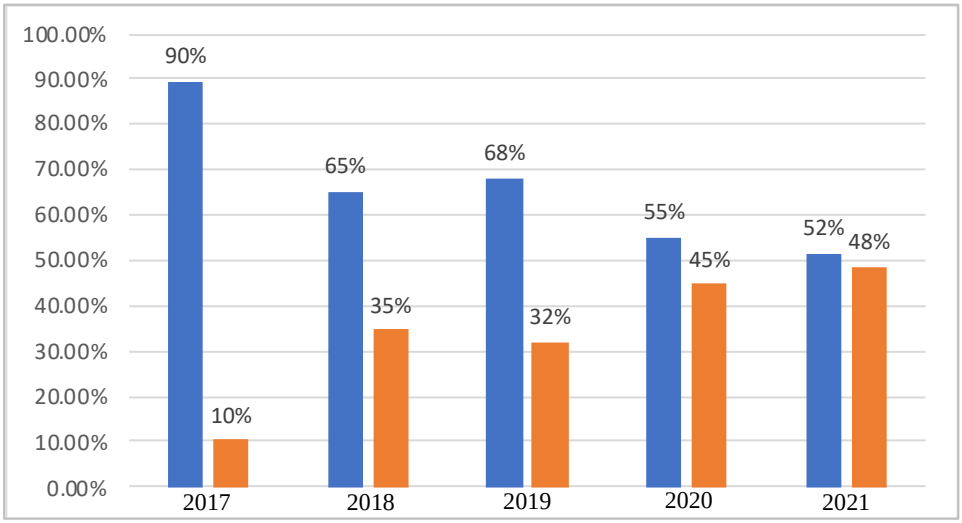

Figure 1. Customer Satisfaction Level

The business model used by Store X is business-to-business (B2B) and business-to-customer (B2C) so that they are not only connected to other business but also reaches the end customer directly. This company is already operating with the STR standard (Registration Certificate) for Health Workers and has suppliers who have permission from the Minister of Health of Indonesia so the optometric equipment sold by this company already has a special standardization in which eye health services are handled by Optic Refractionist (RO). The strategy used in meeting the needs of its customers is make-to-order and make-to-stock. The make-to-stock strategy implemented starts with ordering from several suppliers if the product stock is below the minimum limit (safety stock). After 7 days, the supplier will confirm the availability of the ordered goods and if a purchase order has been made, the required lead time is 3 weeks. Each supplier has varying minimum order requirements. After the company's inventory is fulfilled, then the company will confirm it to the patient. In the course of its business, Store

X evaluates it by distributing questionnaires to see the level of customer satisfaction based on three aspects, namely convenience of place, optical service, and product availability. This was also done as part of the agreement between the company and BPJS Indonesia (Social Security Agency on Health) so that the results of collecting this questionnaire were fully given to BPJS.

The questionnaire distributed used a Likert scale instrument. The Likert scale is a psychometric scale commonly used in questionnaires and is the most widely used scale in survey-related research [12]. The Likert scale used is a 5-point Likert scale with 5 choices, namely Very Disappointing (1 point), Disappointing (2 points), Neutral (3 points), Satisfied (4 points), and Very Satisfied (5 points). From the results of the questionnaire, a recapitulation is carried out by calculating the percentage of customers who choose a scale of 4 (Satisfied) and a scale of 5 (Very Satisfied) each year. From the data obtained from 2017 to 2021, we can see Fig. 1 is a graph that compares the level of customer satisfaction between scales 1-3 (in blue) and scales 4-5 (in orange) at Store X based on product availability. The best possible condition is when all feedback comes in a value of 5 showing the highest level of satisfaction.

From Fig. 1, it can be seen that there has been a significant increase in customer satisfaction from 2017 to 2021 (from 10% to 48%) but the number of respondents who chose a scale of 1-3 is still bigger than the number of respondents who chose a scale of 4-5. This means that the level of customer satisfaction based on product availability is constantly low even after 5 years. As most businesses define goals, this company also wants to increase their level of customer satisfaction in the future which can not be separated from good supply chain management. Therefore they implement a responsive supply chain strategy because they want to meet as many customer needs as possible. The problems that often occur in this strategy are stock-out when patients need it and overstock on several products whose demand does not match the supply provided by the company. Both of these occur because the number of postoperative patients is unpredictable and proper calculations have not been carried out to determine the appropriate safety stock and reorder point. When a stock out occurs, the company's service quality decreases, so it is necessary to determine the right service level in accordance with the company's sales target. Conversely, when there is overstock, some products become damaged. Every lens sold has an expiration date and if the item is not used before the expiration date, the lens will turn yellow (damage) because the coating on the lens fades so the product cannot be resold. These defective products will eventually be discarded or donated to other parties.

Based on the results of discussions with the company, the inventory control system currently used by the company is to set a minimum stock quantity of 200 pairs per type of lens and a maximum stock quantity of 1,800 pairs per type of lens as a consideration. When the amount of available stock is below the minimum stock limit value, the company re-stocks as much as the maximum stock amount. Thus, in determining the number of lenses to be purchased, the company does not adjust to the predicted number of lens demand in the future. This causes a stock out because the lens product inventory that is prepared cannot meet demand and there is no safety stock. Inventory that runs out before this time also causes lost sales so the revenue that the company gets is less than optimal. In essence, in carrying out inventory control, the stage of forecasting or predicting demand is an important initial step so that when you want to order lenses, you can adjust them to predict the number of demands for lenses in the future. Fig. 2 illustrates the supply chain model occupied in the field.

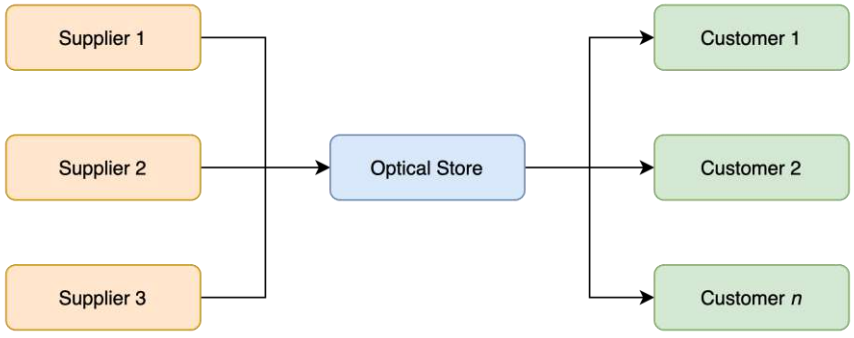

Figure 2. Observed Supply Chain Network

The company applies a three-echelon supply chain model, in which the model consists of suppliers, optical shops (stores), and customers. The store has several suppliers providing the lenses while they also serve multiple customers who are buying the products. This situation is further complicated by the availability of products owned

by suppliers. Store X has exactly three main suppliers to supply its lens products. Two of them set a minimum order quantity of 2,000 pairs per order and the rest set a minimum order quantity of 1,000 pairs per order. Sometimes when the situation with the demand decreases, the supplier who has the availability of the product ordered is the supplier with a minimum order of 2,000 pairs per order. Determining the minimum number of orders by these suppliers is one of the factors that can increase the risk of overstock at Store X. Figs. 3 and 4 are examples of stock-out and overstock data mapping for certain types of lenses observed in this study (November 2019-October 2022). It can be seen from Fig. 3 and 4 that out-of-stock and excess inventory often occur. Out-of-stock happens when demand in the blue line surpasses the available stock at the store (in orange in the graph) that can be seen in 1st, 2nd, 3rd, 7th, 8th, 13th to 15th, 33rd to 35th month for Single Vision -0,75 lens while for Single Vision +2,25 lens, it happens on the month of 1st, 2nd, 4th, 7th, 15th, 18th, 30th, and 33rd. We can infer that out-of-stock situation is more common to Single Vision -0,75 lens compared to Single Vision +2,25 lens therefore the surplus found more to the latter.

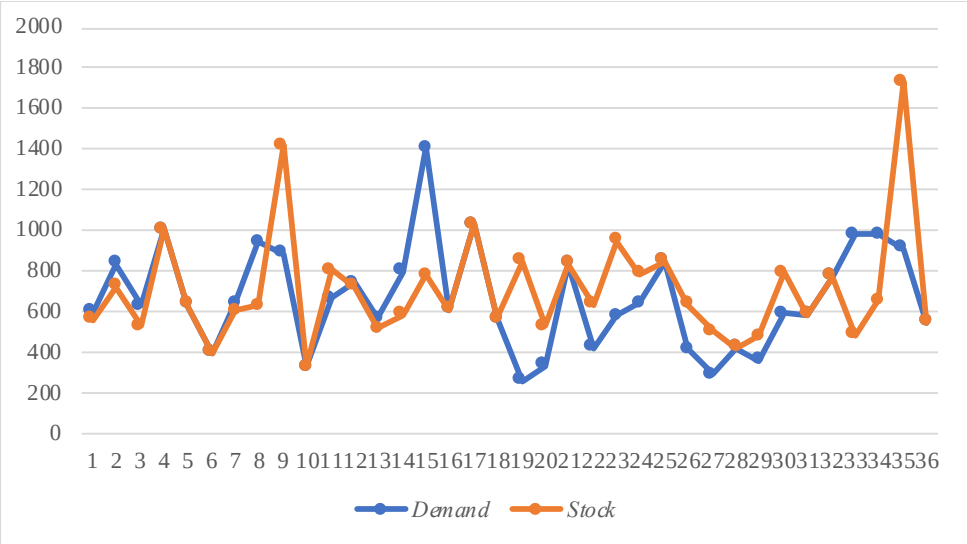

Figure 3. Stock-Out dan Over Stock Single Vision -0,75 Lens

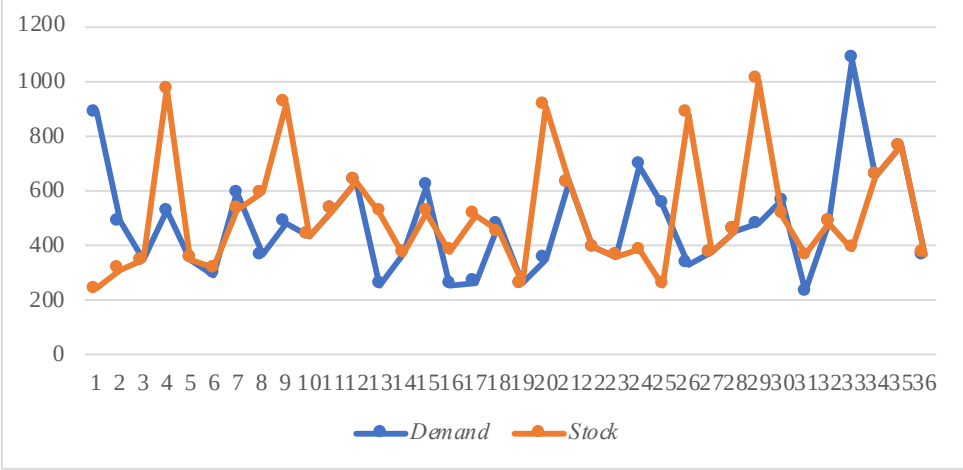

Figure 4. Stock-Out dan Over Stock Single Vision +2,25 Lens

Out-of-stock is the most common situation compared to excess inventory. This can happen because the company has not determined the safety stock to avoid out-of-stock situations and the determination of reorder points that need improvement therefore in this study, forecasting the number of lenses in the future and interpreting the forecast results with the selected method for each type of lens. Reviewing research conducted by [13] regarding production forecasting at battery cage manufacturing companies, the cyclic model was chosen as the best forecasting model compared to the exponential model because it has a higher level of accuracy. According to research conducted by [14] regarding pozzolan inventory control, the cyclical trend model is a forecasting model

that has the highest level of accuracy when compared to exponential, quadratic, linear, and cyclical models. This means that the trend parameter has an influence on the accuracy of forecasting results. Research conducted by [15] shows that the implementation of the ARIMA model in forecasting shows a high level of accuracy with a recorded error value (using the MAPE method) of 16.48%. After reviewing previous research and seeing the pattern of demand shown in the demand for single vision and bifocal lenses, several models selected in this study are models that are included in the time series statistical method, namely cyclical, cyclical trend, ARIMA (Autoregressive Integrated Moving Average). Based on research [16], [17], and [18] considering the forecasting model used in this study, in calculating errors we use the MAPE (Mean Absolute Percentage Error), MAD (Mean Absolute Deviation), and MSE (Mean Square Error) methods. After obtaining product forecasting results from the best forecasting method, a safety stock calculation is carried out that is adjusted to the company's service level. After that, a reorder point is determined based on the lead time, average demand, and safety stock that has been obtained from the previous stage.

2. Methodology

In this study, the method used was the descriptive method with a quantitative approach. Several steps are taken to conduct this research they are:

1. Observations are made for lens sales activities at the store. In this stage, the business activity processes that exist are studied to understand the systems applied.
2. Identification of the problem. After carrying out the observation process, we identify the main problem based on a study of the literature and investigate the existing conditions. This stage is carried out to determine the research focus by selecting the problems to be researched and resolved. The formulation of the problem is done by asking questions about the problem to be solved.
3. A literature study is carried out to increase knowledge about problems that are similar to the problems found at the observation sites that have been studied before.
4. Data collection is done by collecting the data needed in the research process. The data are divided into two types based on how to obtain them, namely primary data and secondary data. Primary data was obtained through observation and interviews, while secondary data was obtained from historical data from the store. The data collected in this study were:
    a. Primary data:
        i. The most frequently stocked out or overstocked lenses.
        ii. Data on customer satisfaction levels.
        iii. Lead time data.
        iv. Company-level service data.
        v. Data on the number of reorders.
    b. Secondary data:
        i. The organizational structure of the store.
        ii. Monthly demand in 2018-2022.
5. Data processing is one of the important processes in conducting research. The following are the steps taken in the data processing:
    a. Aggregation of Lens Demand Data

        In the initial stages of data processing, aggregation of lens demand data was taken for product types that have a critical demand and are most often experiencing stock out or over stock.

    b. Plotting of Aggregated Data Results

        Plotting the result of the aggregation to visualize the data pattern formed from the single vision and bifocal lens demand data that had been aggregated in this study.

    c. Data Stationarity Test

A stationary test was carried out using the ADF Test (Augmented Dickey-Fuller Test) to ascertain whether the data possessed could be processed using the ARIMA forecasting model. This stage ensures the forecasting results are not biased and the selected forecasting model is the best model.

d. Determination of the Parameters of the Forecasting Method

Forecasting parameters are determined to control several aspects of demand forecasting, such as handling missing values, detecting outliers, validating fit and forecasting, and forecasting sparse data. For cyclic and cyclic trend models, the parameters are determined using the sine and cosine (trigonometry) approach which forms special equations with the parameter names *a*, *b*, and *c*. As for the ARIMA model, the parameters are determined by the number of lag observations, the number of differencing transformations needed to become stationary values, and the component that shows the lag of the error component which is part of the time series. However, in this study, the forecast with the best ARIMA model feature was used in determining the best parameters of *p*, *d*, and *q*.

e. Lens Demand Forecasting

Demand forecasting is applied for the next one-year period, using cyclical models, cyclical trends, and ARIMA (Autoregressive Integrated Moving Average). The determination of these methods was referred to comparison compatibility regarding data type, number of data available, and also planning horizon, as resumed from [19] and shown in Table 1.

Table 1. Demand Forecasting Methods using Statistics and Machine Learning

Forecasting Method	Data Type	Number of Datapoint	Forecasting Planning Horizon
Naive	Stationary	1-2	Very short
Moving Average	Stationary	As minimum as same with its moving average period	Very short
Simple Exponential Smoothing	Stationary	5-10	Short
Adaptive Response Exponential Smoothing	Stationary	10-15	Short
Holts Exponential Smoothing	Trend Linear	11-15	Short to Medium
Winters Exponential Smoothing	Trend and Stationary	Minimum 4 or 5 for each season	Short to Medium
Trend Regression	Trend Linear and Non-Linear, with or without Seasonal	Minimum 10 with 4-5 for every season if applied	Short to Medium
Causal Regression	All kinds of data	Minimum 10 for the independent variable	Short, Medium, and Long

Time Series Decomposition	Trend, Seasonal, and Cyclic	Minimum 2 peak points in a cycle	Short, Medium, and Long
ARIMA	Stationary	50	Short, Medium, and Long

f. Forecasting Validation

The forecast validation stage is done by calculating and selecting the lowest error to determine the appropriate forecasting method for the lens demand pattern. The error measurement methods used are Mean Absolute Percentage Error (MAPE), Mean Absolute Deviation (MAD), and Mean Square Error (MSE).

g. Forecasting Verification

After obtaining the results of forecasting with the selected method (with the lowest error), a verification process is conducted using the moving range chart method. This stage is implemented to ensure that the model used is mathematically appropriate and already reflects the conceptual model before executing the analysis of the results. The moving range chart method is used to test the stability of the causal system that affects demand.

h. Calculation of Safety Stock Size

After obtaining the results of demand forecasting, a safety stock calculation is calculated by multiplying the selected forecasting results with the service level set by the company. The service level value is shown in percentage form with a maximum limit of 100%. In the safety stock calculation, the service level is converted to a constant obtained from the normal distribution z table.

i. Determination of the Reorder Point

After forecasting demand and calculating safety stock, a reorder point is determined. The reorder point is the time when inventory conditions have reached a certain level, a product must be reordered to balance the product inventory. In determining the reorder point, a calculation is done involving three elements, namely the demand, safety stock, and lead time.

6. Analysis of Calculation Results

At this stage, an interpretation of all the results of the calculations carried out in this study is conducted by elaborating the results of data processing so that conclusions can be drawn in the form of the selected forecasting method, predictions of demand for the next 12 periods, amount of safety stock, and reorder points. This stage is also carried out to facilitate the process of drawing conclusions and suggestions in the last stage of this research.

3. Result and Discussion

A. Cyclic Model

The data used is historical data on demand for single vision and bifocal lenses from the Operations Division. The data obtained is daily data which is accumulated into monthly data for the period of November 2018 - October 2022 as shown in Table 2. Table 3 covers the detailed list of single-vision and bifocal lens products that are considered the object of this study.

Table 2. Number of Demand for Single Vision Lenses and Bifocals for the 1st Year

Month	Demand Data	
	Single Vision	Bifocal Kryptok
1	2,270	2,156
2	1,802	1,767
3	1,461	1,295
4	2,373	2,111

5	1,374	1,547
6	1,195	1,212
7	1,738	1,963
8	1,850	1,765
9	1,996	1,590
10	990	1,866

Table 3. Detailed Data Name and Type of Lens

No.	Lens Name	Lens Type
1	Single Vision -0.75	Single Vision
2	Single Vision +2.25	
3	Single Vision +3.5	
4	Bifocal Kryptok SPH 0 ADD 1.25	Bifocal Kryptok
5	Bifocal Kryptok SPH 0.25 ADD 2.25	
6	Bifocal Kryptok SPH 0.5 ADD 3	

Calculation of the constant values of other parameters is conducted using the parameter equations in the cyclic model. After obtaining the constant values of parameters *a*, *b*, and *c*, forecasting calculations (y') are performed. The following is a forecasting calculation with a cyclical model in period 36:

$$y' = a + b\cos\frac{2\pi t}{n} + c\sin\frac{2\pi t}{n}$$
$$y' = 3.334{,}0278 + 114{,}66649 \times 1 + 241{,}070309 \times 0$$
$$y' = 3.448{,}69 \text{ pairs}$$
$$y' \approx 3.449 \text{ pairs}$$

After obtaining the forecasting results using the cyclical model, error calculations are performed using the MAPE, MAD, and MSE methods as follows in Table 4.

Table 4. Cyclical Model Error Calculation

Period	t	t^2	Actual (y)	Forecast (y')	Error ($e = y - y'$)	Percentage of Error	Absolute Error	e^2
25	25	625	3,619	3,069	550	15%	550	302,500
26	26	676	2,510	3,077	-567	23%	567	321,489
27	27	729	2,540	3,093	-553	22%	553	305,809
28	28	784	3,666	3,117	549	15%	549	301,401
29	29	841	2,263	3,147	-884	39%	884	781,456
30	30	900	2,636	3,183	-547	21%	547	299,209
31	31	961	2,284	3,224	-940	41%	940	883,600
32	32	1,024	3,992	3,267	725	18%	725	525,625
33	33	1,089	4,514	3,313	1201	27%	1201	1,442,401
34	34	1,156	3,610	3,360	250	7%	250	62,500
35	35	1,225	3,562	3,406	156	4%	156	24,336
36	36	1,296	3,501	3,449	52	1%	52	2,704

Total	233%	6,974	5,253,030

Getting the errors using the three methods of MAPE, MAD, and MSE, the results summary of the error calculations is carried out in Table 5.

Table 5. Summary of Error Calculation for Cyclical Model

MAPE	MAD	MSE
19,42%	581.167	43,7752.5

B. Autoregressive Integrated Moving Average

Forecasting with the ARIMA model is executed using the Minitab 21.3 software. In the first stage, 36 periods of historical data were input and data plotted. Continued, a stationary test was carried out using the Augmented Dickey-Fuller (ADF) test, as a requirement for forecasting with the ARIMA model. In the stationary test using the ADF Test, there are two hypotheses with the following information:

H_0 (null hypothesis): Non-stationary data

H_1 (alternative hypothesis): Stationary data

With a statistical test of -5.94371 and a specified significance level of 0.05 (95% confidence level), it can be concluded reject the null hypothesis because the data is stationary without differencing (the result of statistical test ≤ critical value -2.94851). Because the data is stationary, there is no need for a data transformation process hence we determine the best model using the best ARIMA model feature in Minitab. This stage is utilized to determine the parameters of *p* (the number of lag observations), *d* (the number of differencing transformations required by the time series data so that the data is stationary), and *q* (the lag of the error component). From the use of the Best ARIMA Model in Minitab, the parameter estimation results can be seen in Fig. 5.

Final Estimates of Parameters

Type		Coef	SE Coef	T-Value	P-Value
AR	1	0.99991	0.00287	348.18	0.000
MA	1	0.893	0.196	4.54	0.000
MA	2	0.134	0.216	0.62	0.538
MA	3	-0.054	0.181	-0.30	0.769

Figure 5. Parameter Estimation Result

It was found that the best model was ARIMA (1,0,3) with the smallest corrected Akaike Information Criterion (AIC) value of 594,909. After obtaining the best ARIMA model, forecasting was calculated for the next 12 periods. The ARIMA model used is (1,0,3) and forecasting is done using the ARIMA feature found on the Stats Tab and the Time Series Menu. Fig. 6 is the result of forecasting using the ARIMA model (1,0,3) for 25th to 36th month.

C. Forecasting Validation

After forecasting is tried using several models, namely Cyclic, Cyclical Trend, and Autoregressive Integrated Moving Average (ARIMA), the validation stage is continued by summarizing the error measurement results in percentage form to determine the best forecasting method with the smallest error value. From the results of the error recapitulation shown in Table 6, it can be concluded that the best forecasting method selected for single vision and bifocal lenses is the cyclical trend model with an error value of 15,29% (MAPE); 538.333 (MAD); and 466,615 (MSE).

D. Forecasting Verification

After getting the results of forecasting with the selected method (with the lowest error), a verification process is performed using the moving range chart method, to ensure that the model used is mathematically appropriate and already reflects the conceptual model before carrying out the analysis of the calculation results. The moving range chart method is used to test the stability of the causal system that affects demand. The following chart in Fig. 7 is a recapitulation of the Moving Range calculation in which the orange line represents the upper control

limit (UCL) while the green line represents the lower control line (LCL). The UCL value is a little bigger than 2.000 units, so does the LCL but in negative direction.

Table 6. Recapitulation of Error Calculations for Each Forecasting Model

No.	Forecasting Model	Error Calculation Method		
1	Cyclical	19,42%	581.167	437,753
2	Cyclical Trend	15,29%	538.333	466,615
3	ARIMA (1,0,3)	21,71%	612.493	529,754

Forecasts from Time Period 24

Time Period	Forecast	SE Forecast	95% Limits Lower	95% Limits Upper	Actual
25	3469.97	736.895	2025.36	4914.57	3619
26	3370.86	741.092	1918.03	4823.69	2510
27	3395.19	741.366	1941.82	4848.56	2540
28	3394.88	741.619	1941.02	4848.75	3666
29	3394.57	741.871	1940.21	4848.93	2263
30	3394.26	742.123	1939.40	4849.11	2636
31	3393.95	742.376	1938.60	4849.30	2284
32	3393.64	742.628	1937.79	4849.48	3992
33	3393.32	742.880	1936.99	4849.66	4514
34	3393.01	743.131	1936.18	4849.84	3610
35	3392.70	743.383	1935.38	4850.03	3562
36	3392.39	743.635	1934.57	4850.21	3501

Figure 6. ARIMA Model Calculation Results

Seeing Fig. 7, we can conclude that there are no sudden trend fluctuations or cycles that cause a decrease in forecasting accuracy. This is indicated by the moving range values which are below UCL and above LCL thus the forecasting results of the cyclical trend model are verified to be acceptable.

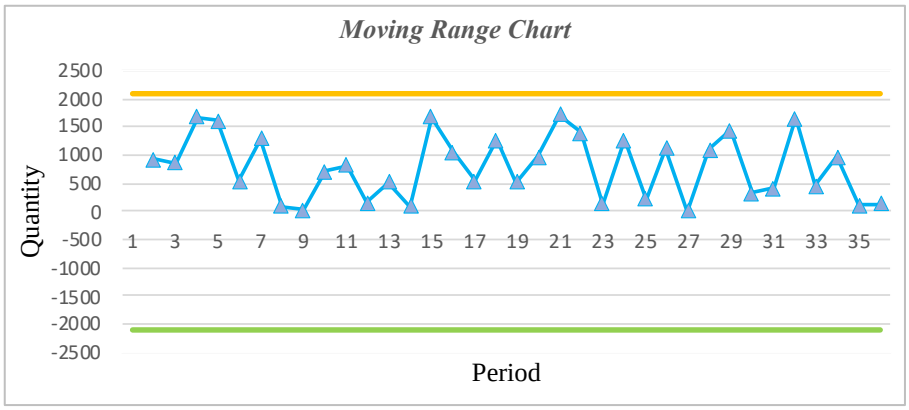

Figure 7. Moving Range Chart

The following stage is the calculation of next year's demand forecasting, safety stock and reorder point determinations for each lens type. Continued scenario experiments show that the size of the safety stock that must be determined by the company will adjust to the service level that has been defined, as well as the reorder point. Fig. 8 is a graph of the relationship between the specified service level and the determination of the size of the safety stock.

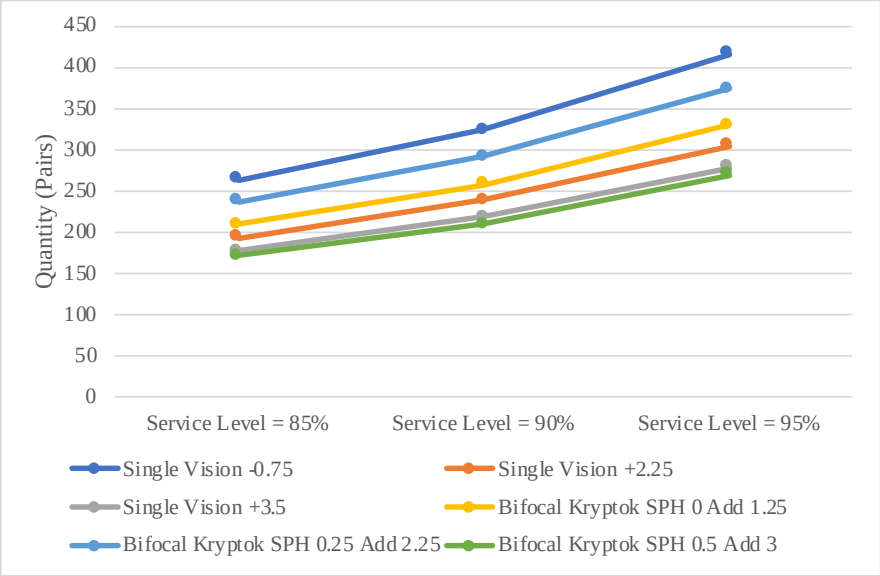

Figure 8. Relationship between Service Level and Safety Stock Quantity

We can see that the higher the service level, the greater the size of the safety stock, and also the reorder point. From Fig. 9 it can be known that the higher the service level, the faster the store has to place an order again (reorder). Considering this condition and the targets set by the store, the calculation shows that a service level of 90% is the most likely service level to be implemented.

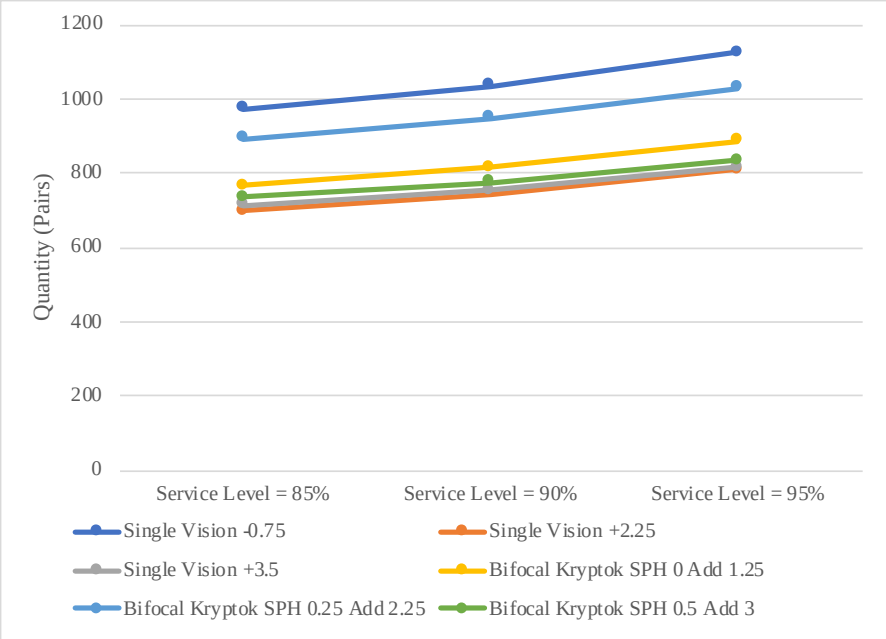

Figure 9. Relationship between Service Level and Reorder Point

4. Conclusion

The forecasting method chosen to meet the demand for single vision and bifocal lens products is the Cyclical Trend method with an error value of 15.29% (MAPE); 538.333 (MAD); and 466,615 (MSE). The results of forecasting the demand for single vision and bifocal lens products for the next year in Store X are for Single Vision -0.75 lenses of 8,511 pairs, Single Vision +2.25 lenses of 6,059 pairs, Single Vision +3.5 lenses of 6,437 pairs, Bifocal Kryptok SPH 0 ADD 1.25 of 6,692 pairs, Kryptok Bifocal lenses SPH 0.25 ADD 2 .25 of 7,866 pairs, and 6,761 pairs of Kryptok SPH 0.5 ADD 3 bifocal lenses. The safety stock for each product is 415 pairs of Single Vision -0.75 lenses, 305 pairs of Single Vision +2.25 lenses, 278 pairs of Single Vision +3.5 lenses, 374 pairs of SPH 0 ADD 1.25 Kryptok Bifocal lenses, 374 pairs of SPH Kryptok Bifocal lenses 0.25 ADD 2.25, and SPH

Kryptok Bifocal lenses 0.5 ADD 3 as many as 269 pairs. The number of reorder points for each product will be ordered again when the supply condition has reached a certain level where 1,125 pairs of Single Vision -0.75 lenses, 810 pairs of Single Vision +2.25 lenses, 815 pairs of Single Vision +3.5 lenses, 887 pairs of Bifocal Kryptok SPH 0 ADD 1.25, 1.0 Bifocal Kryptok SPH 0.25 ADD 2.25 30 pairs, and 833 pairs of Kryptok SPH 0.5 ADD 3 bifocal lenses.

Future research can advance the experiment by investigating other forecasting methods to enrich comparative analysis using such these models: the Linear Regression model, Exponential Smoothing, Multiplicative Holt-Winters, Additive Holt-Winters, Double Seasonal Holt-Winters, SARIMA, and other time series forecasting models.

References

[1] T. Beldek, A. K. Konyalıoğlu, dan H. C. Akdağ, "Supply Chain Management in Healthcare: A Literature Review," in *Lecture Notes in Mechanical Engineering*, Istanbul, Springer, 2019, pp. 570-579.

[2] Dedi, E. T. B. Waluyo, dan L. Septiananingrum, "Sistem Informasi Pengendalian Persediaan Stok Lensa Berbasis Web pada Optik Trio Jaya Cabang Tangerang," *Jurnal SISFOTEK GLOBAL*, pp. 59-64, 2019.

[3] R. S. Russell dan B. W. Taylor, "Operations Management: Creating Value Along the Supply Chain, 7th ed.," New York: John Wiley and Sons, 2011.

[4] S. Tannan, "Demand Forecasting," 2020.

[5] Y. T. Sulistyo dan M. Abdulrahim, "Perencanaan Kebutuhan Kapasitas Produksi untuk Memenuhi Permintaan Songkok di UD Songkok Nizam Gresik dengan Menggunakan Metode RCCP," 2018.

[6] A. D. Cahyo, I. Priadythama, R. C. Y, dan H. W. Sari, "Analisis Peramalan Kebutuhan, Penentuan Safety Stock, dan Reorder Point Material MCB Bidang Distribusi PT PLN (Persero) Distribusi Jakarta Raya dan Tangerang Area Pondok Gede," in *Industrial Engineering Conference*, Surakarta, 2015.

[7] T. Hendriani, M. Yamin, dan A. P. Dewi, "Sistem Peramalan Persediaan Obat dengan Metode Weight Moving Average dan Reorder Point (Studi Kasus: Puskesmas Soropia)," *semanTIK*, pp. 207-214, 2016.

[8] H. Sarjono dan E. A. Kuncoro, "Analisis Perbandingan Perhitungan Re-order Point," *Binus Business Review*, Vol. 5, No. 1, pp. 288 - 300, 1 May 2014.

[9] J. Berg, "Single Vision vs Bifocal vs Progressive Lenses," 8 November 2021. [Online]. Available: https://www.sportrx.com/blog/single-vision-vs-bifocal-vs-progressive-lenses/#.

[10] "Informasi Kesehatan Mata," 26 Agustus 2020. [Online]. Available: https://kmu.id/ini-2-kacamata-bifokal-yang-prlu-diketahui/.

[11] A. Essilor, "Bagaimana Cara Membaca Resep Kacamata & Hasil Pemeriksaan Mata?," West Jakarta, 2023.

[12] D. Taluke, R. S. M. Lakat, dan A. Sembel, "Analisis Preferensi Masyarakat dalam Pengelolaan Ekosistem Mangrove di Pesisir Pantai Kecamatan Loloda Kabupaten Halmahera Barat," *Jurnal Spasial Perencanaan Wilayah dan Kota,* Vol. 6, No. 2, pp. 531-540, 2019.

[13] M. Sayuti, "Aplikasi Perhitungan Metode Peramalan Produksi pada CV X," *Jurnal Teknovasi,* Vol. 1, No. 1, pp. 35-43, 2014.

[14] P. Fithri dan A. Sindikia, "Pengendalian Persediaan Pozzolan di PT Semen Padang," *Jurnal Optimasi Sistem Industri,* Vol. 13, No. 2, pp. 665-686, 2014.

[15] A. H. Al Rosyid, C. D. N. Viana, dan W. A. Saputro, "Penerapan Model Box Jenkins (ARIMA) dalam Peramalan Harga Konsumen Bawang Merah di Provinsi Jawa Tengah," *Jurnal Agri Wiralodra,* Vol. 13, No. 1, pp. 29-37, April 2021.

[16] Nurulita, "Penerapan Metode Peramalan ARIMA (*Autoregressive Intergrated Moving Average*) untuk Penentuan Tingkat *Safety Stock* pada Industri Elektronik," 2010.

[17] M. I. Ibrahim, "Peramalan Volume Penjualan Kacamata di Perusahaan Optik Akur Jogjakarta dengan Metode Box-Jenkins (ARIMA)," 2004.

[18] D. Rahmayanti dan A. Fauzan, "Optimalisasi Sistem Persediaan Bahan Baku Karet Mentah (Lateks) dengan Metode *Lot Sizing* (Studi Kasus - PT Abaisiat Raya)," *Jurnal Optimasi Sistem Industri,* Vol. 12, No. 1, pp. 317-325, 2013.

[19] J. H. Wilson dan B. Keating, "Business Forecasting: With Accompanying Excel-Based Forecast Software, 4th ed.," Boston: McGraw-Hill, 2002.

Biographies of Authors

Thobias Adriel Silaen is a student at the Department of Logistics Engineering, Universitas Pertamina.

Yelita Anggiane Iskandar completed her bachelor's degree in Industrial Engineering from Universitas Indonesia (UI) in 2007 with a concentration in system modeling. In 2013, she obtained a master's degree from Institut Teknologi Sepuluh Nopember (ITS) in Surabaya, East Java, Indonesia in the field of logistics and supply chain management, with cum laude predicate. Currently pursuing doctoral education in Industrial Engineering, especially in the area of scheduling at Pusan National University, South Korea; while also actively working as a lecturer at the Department of Logistics Engineering at Universitas Pertamina. Previously, he worked at PT Freeport Indonesia in Tembagapura, Papua in the Maintenance Department; and at PT Fonterra Brands Indonesia in Jakarta, handling imported products and supply planning.

Vol. 2, No. 2, October 2023, pp. 99-108
p-ISSN: 2963-8577
e-ISSN: 2964-3511
DOI: 10.57102/jescee.v2i2.66

RELIABILITY ANALYSIS OF 3 PHASE GENERATOR SET AS AN EMERGENCY POWER SUPPLY IF THERE ARE ELECTRICITY OUTAGES AT PT. INTRACAWOOD MANUFACTURING

Musmuliadi[1]*, Ismit Mado[1], Achmad Budiman[1], Subarianto[2], Agustinus Rantepadang[2]
[1]Electrical Engineering Study Program, Faculty of Engineering, University Borneo Tarakan, Indonesia
[2]PT. Intracawood Manufacturing, Tarakan, Indonesia

Abstract
The need for electricity is a problem that occurs every year, especially in environments that really need a very high supply of electricity, such as companies, industries, offices, and lecture buildings. To maintain the continuity of the supply of electrical energy in the event of a disturbance, it is necessary to back up the generating system. As with the operation of a power generation system, it is also necessary to maintain the continuity and reliability of this backup power plant. To determine the level of reliability and availability, equipment data, operational data and damage data are needed. This study calculates the specified operating time (SOT), the total number of damages and the number of generators that are not operated due to routine or scheduled maintenance needs. calculating maintenance hours (S) and total maintenance time for each generator within a predetermined period. From SOT minus the total maintenance time, you will get the actual operating time (AOT) value of each generator. SOT and AOT data are needed to calculate the level of availability of generators individually and the level of availability of generators as a backup power supply. Furthermore, this research calculates the mean time between failure (MTBF) for each generator. The results of the study show that in 2022 the reliability level of PT. Intracawood Manufacturing by 99%. The generator set reliability level is included in the group that rarely experiences disturbances or damage (R≥ 90%) and the average generator set availability rate in 2022 is 98.5%. This study shows that the operating target of the power generation system at PT. Intracawood Manufacturing rarely experiences interruptions.

Keywords:
Generator; reliability; availability; MTBF;

Article History:
Received: August 24th, 2023
Revised: September 24th, 2023
Accepted: October 24th, 2023
Published: October 31st, 2023

Corresponding Author:
Musmuliadi
Electrical Engineering Study Program, Faculty of Engineering, Borneo Tarakan University, Indonesia
E-mail:
musmuliadi2000@gmail.com

1. Introduction

At this time, it is known that the development of technology in our country is growing quite rapidly in the field of industry, companies, offices, and other sectors. This technological improvement is in line with the increasing need for electrical equipment. The need for electricity is a problem that occurs every year, especially in environments that really need a very high supply of electricity. In addition to the increasing demand for electricity supply, North Kalimantan province is also one of the areas that still has a deficit of electricity. Statistical data for 2021 shows that the capacity is still lower than the peak load[1]. To need backup generator sets in various industrial sectors and groups with large electricity loads.

The back up of electric power is in the form of a power generation system called a generator, both generators in power plants such as diesel power plants (PLTD), and generator sets. Generator set is equipment used to convert motion energy into electrical energy. The generator set functions to provide electrical energy that is needed by the community and industry. Genset performance is needed so that reliability and availability meet performance standards.

Reliability is defined as the ability of various components of equipment and systems to perform the required work functions under operating conditions. Generator reliability will change over time and the equipment ages. To get the optimal generator set performance value.

Researchers have conducted studies from various aspects related to the performance of generator sets as a back-up supply of electrical energy. Ilmi & Ayong (2019) analyzes the economic side of the generator operating system by arranging PT. Telecommunications (Tbk) Pontianak using the method *Lagrange Multiplier[2]. Tsuuri*

*and Deni (2017)*regarding the design of an Automatic Transfer Switch (ATS) generator with a capacity of 1200 VA for the operation of backup electrical energy in emergency conditions. This research is able to integrate the connection between PT. PLN (Persero) and a generator as a backup[3].

Yusniati and Nurcholish (2020) examined the loading system when there was an increase in the demand for electric power which required the generator to carry the overload [4]. Meanwhile, Restu and Ismit (2022) is a research on PLTD loading analysis in the Tana Merah sub-district, Tana Tidung Regency, North Kalimantan province. Qualitative research based on measurement results in the field recommends a parallel loading system with a percentage of 73% of the generating capacity in the area [5]. And to achieve the best performance it is necessary to carry out maintenance, one of which is by using the total productive maintenance method [6]. Generator set reliability analysis has been carried out by researchers (Budi, 2017) by looking at the effect of generator electric torque on generator frequency values [7].

PT. Intracawood Manufacturing, located in Tarakan City, North Kalimantan, is one of the major Indonesian plywood companies. There are 6 generator sets owned by PT. Intracawood Manufacturing, each of the generator sets has a capacity of 3 units of 1000 Kva, 2 units of 1360 KVa and 1 unit of 1400 KVa as a backup power supply for the entire electrical load at PT. Intracawood Manufacturing. Given the importance of the generator as a power generator in the corporate environment, buildings and other mechanical equipment, the researcher wants to know how reliable the performance of the generator is so that it can produce a stable electric power output and have reliable performance and the availability of an optimal supply of electrical energy for the continuity of the company's work. .

2. Methods

This study uses qualitative data based on analytical descriptive methods [5]. Qualitative data is in the form of observation where data is collected on the required object. This research was conducted in approximately 6 months starting from March to August 2022. Data analysis was carried out when 6 generator sets were operating either in parallel or periodically as a back up supply of electrical energy when there was a disruption to PLN operations or scheduled blackouts at PT. Intracawood Manufacturing.

A. Calculation and Data Processing

To determine the level of operational reliability and availability of the generator set, it is necessary to calculate the level of availability and operational data and damage obtained from the generator operational data. Then the specified operating time (SOT) is collected, the total amount of damage and the number of generators not operated for routine or scheduled maintenance, due to maintenance (S) and the total maintenance time for each generator within a predetermined period. From SOT minus the total maintenance time, you will get the actual operating time (AOT) value of each generator. SOT and AOT data are needed to calculate the level of availability of generators individually and the level of availability of generators as a backup power supply. Next AOT=SOT-(S+T), the amount of damage is needed to calculate the mean time between failure (MTBF) of each generator. After obtaining the MTBF value, together with the total failure time (T), the level of reliability and availability can be calculated.

B. Generator Evaluation

To evaluate the performance of the generator set in order to achieve the desired reliability of the generator set, some data is needed, such as generator set maintenance data in the form of a maintenance schedule, generator set failure data, generator set operational data in a year and also analytical calculation data in the form of generator set operational data. which has been set or Specified Operating Time (SOT), real generator set operational data or Actual operating time (AOT), the average time between failures or Mean time between failure (MTBF), reliability or reliability and availability or availability. To be able to find out that the maintenance program has met the standards of the objectives to be achieved, each technician has the responsibility to evaluate the maintenance program that has been implemented. So that the performance of the equipment can meet the standards set. What is meant by maintenance technique is scheduled prevention including weekly and monthly maintenance. What is meant by the performance of the generator is the result of work which is the operation of the generator.

Generator set analysis to achieve the desired generator set reliability is divided into:

1. *Specified operating time (SOT)*

*Specified operating time (SOT)*or the amount of operating time that has been set is written in the following equation [6]:

$$SOT = A \times B \quad (1)$$

With:

A = Total standby Genset Operation time
B = Number of days in a year

2. *Actual operating time (AOT)*

*Actual operating time*or the amount of actual operating time and remaining on standby for the generator set for 24 hours a day is written in the following equation [8]:

$$AOT = SOT - (S + T) \quad (2)$$

With:
AOT = Actual Operating Time
SOT = specified operating time
S = Total scheduled maintenance time in 1 year
T = Total unscheduled maintenance time in 1 year

3. *Mean Time Between Failures (MTBF)*

Mean Time Between Failures(MTBF) or the average time between failures is written in the following equation [6]:

$$MTBF = \frac{AOT}{Number\ of\ failures\ in\ a\ year} \quad (3)$$

With:
MTBF= *Mean Time Between Failures*
AOT = *Actual Operating Time*

4. Reliability

The equation for finding the reliability value is written in the following equation:

$$R = 100.e-t/m \quad (4)$$

With:
R = Reliability
e = 2.718
t = SOT
m = MTBF

5. Availability

The equation for finding the availability value is written in the following equation[8]:

$$A = \frac{(AOT)}{(SOT)}\ x\ 100\% \quad (5)$$

With:
A = Availability (Availability).
AOT = Actual Operating Time (actual operating time).
SOT = Specified Operating Time (specified operating time.

3. Results and Discussion

To obtain generator set performance results, several calculations are carried out, namely by determining the specified operating time (SOT), the actual operating time (AOT), the average time between failures or the mean time between failures. (MTBF), reliability and availability for each generator set unit.

Calculation of Generator Set Performance

The SOT calculation uses the equation for one of the generator sets in 2022.

A. Calculation of SOT in January 2022 is as follows.

- For generator set 02

  SOT = 24 × 31

  SOT = 744 Hours

Calculation of the specified operating time (SOT) generator set 02 in January. The calculation above is the same as the calculation for generator sets 06, 07, 09, 11, 12 and according to the number of days in the following month. Calculation of SOT Generator Set is presented in table 1.

Table 1. SOT Generator Set in 2022

No	Generator	SOT 2022			SOT (HOURS)
		Month	Hours/day	Total Days	
1	G2, G6, G7, G9, G11, G12	January	24	31	744
2	G2, G6, G7, G9, G11, G12	February	24	28	672
3	G2, G6, G7, G9, G11, G12	March	24	31	744
4	G2, G6, G7, G9, G11, G12	April	24	30	720
5	G2, G6, G7, G9, G11, G12	May	24	31	744
6	G2, G6, G7, G9, G11, G12	June	24	30	720
7	G2, G6, G7, G9, G11, G12	July	24	31	744
8	G2, G6, G7, G9, G11, G12	August	24	31	744
9	G2, G6, G7, G9, G11, G12	September	24	30	720
10	G2, G6, G7, G9, G11, G12	October	24	31	744
11	G2, G6, G7, G9, G11, G12	November	24	30	720
12	G2, G6, G7, G9, G11, G12	December	24	31	744
Total					**8760**

B. Scheduled Maintenance Time (S)

Generator set (Genset) PT. Intracawood Manufacturing is not operated because routine scheduled maintenance is carried out by technicians to prevent errors or failures. On average per month, scheduled routine maintenance and inspections are carried out within 10 hours (10*12 months) = 120 hours (S). SOP set by PT. Intacawood Manufacturing as a generator set is carried out routine maintenance and inspection every month.

C. Total Breakdown Time (T)

The total breakdown time is the number of times the generator set is not operating (hours) for 12 months in 2022 caused by damage shown in table 2 below.

Table 2. SOT Generator Set in 2022

Year		Month											T Broken	
2022		**Jan**	**Feb**	**Mar**	**Apr**	**May**	**Jun**	**Jul**	**Aug**	**Sept**	**Oct**	**Nov**	**dec**	**(O'clock)**
Generator Sets	**G2**													0
	G6													0
	G7													0
	G9								3					3
	G11							2			2	4		8
	G12									4			2	6

D. *Actual Operating Time (AOT)*

The AOT calculation uses equation 2.5 for 6 generator set units in 2022
The calculation of AOT in January 2022 is as follows

- For Generator Sets 02
  Scheduled maintenance (S) = 10 Hours

Unscheduled maintenance (T)= 0 Hours
Total equipment not operating = 10 hours
Then,AOT G02 = 744 - (10+0)
AOT G02 = 744 - 10
AOT G02 = 734 Hours

- For Generator Set 06
  Scheduled maintenance (S) = 10 Hours
  Unscheduled maintenance (T)= 0 Hours
  Total equipment not operating = 10 hours
  Then,AOT G02 = 744 - (10+0)
  AOT G02 = 744 - 10
  AOT G02 = 734 Hours
- For Generator Sets 07
  Scheduled maintenance (S) = 10 Hours
  Unscheduled maintenance (T)= 0 Hours
  Total equipment not operating = 10 hours
  Then,AOT G02 = 744 - (10+0)
  AOT G02 = 744 - 10
  AOT G02 = 734 Hours
- For Generator Set 09
  Scheduled maintenance (S) = 10 Hours
  Unscheduled maintenance (T)= 0 Hours
  Total equipment not operating = 10 hours
  Then,AOT G02 = 744 - (10+0)
  AOT G02 = 744 - 10
  AOT G02 = 734 Hours
- For Generator Sets 11
  Scheduled maintenance (S) = 10 Hours
  Unscheduled maintenance (T)= 0 Hours
  Total equipment not operating = 10 hours
  Then,AOT G02 = 744 - (10+0)
  AOT G02 = 744 - 10
  AOT G02 = 734 Hours
- For Generator Sets 12
  Scheduled maintenance (S) = 10 Hours
  Unscheduled maintenance (T)= 0 Hours
  Total equipment not operating = 10 hours
  Then,AOT G02 = 744 - (10+0)
  AOT G02 = 744 - 10
  AOT G02 = 734 Hours

To find the AOT Generator Set value in February-December in 2022, the same calculation is carried out as the calculation above, the results are presented in table 3.

Table 3. Calculation results of AOT Generator Set in 2022

Genset 2022	**Month**											
	Jan	**Feb**	**Mar**	**Apr**	**May**	**Jun**	**Jul**	**Aug**	**Sept**	**Oct**	**Nov**	**dec**
G2(Hour)	734	662	734	710	734	710	734	734	710	734	710	734
G6(Hour)	734	662	734	710	734	710	734	734	710	734	710	734
G7(Hour)	734	662	734	710	734	710	734	734	710	734	710	734
G9(Hour)	734	662	734	710	734	710	734	731	710	734	710	734
G11(Hour)	734	662	734	710	734	710	732	734	710	732	706	734

G12(Hour)	734	662	734	710	734	710	734	734	706	734	710	732

E. Mean Time Between Failure (MTBF)

The MTBF calculation uses actual operational data and the number of failures in a year as in equation 3 for 6 generator sets in 2022.

The calculation of MTBF Generator Set in January 2022 is as follows.

- $MTBF\ G02 = \frac{734}{0} = \infty$ hour
- $MTBF\ G06 = \frac{734}{0} = \infty$ hour
- $MTBF\ G07 = \frac{734}{0} = \infty$ hour
- $MTBF\ G09 = \frac{734}{0} = \infty$ hour
- $MTBF\ G11 = \frac{734}{0} = \infty$ hour
- $MTBF\ G12 = \frac{734}{0} = \infty$ hour

To find the SOT Generator Set value in February-December in 2022, the same calculation is carried out as the calculation above, the results are shown in table 4.

Table 4. 2022 Generator Set MTBF Calculation Results

Genset 2022	Month												
	Jan	**Feb**	**Mar**	**Apr**	**May**	**Jun**	**Jul**	**Aug**	**Sept**	**Oct**	**Nov**	**dec**	**Average**
G2 (Hour)	∞	∞	∞	∞	∞	∞	∞	∞	∞	∞	∞	∞	∞
G6 (Hour)	∞	∞	∞	∞	∞	∞	∞	∞	∞	∞	∞	∞	∞
G7 (Hour)	∞	∞	∞	∞	∞	∞	∞	∞	∞	∞	∞	∞	
G9 (Hour)	∞	∞	∞	∞	∞	∞	∞	244	∞	∞	∞	∞	20.30556
G11 (Hour)	∞	∞	∞	∞	∞	∞	366	∞	∞	366	177	∞	75.70833
G12 (Hour)	∞	∞	∞	∞	∞	∞	∞	∞	177	∞	∞	366	45.20833

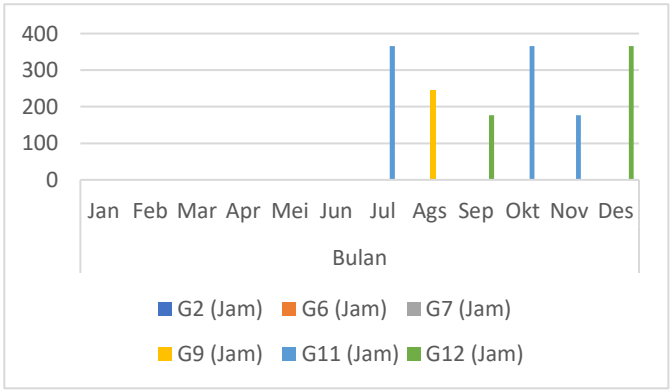

Figure 1. Graph of 2022 Generator Set MTBF

F. Level of Reliability (Reliability)

To calculate the reliability level of the generator set, it takes data on the actual operating time of the generator set and the number of damage to the generator set in 2022 based on (4). Calculation of the reliability level of the generator set in January 2022

- $R\ G02 = 100\ \times 2{,}718^{-\frac{0}{734}}$
  $R\ G02 = 100\%$
- $R\ G06 = 100\ \times 2{,}718^{-\frac{0}{734}}$
  $R\ G06 = 100\%$
- $R\ G07 = 100\ \times 2{,}718^{-\frac{0}{734}}$
  $R\ G07 = 100\%$
- $R\ G09 = 100\ \times 2{,}718^{-\frac{0}{734}}$
  $R\ G09 = 100\%$
- $R\ G11 = 100\ \times 2{,}718^{-\frac{0}{734}}$
  $R\ G11 = 100\%$
- $R\ G12 = 100\ \times 2{,}718^{-\frac{0}{734}}$
  $R\ G12 = 100\%$

Table 5. Generator Set Reliability Calculation Results for 2022

Genset 2022	Month												
	Jan	Feb	Mar	Apr	May	Jun	Jul	Aug	Sept	Oct	Nov	dec	Average
G2 (%)	100	100	100	100	100	100	100	100	100	100	100	100	100
G6 (%)	100	100	100	100	100	100	100	100	100	100	100	100	100
G7 (%)	100	100	100	100	100	100	100	100	100	100	100	100	100
G9 (%)	100	100	100	100	100	100	100	99.6	100	100	100	100	99.96
G11 (%)	100	100	100	100	100	100	99.7	100	100	99.7	99.4	100	99.90
G12 (%)	100	100	100	100	100	100	100	100	99.4	100	100	99.7	99.93

Information:
< 70% (Very frequent interruptions)
70%-95% (Frequent crashes)
≥ 90% (Rarely experience interference)

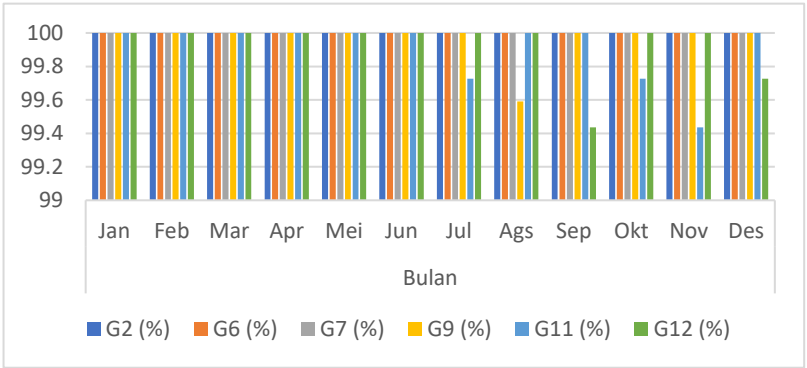

Figure 2. Generator set Reliability Graph for 2022

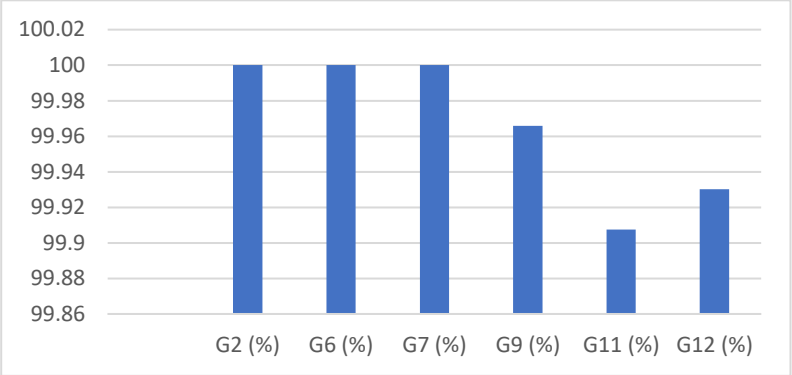

Figure 3. Graph of average Reliability of Generator sets in 2022

G. Availability

To calculate the level of availability of the generator set, data on the actual operating time of the generator set and the operating time of the generator set are required in 2022 based on (5).
Calculation of the level of availability of generator sets in January 2022

- $A\ G02 = \frac{734}{744} \times 100\% = 98.6\%$
- $A\ G06 = \frac{734}{744} \times 100\% = 98.6\%$
- $A\ G07 = \frac{734}{744} \times 100\% = 98.6\%$
- $A\ G09 = \frac{734}{744} \times 100\% = 98.6\%$
- $A\ G11 = \frac{734}{744} \times 100\% = 98.6\%$
- $A\ G12 = \frac{734}{744} \times 100\% = 98.6\%$

To find Generator Set Availability in February-December in 2022, the same calculation is carried out as the calculation above, the results are shown in table 6.

Table 6. Generator Set Availability Calculation Results for 2022

Genset 2022	**Month**											
	Jan	**Feb**	**Mar**	**Apr**	**May**	**Jun**	**Jul**	**Aug**	**Sept**	**Oct**	**Nov**	**dec**
G2 (%)	98.7	98.5	98.7	98.6	98.7	98.6	98.7	98.7	98.6	98.7	98.6	98.7
G6 (%)	98.7	98.5	98.7	98.6	98.7	98.6	98.7	98.7	98.6	98.7	98.6	98.7
G7 (%)	98.7	98.5	98.7	98.6	98.7	98.6	98.7	98.7	98.6	98.7	98.6	98.7
G9 (%)	98.7	98.5	98.7	98.6	98.7	98.6	98.7	98.3	98.6	98.7	98.6	98.7
G11 (%)	98.7	98.5	98.7	98.6	98.7	98.6	98.4	98.7	98.6	98.4	98.1	98.7
G12 (%)	98.7	98.5	98.7	98.6	98.7	98.6	98.7	98.7	98.1	98.7	98.6	98.4

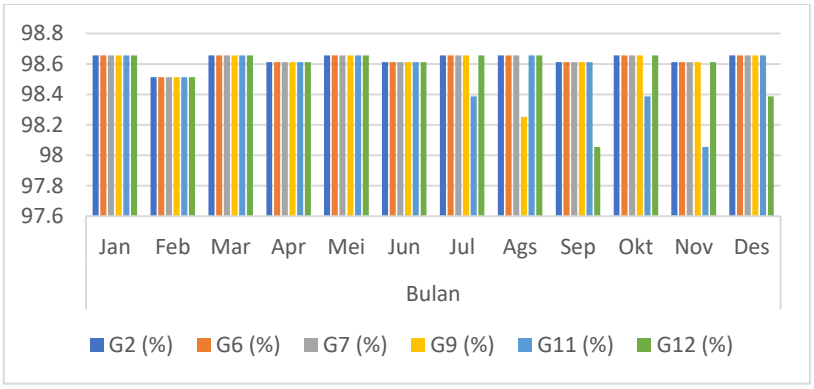

Figure 4. Graph of the level of availability of generator sets in 2022

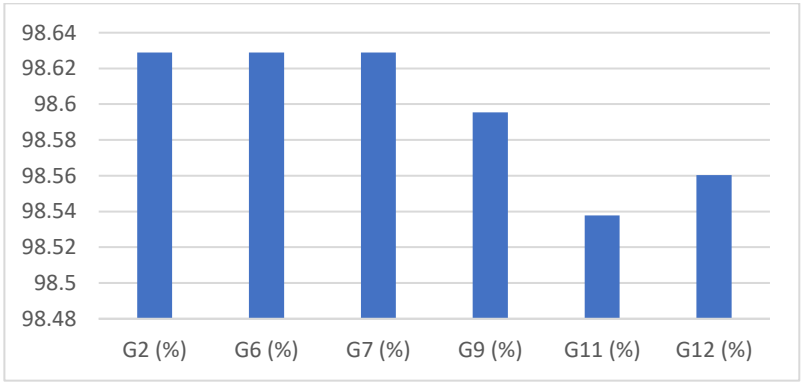

Figure 5. Graph of the average availability of generator sets in 2022

4. Conclusion

Generator set performance at PT. Intracawood Manufacturing is very reliable as a replacement or emergency supply when the power goes out. The average generator set reliability rate in 2022 has an average of 99%. The reliability level of the generator set is included in the group that rarely experiences disturbance or damage (R≥ 90%) and the average level of availability (*Reliability) of generator sets in 2022 is 98.5% and is included in the group that rarely experiences disturbances.*

References

[1] PLN, "Statistik PLN 2021," Indonesia, 2021. [Online]. Available: https://web.pln.co.id/statics/uploads/2022/03/Statistik-PLN-2021-Unaudited-21.2.22.pdf

[2] M. Ilmi, Junaidi, and A. Heidro, "Analisis Tekni-Ekonomis Generator Set (Genset) Sebagai Sumber Energi Listrik Cadangan Pada PT. Telekomunikasi Indonesia Tbk. Pontianak," *Universitas Tanjung Pura*. 2015.

[3] I. S. Tsauri and D. Hendarto, "Rancang Bangun Perangkat Automatic Transfer Switch (Ats) Genset 1 . 200 Va Sebagai Energi Listrik Cadangan," *J. Tek. Elektro Univ. Ibn Khaldun Bogor*, vol. 4, no. 2, pp. 1–10, 2017.

[4] Yusniati and Matondang NNS, "Analisis sistem pembebanan pada generator di PT.PLN (persero) pembangkit listrik tenaga diesel titi kuning," *Semnastek Uisu* , pp. 59–64, 2020.

[5] K. Tana, T. Provinsi, and K. Utara, "Analisis Pembagian Beban Generator Unit PLTD Desa Tana Merah," pp. 387–392, 2022.

[6] B. Pamungkas, Deni Rosiyanto. Bhirawa, W.T. dan Arianto, "Analisa Performansi Pemeliharaan Generator Set (Genset) dengan Metode TPM (Total Productive Maintanance) untuk Meningkatkan Kerja di PT. Lativi Media Karya," *Tek. Ind.*, vol. 8, no. 1, p. 5, 2019, [Online]. Available: https://journal.universitassuryadarma.ac.id/index.php/jtin/article/view/803

[7] B. SAPUTRO, "Analisis Keandalan Generator Set Sebagai Power Supply Darurat Apabila Power Supply Dari Pln Mendadak Padam Di Morodadi Poultry Shop Blitar," *J. Qua Tek.*, vol. 7, no. 2, pp. 17–25, 2017, doi: 10.35457/quateknika.v7i2.239.

[8] M. S. Siregar, J. Junaidi, A. Irwan, H. Ibrahim, and Novendis, "Analisis Pemeliharaan Berkala Dengan Kinerja Generator Set 670 KVA Dan 530 KVA di PT.Ramayana Sentosa Pematang Siantar," *SINERGI POLMED J. Ilm. Tek. Mesin*, vol. 6, no. 1, p. 103, 2022.

Biographies of Authors

Musmuliadi has been an Electrical Engineering student at Borneo Tarakan University since 2017. The author was born in Tawau July 26 1999. Before becoming a student the writer had completed his education in the Department of Computer and Network Engineering at Mutiara Bangsa Vocational School, Sebatik District, Nunukan Regency, North Kalimantan Province. Majoring in final project in the field of loading systems and generator dynamics in the field of expertise in electric power systems.

Ismit Mado Lecturer in Electrical Engineering since 2001. Graduated from the Doctoral Electrical Engineering Program at ITS Surabaya in 2019. Currently serves as Head of the Power System Stability Laboratory in the Electrical Engineering Department, Borneo Tarakan University. Interest in stability and control studies of power generation systems, studies of electric load forecasting based on time series models and fuzzy modeling.

Achmad Budiman, Lecturer in Electrical Engineering since 2022. Bachelor of Electrical Engineering, Gadjah Mada University, Yogyakarta and graduated in 2001. Master of Electrical Engineering, ITS Surabaya and graduated in 2010. Currently serves as Chair of the Electrical Engineering Department, Borneo Tarakan University. Study of the stability of the electric power distribution and transmission system.

Subarianto graduated from Electrical Engineering at SMK Negeri 2 Tarakan. Currently serves as Electrical Supervisor, Revinding and Generator at PT. Intracawood Manufacturing, Tarakan, North Kalimantan.

Agusthinus Rantepadang with a degree in electrical engineering, IKIP Ujung Pandang, Makassar. Currently serving as Foreman at PT. Intracawood Manufacturing, Tarakan, North Kalimantan.

Vol. 2, No. 2, October 2023, pp. 109-124
p-ISSN: 2963-8577
e-ISSN: 2964-3511
DOI: 10.57102/jescee.v2i2.67

RELIABILITY ANALYSIS OF PLTMG SYSTEM OPERATION PT PERTAMINA EP. BUNYU BASED ON LOAD LOSS PROBABILITY INDEX

Rendy Rusady[1*], Ismit Mado[2]
[1]Department of Electrical Engineering, Faculty of Engineering, Universitas Borneo Tarakan, North Kalimantan, Indonesia
[2]PLTMG PT Peramina EP Bunyu, Bunyu Island, [2]North Kalimantan, Indonesia

Abstract
Power plants are equipment used to generate electricity by converting an energy into electrical energy. In power plants, it is necessary to pay attention to the reliability of the generating system in meeting the needs of a load. The reliability of the generating system can be described by the plant reliability index. To pay attention to the reliability of the generating system, an analysis is needed that is used to evaluate the reliability index of the plant, one of which is Loss of Load Probability (LOLP). This study presents the calculation of the LOLP value at the PT Pertamina EP Bunyu PLTMG in 2022. In calculating the LOLP value, namely by using Microsoft Exel and Matrix laboratory simulation. PT Pertamina EP Bunyu PLTMG has 4 generating units with each capacity having a power of 1000 KW. The duration of disruption of the generating unit affects the Forced Outage Rate (FOR) value which will be used to find the probability of each combination of generating units. From this probability value, the LOLP value is obtained. At the PT Pertamina EP Bunyu PLTMG, the LOLP value is 0.00005579646% with an outage probability of 0.0203657079 days/year. While the standard set by PT PLN (Persero) in the 2018-2027 PLN RUPTL of LOLP is smaller than 0.274% or equivalent to a probability of outage of 1 day / year, it can be said that the reliability index of the power plant at PT Pertamina EP Bunyu PLTMG in 2022 is in the reliable category.

Keywords:
PLTMG; reliability; probability; LOLP

Article History:
Received: September 7th, 2023
Revised: October 7th, 2023
Accepted: October 21st, 2023
Published: October 31st, 2023

Corresponding Author:
Rendy Rusady
Department of Electrical Engineering, Universitas Borneo Tarakan, Indonesia
Email:
Rendyzeroseven51@gmail.com

1. Introduction

As time goes by, electricity is an energy needed for households and industries. There are industries that have their own power plants, for example PT Pertamina EP BUNYU. Where the generation system is independent of PT PLN (Persero), PT Pertamina EP Bunyu has 4 generating units, namely the Gas Engine Power Plant (PTMG). In the generation system, one of the important things to maintain is its reliability. In generation units, disturbances often occur. To minimize the disturbance, periodic maintenance is carried out or maintenance. The power in the system will decrease when several generating units occur simultaneously. This results in system outages and load loss.

The changing nature of the generating system load is accompanied by the characteristics of the electricity load which is increasing along with the development of technology, so the reliability of the generating system is increasingly needed to remain reliable in operation [1].

In the power generation system, the reliability of a power generation unit must be considered. Therefore, the calculation of the power plant reliability index is very important to ensure the availability of power. Loss of Load Probability (LOLP) is one of the methods used to calculate the reliability index [2].

LOLP LOLP describes the chances of load loss due to lack of available power in the system. Based on this, the author feels the need to conduct a study of this matter. Calculation and analysis of LOLP will be done manually and use the help of matrix laboratory software (MATLAB) to simulate the addition of generators to the PT Pertamina EP Bunyu PLTMG. Plant planning is simulated up to 1 year ahead with utilizing the Graphic User Interface (GUI) tool, making it easier to calculate and analyze system reliability.

2. Theory Foundation

A. Loss Of Load Probability (LOLP) Theory

LOLP is a reliability index that considers the chance of a plant when the system load exceeds the available generating capacity [3]. With the LOLP index, the company can make a target to determine the ability of the plant in the coming year, whether the plant can meet the load or not. High LOLP indicates a low plant reliability index, while a low LOLP indicates a high plant reliability index [4]. The LOLP reliability index is expressed in days per year. This figure shows the number of days that may occur per year, where the disturbance capacity of a system will be equal to or greater than the system's reserve capacity. Therefore, the value of the possible loss of load is the annual risk faced by the generating system in serving load demand [5]. The LOLP reliability index standard set by PT PLN (Persero) in the PLN 2018-2027 Electricity Supply Business Plan (RUPTL) is less than 0.274% or equivalent to 1 day/year [3].

$$LOLP = \sum_{t=1}^{t=365} \mathrm{P} \times t \quad (1)$$

Description:

P = Cumulative probability

t = Duration of Load Loss

A measure that states the value of a generating unit experiencing frequent interruptions is expressed by the Forced Outage Rate (FOR), namely: [3].

$$\mathrm{FOR} = \frac{\text{Number of unit hours disrupted}}{\text{Number of unit hours operating} + \text{Number of unit hours disrupted}} \quad (2)$$

The value of Forced Outage Rated (FOR) gives an understanding that the smaller the FOR, the higher the reliability assurance obtained, conversely the greater the FOR, the smaller the reliability assurance obtained.

B. LOLP (Lost of Load Probability)

The LOLP index is calculated by summing the length of time of disturbance against all possible loss of load in the period of a certain time. The LOLP index can be calculated using (1) [3].

$$LOLP = \sum_{n=1}^{i} P^i \times t^i \quad (3)$$

Description:
P : Cumulative probability of combination
t : Duration of load loss
n : Number of combinations
i : Combination index

C. Determining Plant Reliability

The reliability of units in electricity generation can be seen from the value influenced by various factors. These factors are often used as parameters in determining the reliability of the power generation system. The parameters include the following: [6].

Load Factor, which is the ratio between the magnitude of the average value in a certain time interval and the value of the load

1. Load Factor, which is the ratio between the average value in a given time interval and the peak load value in the same time period.
   $$\text{Load Factor} = \frac{\text{average load rate(MW)}}{\text{peak load(MW)}} x100\% \quad (4)$$
   The load factor shows the characteristics of the load, where the greater the load factor (100%), the flatter the system load, the better the reliability of the plant.

2. Availability Factor, which is the ratio of the amount of power available at a certain time period to the power installed in the system at the same time period.
   $$\text{Availability Factor} = \frac{installed\ power}{power\ available} x100\% \quad (5)$$

The availability factor shows the operating readiness of the generating unit in the system. The higher the availability factor (100%), the better the reliability of the generating unit.

3. Usage Factor, which is the ratio of the peak load value to the power installed in the system.
   Usage Factor = $\frac{\text{Peak Load}}{installed\ power} x100\%$ (6)
   The usage factor shows a large picture of the installed capability (installed power) in the installation that is utilized in terms of usage. When the usage factor has reached the value installed in the system, the usage factor shows the magnitude of the installed capability (installed power) in the installation that is utilized in terms of usage. When the usage factor has reached the value installed in the system.

4. Capacity Factor Capacity Factor (CF) shows how much a generating unit is utilized. The annual capacity factor (8760 hours) is defined as:
   CF = $\frac{Energy\ Production\ (MWh)\ In\ one\ day}{Capable\ Power\ (MW) x\ 24\ hours} x100\%$ (7)
   Capacity factor shows the utilization of energy utilization of the generating unit in one year from the production capability. The higher the capacity factor (100%), the better the reliability of the generating unit.

3. Methods

A. Data Collection

The process of collecting data that supports the completion of research is obtained from PT Pertamina EP Bunyu. The data obtained includes the duration of interference for each plant, operating hours for each plant, daily load for each plant and peak load data.

B. Research Stages

The author performs several stages that must be carried out as follows:

1. Conduct a literature study.
   Collecting some reference data as a reference for completing this research such as journals, books and other reference sources.
2. Data collection
   The data required in this study at PT Pertamina EP Bunyu for the past year. The data obtained includes the duration of interference each plant, operating hours of each plant, daily load of each plant and peak load data
3. Analyzing the reliability index based on the possibility of loss of load.
4. Calculating the reliability index value using Loss of Load Probability (LOLP). Of Load Probability (LOLP).
5. Take load data consisting of daily data, average daily load data and peak load data. Data and peak load data used as the basis for calculating the load factor. load factor whether it is in accordance with the PLN 2018-2027 RUPTL standard.
6. Making conclusions.

C. Stages of data processing

After the required data has been fulfilled, the calculation and analysis of the reliability index based on the probability of loss of load will be carried out as follows:

1. Data processing, After obtaining the required data, analyze the data and analyze the capacity of the generating system.
2. Performing FOR calculations to get the percentage of load loss and then adjusting to the PLN RUPTL standard value to measure the reliability index of each PLTMG unit.
3. Taking load data consisting of daily data, daily average load data and peak load data is used as a basis for calculating the PLTMG load factor whether it is in accordance with PLN RUPTL standards.
4. Calculate the availability factor, daily usage factor, daily capacity factor and outage factor.
5. From the results of load factor analysis, load availability factor, usage factor, capacity factor and outage factor. Furthermore, the reliability of the plant is calculated using LOLP.

4. Results and Discussion

A. Power Plant

Gas Engine Power Plant (PLTMG) is a power generation system managed by PT Pertamina EP. Bunyu which is used for Pertamina's distribution system, where PT Pertamina EP. Bunyu has 4 generating units. Where each generating unit has a maximum power capacity of 1000 KW so that the total installed power capacity of PT Pertamina EP. Bunyu amounted to 4000 KW.

B. System Data

The data used in this study uses power plant operation data for 2022, including

1. Power Capacity Data
   PT Pertamina EP. Bunyu has 4 power plant units, each with a capacity of 1000 KW, where the details of the data are shown in table 1.

Table 1. Generating Unit Data of PT Pertamina EP. Bunyu

No	Generator	Capacity (KW)
1.	Unit D	1000
2.	Unit E	1000
3.	Unit F	1000
4.	Unit G	1000

2. Forced Outage Rate (FOR) Data

The Forced Outage Rate (FOR) value at PT Pertamina EP. Bunyu is obtained from daily operating data, dividing the number of hours of disturbed generating units removed from the system by the number of hours of disturbed generating units from the system added to the number of hours the generating unit operates during the year. Obtained the FOR index of each unit of PT Pertamina EP. Bunyu during the year 2022 operates as in table 2.

Table 2. FOR Index of PT Pertamina EP. Bunyu Year 2022

Generator	FOR (%)	Innage Rate (%)
Unit D	0,032697	99,967
Unit E	0,031916	99,968
Unit F	0,028311	99,971
Unit G	0,027974	99,972

3. Load Data

The load data used as experimental data is using the plant operation data recorded in 2022, to calculate the factors that determine the reliability of the plant using parameters such as Load Factor, Availability Factor, Usage Factor, Capacity Factor and Loss of Load Probability (LOLP). November data will be used as experimental data in the calculation because it has the highest average load during 2022. November data has the highest load reaching 635 KW which can be seen in table 3.

Table 3. Load Data November 30, 2022

Hours	Load #D	Load #E	Load #F	Load #G	ROH #D	ROH #E	ROH #F	ROH #G	Total Load	Total ROH
01.00	389	472	390	393	750	750	750	750	1644	3000
02.00	343	409	416	418	750	750	750	750	1586	3000
03.00	400	422	396	390	750	750	750	750	1608	3000

Hours	Load #D	Load #E	Load #F	Load #G	ROH #D	ROH #E	ROH #F	ROH #G	Total Load	Total ROH
04.00	426	453	442	473	750	750	750	750	1794	3000
05.00	399	444	471	445	750	750	750	750	1759	3000
06.00	450	463	405	410	750	750	750	750	1728	3000
07.00	361	487	476	424	750	750	750	750	1748	3000
08.00	372	480	465	430	750	750	750	750	1747	3000
09.00	407	421	531	523	750	750	750	750	1882	3000
10.00	386	447	534	538	750	750	750	750	1905	3000
11.00	395	459	518	524	750	750	750	750	1896	3000
12.00	349	438	555	537	750	750	750	750	1879	3000
13.00	384	444	584	589	750	750	750	750	2001	3000
14.00	359	450	591	572	750	750	750	750	1972	3000
15.00	456	466	635	622	750	750	750	750	2179	3000
16.00	592	476	622	609	750	750	750	750	2299	3000
17.00	406	446	577	560	750	750	750	750	1989	3000
18.00	431	453	540	574	750	750	750	750	1998	3000
19.00	355	452	619	622	750	750	750	750	2048	3000
20.00	370	425	608	613	750	750	750	750	2016	3000
21.00	365	455	533	533	750	750	750	750	1886	3000
22.00	439	471	493	483	750	750	750	750	1886	3000
23.00	366	444	564	562	750	750	750	750	1936	3000
24.00	344	455	514	495	750	750	750	750	1808	3000

Table 4. Average Daily Load Data

No	Hours	Load #D(KW)	Load #E(KW)	Load #F(KW)	Load #G(KW)	Total Load (KW)
1	01.00	389	472	390	393	1644
2	02.00	343	409	416	418	1586
3	03.00	400	422	396	390	1608
4	04.00	426	453	442	473	1794
5	05.00	399	444	471	445	1759
6	06.00	450	463	405	410	1728
7	07.00	361	487	476	424	1748
8	08.00	372	480	465	430	1747
9	09.00	407	421	531	523	1882
10	10.00	386	447	534	538	1905
11	11.00	395	459	518	524	1896
12	12.00	349	438	555	537	1879
13	13.00	384	444	584	589	2001
14	14.00	359	450	591	572	1972
15	15.00	456	466	635	622	2179
16	16.00	592	476	622	609	2299
17	17.00	406	446	577	560	1989
18	18.00	431	453	540	574	1998

No	Hours	Load #D(KW)	Load #E(KW)	Load #F(KW)	Load #G(KW)	Total Load (KW)
19	19.00	355	452	619	622	2048
20	20.00	370	425	608	613	2016
21	21.00	365	455	533	533	1886
22	22.00	439	471	493	483	1886
23	23.00	366	444	564	562	1936
24	24.00	344	455	514	495	1808
Total						45194
Average Load						1883
Peak Load						2299

Table 5. Monthly Average and Peak Load Data

November 2022		
Date	Date Average Load (KW) Peak	Date Average Load (KW) Peak Load
1	1534	1794
2	1625	1782
3	1550	1768
4	1633	1848
5	1825	2077
6	1850	2069
7	1635	1903
8	1808	2005
9	1738	1558
10	1738	1897
11	1773	2062
12	1866	2036
13	1860	1976
14	1708	1910
15	1818	1994
16	1849	1971
17	1787	1930
18	1674	1779
19	1802	2067
20	1823	2023
21	1723	1922
22	1569	1855
23	1731	1929
24	1778	2002
25	1846	2040
26	1781	1998
27	1658	1826

November 2022		
Date	Date Average Load (KW) Peak	Date Average Load (KW) Peak Load
28	1810	2038
29	1886	2052
30	1883	2299

C. Calculation of Plant Loading

The load data table provides data that can be used in determining the reliability of the Power Plant through the following parameters.
Daily Load Factor.

1. Daily Load Factor

$$\text{Load Factor} = \frac{\text{Average Load(KW)}}{\text{Peak Load(KW)}} x100\%$$

$$\text{Load Factor} = \frac{1883\ \text{KW}}{2299\ \text{KW}} x100\%$$

Load Factor = 81.9%

The load factor describes the load distribution on the system, the greater the load factor (100%) the better the reliability of the plant, the PLN standard annual load factor ranges from 70% - 90%, [6]. but from the results of the above calculations obtained a value of 81.90%, meaning that from the load factor parameter the reliability level of PT Pertamina EP. Bunyu can be said to be still in the reliable category.

2. Daily Availability Factor

$$\text{Availability Factor} = \frac{\text{Available Power(KW)}}{\text{Installed Power(KW)}} x100\%$$

$$\text{Availability Factor} = \frac{3000\ \text{KW}}{4000\ \text{KW}} x100\%$$

Availability Factor = 75 %

The Availability Factor shows the operating readiness of the generating units in the system from the results of the above calculations obtained the value of the daily availability factor at PT Pertamina EP. Bunyu is 75%, where the more (80%), [6]. the value of the availability factor, the reliability of the generating unit can be categorized as good / reliable.

3. Daily Usage Factor

$$\text{Utilization Factor} = \frac{Peak\ Load}{Installed\ Power} x100\%$$

$$\text{Usage Factor} = \frac{2299}{4000} x100\%$$

Usage Factor= 57,4 %

The usage factor shows the ability of the installed power to be used. If the value of the usage factor is high, it means that the plant needs to be developed so as not to experience overload, meaning that the value of the usage factor of the PT Pertamina EP generating units. Bunyu which reaches a value of 57.4% can still be categorized as using a reliable unit.

4. Daily Capacity Factor

$$\text{CF} = \frac{\text{Energy Production (MWh)}\ In\ one\ day}{\text{Capable Power (MW)x 24 hours}} x100\%$$

$$\text{CF} = \frac{12.490\ \text{(KWh) in one day}}{4000\ \text{(KW)x 24 hours}} x100\%$$

CF = 74,9 %

The annual capacity factor above is 74.9%, where the capacity factor shows the energy utilization of the generating unit in a day from the production capability, the PLN standard for the generating capacity factor ranges from 70%-90%, [6]. from the calculation of the capacity factor of PT Pertamina EP. Bunyu shows that the plant is still in the reliable category.

D. LOLP Calculation Using Microsoft Exel Application

Table 6. PT Pertamina EP MHP Unit Data. Bunyu in 2022

No. Unit	Power (KW)	FOR	1-FOR
1	1000	0,032697	0,99967
2	1000	0,031916	0,99968
3	1000	0,028311	0,99971
4	1000	0,027974	0,99972

Table 7 Probability Calculation Results

	Operation/Disturbance Unit				Power	
No.					Outage	Probability
	P1	P2	P3	P4		
1	0	0	0	0	0	0,998780557
2	0	0	0	1	1000	0,027947713
3	0	0	1	0	1000	0,028284679
4	0	1	0	0	1000	0,031887284
5	1	0	0	0	1000	0,032667908
6	1	0	1	0	2000	0,000925129
7	0	1	0	1	2000	0,000892265
8	0	1	1	0	2000	0,000903023
9	1	1	0	0	2000	0,001042963
10	1	0	0	1	2000	0,000914108
11	0	0	1	1	2000	0,000791457
12	1	1	1	0	3000	2,95359E-05
13	1	1	0	1	3000	2,9184E-05
14	1	0	1	1	3000	2,58868E-05
15	0	1	1	1	3000	2,52682E-05
16	1	1	1	1	4000	8,26468E-07
Total						1

Description:
0 states the unit is operating
1 denotes unit fault
Probability Formula with Microsoft Excel
No.1
=(IF(B4=1;L2;M2)*(IF(C4=1;L3;M3))*(IF(D4=1;L4;M4)*(IF(E4=1;L5;M5))))
No.2

=(IF(B5=1;L2;M2)*(IF(C5=1;L3;M3))*(IF(D5=1;L4;M4)*(IF(E5=1;L5;M5))))
No.3
=(IF(B6=1;L2;M2)*(IF(C6=1;L3;M3))*(IF(D6=1;L4;M4)*(IF(E6=1;L5;M5))))
No.4
=(IF(B7=1;L2;M2)*(IF(C7=1;L3;M3))*(IF(D7=1;L4;M4)*(IF(E7=1;L5;M5))))
No.5
=(IF(B8=1;L2;M2)*(IF(C8=1;L3;M3))*(IF(D8=1;L4;M4)*(IF(E8=1;L5;M5))))
No.6
=(IF(B9=1;L2;M2)*(IF(C9=1;L3;M3))*(IF(D9=1;L4;M4)*(IF(E9=1;L5;M5))))
No.7
=(IF(B10=1;L2;M2)*(IF(C10=1;L3;M3))*(IF(D10=1;L4;M4)*(IF(E10=1;L5;M5))))
No.8
=(IF(B11=1;L2;M2)*(IF(C11=1;L3;M3))*(IF(D11=1;L4;M4)*(IF(E11=1;L5;M5))))
No.9
=(IF(B12=1;L2;M2)*(IF(C12=1;L3;M3))*(IF(D12=1;L4;M4)*(IF(E12=1;L5;M5))))
No.10
=(IF(B13=1;L2;M2)*(IF(C13=1;L3;M3))*(IF(D13=1;L4;M4)*(IF(E13=1;L5;M5))))
No.11
=(IF(B14=1;L2;M2)*(IF(C14=1;L3;M3))*(IF(D14=1;L4;M4)*(IF(E14=1;L5;M5))))
No.12
=(IF(B15=1;L2;M2)*(IF(C15=1;L3;M3))*(IF(D15=1;L4;M4)*(IF(E15=1;L5;M5))))
No.13
=(IF(B16=1;L2;M2)*(IF(C16=1;L3;M3))*(IF(D16=1;L4;M4)*(IF(E16=1;L5;M5))))
No.14
=(IF(B17=1;L2;M2)*(IF(C17=1;L3;M3))*(IF(D17=1;L4;M4)*(IF(E17=1;L5;M5))))
No.15
=(IF(B18=1;L2;M2)*(IF(C18=1;L3;M3))*(IF(D18=1;L4;M4)*(IF(E18=1;L5;M5))))
No.16
=(IF(B19=1;L2;M2)*(IF(C19=1;L3;M3))*(IF(D19=1;L4;M4)*(IF(E19=1;L5;M5))))

The definition of the Formula above is as follows.

=(IF(P1=1,FOR_P1,1-FOR_P1)*(IF(P2=1,FOR_P2,1-FOR_P2))*(IF(P3=1, FOR_P3,1-FOR_P3))*(IF(P4=1,FOR_P4,1-FOR_P4))

This means that if the Unit 1 generator is binary 1 will enter the FOR value for the unit 1 generator otherwise the 1-FOR (innage rate) value of the unit 1 generator will be entered multiplied if the unit 2 generator is binary 1 will enter the FOR value for the unit 2 generator otherwise the 1-FOR value of the unit 2 generator will be entered multiplied if the unit 3 generator is binary 1 will enter the FOR value for the unit 3 generator otherwise the 1-FOR value of the unit 3 generator will be entered multiplied if the unit 4 generator is binary 1 will enter the FOR value for the unit 4 generator otherwise the 1-FOR value of the unit 4 generator will be entered.

Table 8. LOLP Calculation Results

No.	Power Available	Power Available	Probability	LOLP
1	4000	0	0,998780557	0
2	3000	1000	0,027947713	0
3	3000	1000	0,028284679	0
4	3000	1000	0,031887284	0
5	3000	1000	0,032667908	0
6	2000	2000	0,000925129	0,000925129

7	2000	2000	0,000892265	0,000892265
8	2000	2000	0,000903023	0,000903023
9	2000	2000	0,001042963	0,001042963
10	2000	2000	0,000914108	0,000914108
11	2000	2000	0,000791457	0,000791457
12	1000	3000	2,95E-05	2,95359E-05
13	1000	3000	2,92E-05	0,000029184
14	1000	3000	2,59E-05	2,58868E-05
15	1000	3000	2,53E-05	2,52682E-05
16	0	4000	8,26E-07	8,26468E-07
Total LOLP				0,005579646

LOLP Calculation Formula with Microsoft Excel
No.1
=IF(B3<=C3;D3;0)
No.2
=IF(B4<=C4;D4;0)
No.3
=IF(B5<=C5;D5;0)
No.4
=IF(B6<=C6;D6;0)
No.5
=IF(B7<=C7;D7;0)
No.6
=IF(B8<=C8;D8;0)
No.7
=IF(B9<=C9;D9;0)
No.8
=IF(B10<=C10;D10;0)
No.9
=IF(B11<=C11;D11;0)
No.10
=IF(B12<=C12;D12;0)
No.11
=IF(B13<=C13;D13;0)
No.12
=IF(B14<=C14;D14;0)
No.13
=IF(B15<=C15;D15;0)
No.14
=IF(B16<=C16;D16;0)
No.15
=IF(B17<=C17;D17;0)
No.16
=IF(B18<=C18;D18;0)
The meaning of the formula above is as follows.

=IF(Power Reserve<= Outage Power, Probability Value,0)

This means that if the power reserve value is smaller or equal to the outage power value, it will be equal to the probability value, but otherwise it will be zero (0).

 p-ISSN: 2963-8577
e-ISSN: 2964-3511

E. Calculation of Annual LOLE Reliability Index Using Microsoft Exel

$$LOLP = \sum probabilitas\ capacity\ in\ <\ Load$$

$LOLP$ = 0+0+0+0+0+0,000925129+0,000892265+0,000903023
+0,001042963+0,000914108+0,000791457+0,000025359+0,000029184+0,0000258868
+0,0000252682+0,000000826468

$LOLP$ = 0,005579646 / 100

$LOLP$ = 0,00005579646 %

$LOLE = LOLP \times 365\ days/year$

$LOLE$ = 0,00005579646 × 365 $days/year$

$LOLE$ = 0,0203657079 $days/year$

F. LOLP Calculation using Matlab Application

1. Program Design

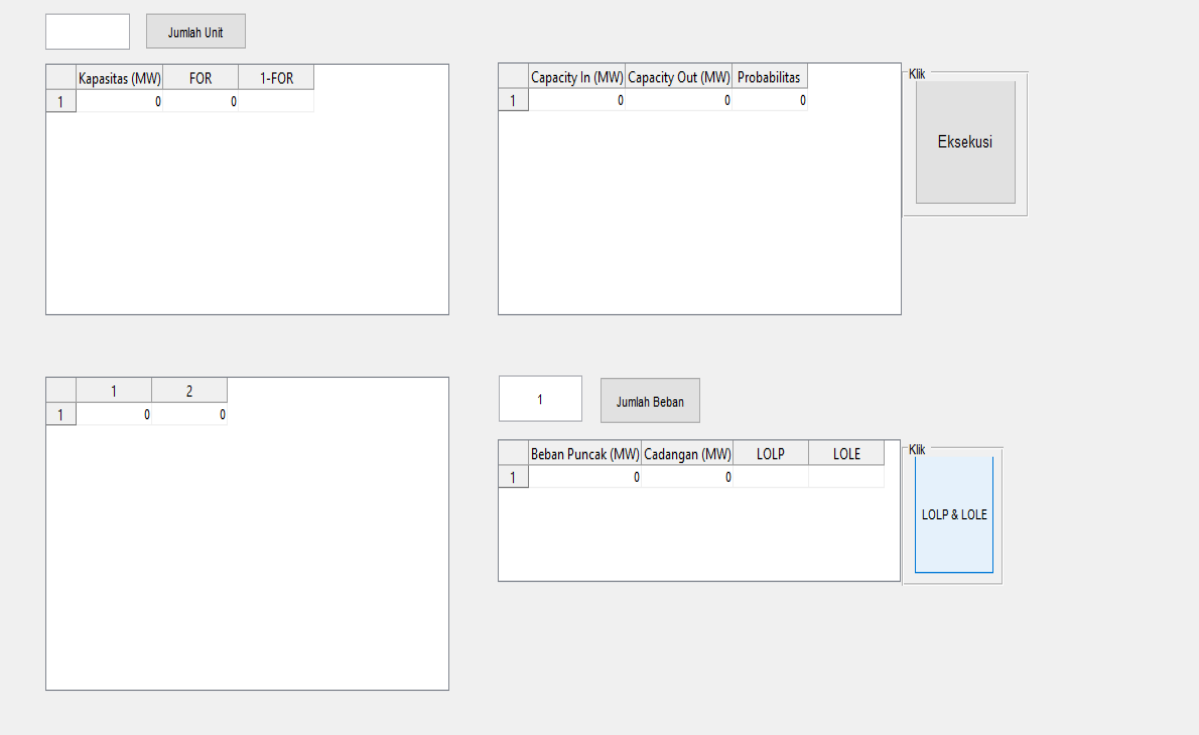

Figure 1. Initial View of the LOLP GUI

```
data = get(handles.uitable1, 'data')
data= [0 0];
set(handles.uitable1, 'data',data);
 data = get(handles.uitable2, 'data')
data= [0 0];
set(handles.uitable2, 'data',data);
data = get(handles.uitable3, 'data')
data= [0 0];
set(handles.uitable3, 'data',data);
data = get(handles.uitable5, 'data')
data= [0 0 0];
set(handles.uitable5, 'data',data);
```

The coding program above is a program that is used to display the initial numbers when the program is run.

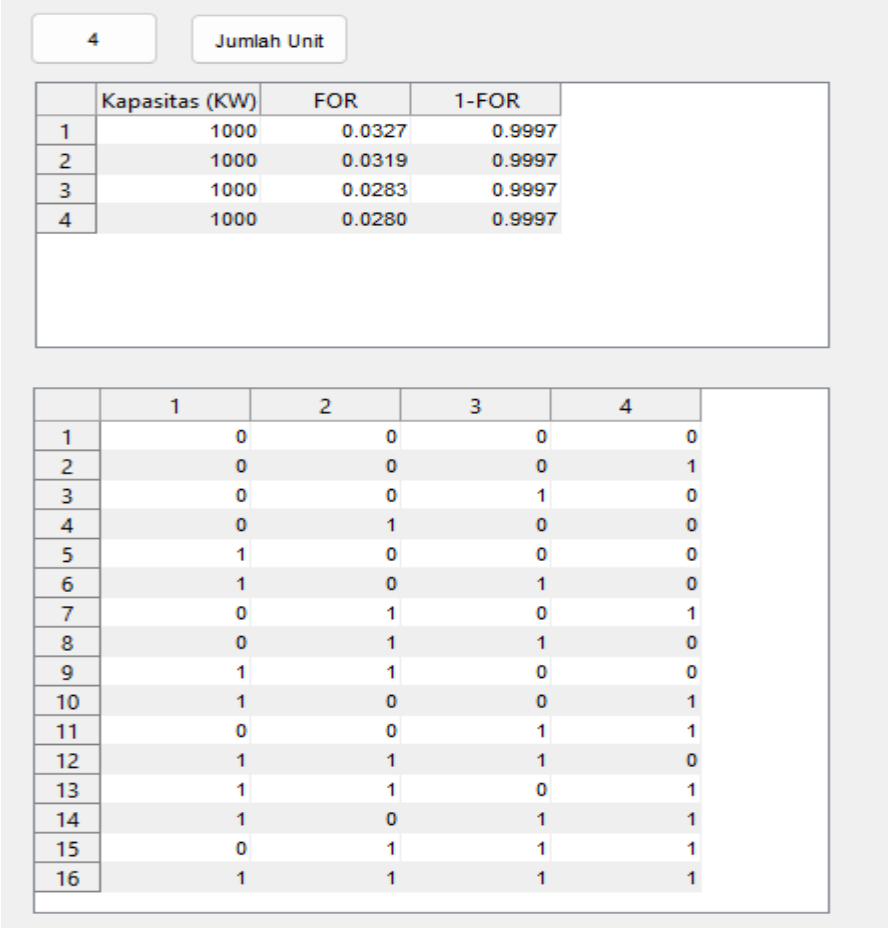

4 Jumlah Unit

	Kapasitas (KW)	FOR	1-FOR
1	1000	0.0327	0.9997
2	1000	0.0319	0.9997
3	1000	0.0283	0.9997
4	1000	0.0280	0.9997

	1	2	3	4
1	0	0	0	0
2	0	0	0	1
3	0	0	1	0
4	0	1	0	0
5	1	0	0	0
6	1	0	1	0
7	0	1	0	1
8	0	1	1	0
9	1	1	0	0
10	1	0	0	1
11	0	0	1	1
12	1	1	1	0
13	1	1	0	1
14	1	0	1	1
15	0	1	1	1
16	1	1	1	1

Figure 2. Many Generators and Binary Disturbance Probability

```
baris =str2num(get(findobj(gcf,'Tag','edit1'),'string'));
data = get(handles.uitable1, 'data');
data(baris,:)=0;
data_1(2^baris,:)=0
set(handles.uitable1,'data',data);
set(handles.uitable5,'data',data_1);

derett=(0:((2^baris)-1))
probb=de2bi(derett)
set(handles.uitable2,'data',probb);
```

The program function above displays the number of plants and displays the number of possible plants experiencing interference in binary form.

 p-ISSN: 2963-8577
e-ISSN: 2964-3511

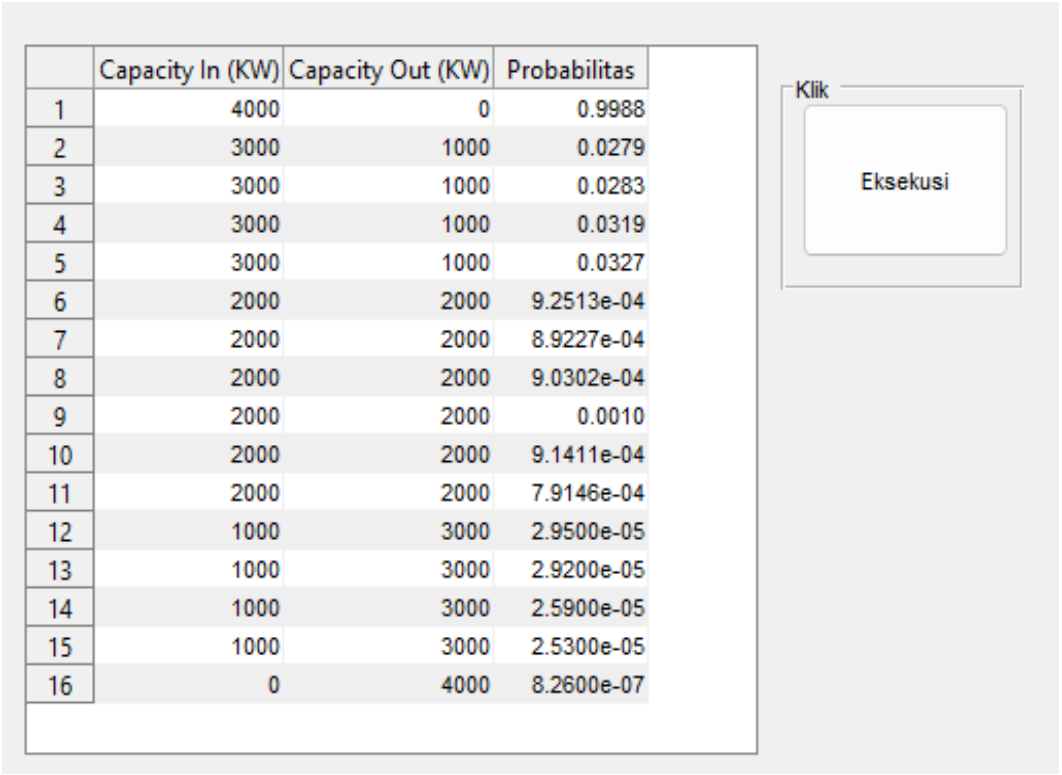

	Capacity In (KW)	Capacity Out (KW)	Probabilitas
1	4000	0	0.9988
2	3000	1000	0.0279
3	3000	1000	0.0283
4	3000	1000	0.0319
5	3000	1000	0.0327
6	2000	2000	9.2513e-04
7	2000	2000	8.9227e-04
8	2000	2000	9.0302e-04
9	2000	2000	0.0010
10	2000	2000	9.1411e-04
11	2000	2000	7.9146e-04
12	1000	3000	2.9500e-05
13	1000	3000	2.9200e-05
14	1000	3000	2.5900e-05
15	1000	3000	2.5300e-05
16	0	4000	8.2600e-07

Figure 3. Probability of Plant Disruption

```
baris =str2num(get(findobj(gcf,'Tag','edit1'),'string'));
data = get(handles.uitable1, 'data');
daya = get(handles.uitable5, 'data');
biner_pembangkit = get(handles.uitable2, 'data');
data(:,4)=1-data(:,2);
set(handles.uitable1,'data',data);
for c=1 : 1 : (2^baris) % baris
        for d=1 : 1 : baris % kolom
          if biner_pembangkit(c,d)==0
        hd=data(d,2);
        else
 hd=data(d,4);
       end
matriks(c,d)=hd;
       end
         end
         daya(:,4)= sum(data(:,1))-daya(:,1);
         daya(:,3)=prod(matriks,2);
         daya(:,1)=mtimes(biner_pembangkit,data(:,1));
         daya(:,2)= sum(data(:,1))-daya(:,1);
set(handles.uitable5,'data',daya);
```

The function of the above coding program is to generate a probability of on each possibility of the plant experiencing interference

2. Calculation of the annual LOLE reliability index using Matlab

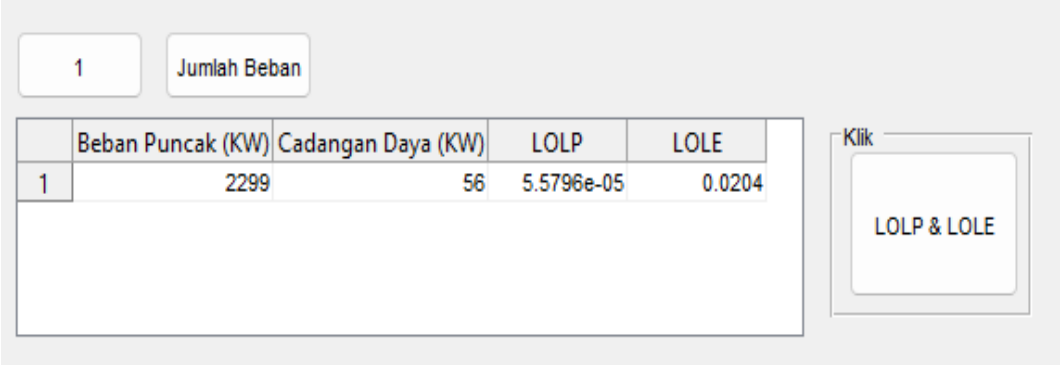

Figure 4. Display of LOLP and LOLE results

```
baris1 =str2num(get(findobj(gcf,'Tag','edit2'),'string'));
daya = get(handles.uitable1, 'data');
daya_beban(baris1,:)=0;
set(handles.uitable3,'data',daya_beban);
Program code to display the load data to be entered
line =str2num(get(findobj(gcf,'Tag','edit1'),'string'));
data = get(handles.uitable1,'data');
power = get(handles.uitable5,'data');
load = get(handles.uitable3, 'data');
binary-generator = get(handles.uitable2, 'data');
row1 =str2num(get(findobj(gcf,'Tag','edit2'),'string'))
peak_load=sum(data)
load(:,2)=peak_load(1,1)-load(:,1)
set(handles.uitable3,'data',load)
for u=1 : 1 : row1 % load row
for t=1 : 1 : (2^row) % probability row
     if power(t,1)<=load(u,1)
       demand=power(t,3)
     else
       demand=0
end
      power_matrix(u,t)=demand
   end
end
load(:,3)=sum(matrix_power,2)
load(:,4)=load(:,3)*365
set(handles.uitable3,'data',load)
```

Program coding to generate LOLE values and LOLP values from the load data entered. Program coding is a language command used to direct the computer to work according to our wishes. In this case the command that is addressed is to calculate the value of LOLP in Matlab from the operating data of the PT Pertamina EP PLTMG plant. Bunyu in 2022.

1. set(handles.uitable1, 'data',data);
This program states that the data to be displayed, namely the data named "data", will be placed in uitable 1.
2. line =str2num(get(findobj(gcf,'Tag','edit1'),'string'));
This program declares that string format (word format) is converted to
into the number format and the variable to be
is taken from the tag number in edit1.
probb=de2bi(derett)
This program code tells the definition of probb as a variable
that comes from a decimal sequence number to be converted into a binary number.
binary number.
4. data(:,3)=1-data(:,2);

This program tells the contents of the data matrix all rows of column 3
equal to one minus all rows in column 2 (1FOR calculation).
5. power(:,1)=mtimes(binary-generator,data(:,1));
This program expresses that power in all rows of column 1 is multiplication of the data from the binary generator with the data value in the data "(:,1)".

3. Program Simulation
Simulation of 4 Generating Units

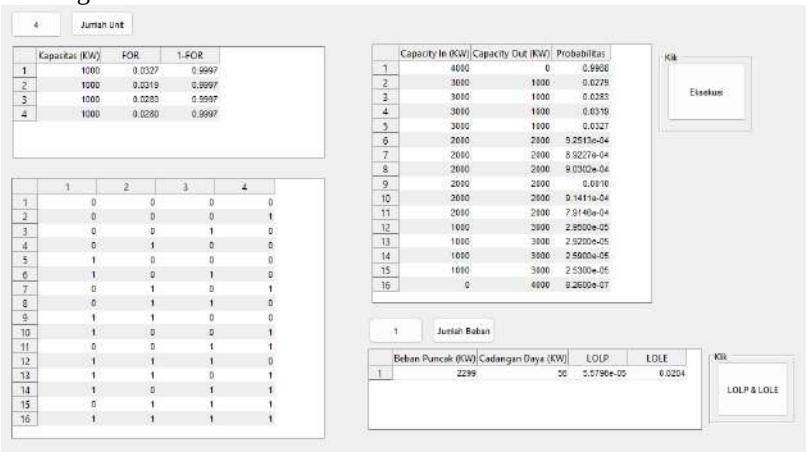

Figure 5. LOLP Results of 4 Generating Units

From the results of the calculation using the Matlab application program above, the LOLP result is 0.00005579646 and LOLE is 0.0203657079 days / year where these results have the same value as doing manual calculations using Microsoft Excel, namely LOLP 0.00005579646 and LOLE 0.0203657079, in this case it means that calculating LOLP can use Microsoft Excel and Matlab applications because they have the same results but the results of the matlab program have a higher level of accuracy. in Microsoft Excel there will also be weaknesses when you want to calculate LOLP with more generating capacity, in Microsoft Excel you have to use a different formula and the addition of binary probabilities will double and the occurrence of human error is higher in making the formula, Microsoft Excel will also find weaknesses when you want to calculate LOLP with more generating capacity, in Microsoft Excel you have to use a different formula and the addition of binary probabilities will multiply and the occurrence of human error is higher in making the formula. The LOLP and LOLE values obtained are smaller than the standards set by the 2018-2025 PLN RUPTL, namely LOLP < 0.274% and LOLE < 0.274%. Reserve margin = 40%, where the simulation of 4 plants against a peak load of 2299 KW is worth LOLP = 0.00005579646 and LOLE = 0.0203657079 days / year, respectively, meaning that the PT Pertamina EP Bunyu plant is good and can be categorized as reliable.

5. Conclusion

A. From the results of the calculation of the reliability of the plant using the LOLP index, the reliability value of the PT Pertamina EP plant is obtained. Bunyu with a Loss of Load Probability (LOLP) value of 0.00005579646% with an outage probability of 0.0203657079 days a year due to the availability of PT Pertamina EP Bunyu's power plant of 75% which can be categorized as good and reliable.
B. The results of the analysis of the calculation value of the reliability of the PT Pertamina EP plant. Bunyu in 2022 shows that the reliability of the plant can be categorized as reliable because it is in accordance with the reliability criteria used, namely LOLP is smaller than 0.274% or equivalent to a probability of outage of 1 day / year based on PT PLN's RUPTL in the Decree of the Minister and Energy and Mineral Resources of the Republic of Indonesia Number 1567 K/21 / MEM / 2018 RUPTL 2018-2027.

References

[1] U. Albab, D. Y. Sukma, and K. H. Binawidya Jl Soebrantas Km, "Upaya Peningkatan Indeks Keandalan Sistem Pembangkit dengan Peningkatan Kapasitas Sistem Pembangkit," *Jom FTEKNIK*, vol. 6, no. 2, pp. 1–6, 2019.
[2] R. M. AKBAR, "Studi Analisa Indeks Keandalan Menggunakan Analisa Perhitungan Eens (Expected Energy Not Supplied) Pada Pembangkit Listrik Tenaga Uap (Pltu) Pt. Pjb Up Gresik," *Http://Eprints.Umm.Ac.Id/*, vol. 1, no. 2, pp. 96–107, 2020, [Online]. Available: http://eprints.umm.ac.id/54456/
[3] R. Apriani and R. Thayib, "Perhitungan Loss of Load Probability (Probabilitas Kehilangan Beban) Sistem Tenaga Listrik Di Pt.Pupuk Sriwidjaja," *2355 - 0457* , vol. 2, no. 1, pp. 22–37, 2015.
[4] A. A. P. Yulius Indra Kurniawan, "Loss of Load Probability (LOLP) Index untuk Menganalisis Keandalan Pembangkit Listrik," *Pros. Semin. Nasioanl Mat. dan Pendidik. Mat. UMS*, pp. 582–588, 2015.
[5] V. Pillai, "Loss of Load Probability of a Power System Fundam," *J. Fundam. Renew. Energy Appl.*, vol. 5, no. 1, pp. 1–9, 2015, doi: 10.4172/20904541.1000149.
[6] D. Marsudi, "Daftar Isi Daftar Isi :," no. April, pp. 2–5, 2009.

Biographies of Authors

Rendy Rusady is an Electrical Engineering Student at Universitas Borneo Tarakan in 2018. The author was born in Bunyu Island on February 05, 2000. Before becoming a student, the author had completed his education at SMK Negeri 1 Bunyu

Ismit Mado graduated from the Doctoral Program at ITS Surabaya in 2019. Currently, He is the Head of Power System Stability Laboratory at the Department of Electrical Engineering, Universitas Borneo Tarakan. He is interested in stability and control studies of power generation systems, forecasting studies based on time series models, and fuzzy modeling.

Vol. 2, No. 2, October 2023, pp. 125-130
p-ISSN: 2963-8577
e-ISSN: 2964-3511
DOI: 10.57102/jescee.v2i2.68

JESCEE
Journal of Emerging Supply Chain, Clean Energy, and Process Engineering

TRANSPARENCY AND THERMAL STABILITY OF SILICA AEROGEL SYNTHESIZED FROM SODIUM SILICATE USING AMBIENT PRESSURE DRYING

Egiana Reshi Hardiane[1], Gita Evi Monika Purba[1], Ayu Dahliyanti[1*]
[1]Department of Chemical Engineering, Universitas Pertamina, Simprug, Kebayoran Lama, South Jakarta, Indonesia, 12220.

Abstract
Silica aerogel is a special material due to its low density, high transparency, and high thermal stability. Producing silica aerogels in an inexpensive and environmentally friendly way is the focus of recent research. Here, silica aerogel is synthesized from sodium silicate as silica source and surface modification with organosilanes, followed by ambient pressure drying at various conditions. The resulting aerogels were analyzed for their density, transparency, and thermal stability. Silica aerogel with a low density of 0.4031 g/cm^3 was successfully synthesized with polydimethylsiloxane (PDMS) as modifying agent at 7:50 solvent ratio. The aerogel can withstand heat up to 400°C.This shows the potential of aerogel to be applied as thermal insulator in various fields.

Keywords:
Silica aerogel; sodium silicate; ambient pressure drying; thermal stability

Article History:
Received: September 29th, 2023
Revised: October 13th, 2023
Accepted: October 27th, 2023
Published: October 31st, 2023

Corresponding Author:
Ayu Dahliyanti
Department of Chemical Engineering, Universitas Pertamina, Indonesia
Email:
ayu.dahliyanti@universitaspertamina.ac.id

1. Introduction

Silica aerogel is a solid material that is lightweight, highly porous (nanoporous), non-flammable, and amorphous [1]. Aerogel has a high visual transmission up to 90-99%, low thermal conductivity of 0.004-0.03 W/m.K, low density of 0.01-0.35 g/cm³ and high surface area of around 1600 m²/g [2]. Due to its remarkable properties, silica aerogel has been applied as an adsorbent, catalyst, and thermal insulator [2]. Silica aerogel also has uses in other fields, such as aerospace. In 2005, NASA prepared the use of aerogel as a thermal protection system for Venus spacecraft [3]. Silica aerogel has been developed to be used as transparent window material and wall insulation [4].

Generally, there are two groups of material that are often used as silica aerogel precursors, alkoxide and sodium silicate. The types of alkoxides commonly used consist of Tetraethyl Orthosilicate (TEOS) and Tetramethyl Orthosilicate (TMOS). However, alkoxides are mostly expensive, difficult to obtain, and toxic [5]. Sodium silicate (waterglass) is an alternative raw material that can be used because it contains silica as much as 86.4% by mass [6]. Sodium silicate can produce silica aerogel with large porosity and is more readily available, environmentally friendly, cheaper and has almost the same level of stability as TEOS [7].

The basic technique of silica aerogel synthesis begins with the creation of sol from sodium silicate and an addition of acid or base catalyst. The sol is then aged to form a hydrogel and washed to remove contaminants that are still present. The hydrogel is then dried by the ambient pressure drying method to obtain aerogel [8]. There are several common methods that are often used in the silica aerogel drying process, such as supercritical drying, freeze drying, and ambient pressure drying. Supercritical drying is quite impractical due to its particular temperature and pressure, therefore it is difficult to apply commercially [9]. Freeze drying needs the addition of specific eutectics, solvents, and polymers [7]. Ambient pressure drying is safer because it operates at ambient pressure and low production costs [10]. Silica aerogel must go through a cationic exchange process as well as solvent exchange and surface modification before being dried at ambient pressure conditions.

Strengthening the gel structure beforehand to prevent cracking and rupture is important during the ambient pressure drying process. This can be achieved through surface modification with the help of silane compounds as silylating agents. The previous research which used Hexamethyldisilazane (HMDS), produced silica aerogel with a density 0.15 g/cm³, surface area of 746 m²/g, and porosity of 93% [11]. Whereas the use of Trimethylchlorosilane (TMCS) produces silica aerogel with a density of 0.071 g/cm³, a surface area of 945.8 m²/g and a pore size of 3.8

nm [8]. Polydimethylsiloxane (PDMS) can also be used as a modifying agent to produce silica aerogel with a density of 0.03099 g/cm³, a surface area of 574.38 m²/g, and high porosity [12].

In this study, we compare the effects of different silylating agents and its concentration on the yield, transparency, and thermal stability of silica aerogels synthesized from sodium silicate via sol-gel and ambient pressure drying. Through this research, we hope to investigate the optimum synthesize conditions as an effort to manufacture thermal insulators that have transparent optical properties.

2. Experimental Section

A. Resin activation

The resin was soaked in aquadest for 24 hours before being drained and then immersed in 37% HCl with a resin to HCl mass ratio of 1: 1 for 24 hours. Next, the resin was separated from the solution and washed with aquadest to remove excess HCl. The resin was patted using a tissue to make sure that there was no aquadest left.

B. Silica sol-gel formation

The sodium silicate solution (4%, 6%, and 8%) was mixed with an activated cationic resin with a mass ratio of 1: 2 accompanied by stirring to carry out the ion exchange process. The H^+ ion of the activated cationic resin replaces the Na^+ ion so that the pH of the solution becomes 1-2. Ammonium hydroxide 1 M was then added to the solution dropwise until a stable silica colloid is formed at pH 5. For another mass concentration of 6%, without the addition of resin, HCl as an acid catalyst was added to reach a specified pH. After that, the colloids were poured into silicone molds. Then ethanol was added to a total of 15 ml. When a cloud had formed in the center of the solution, it indicated that sol had been reached. Then it was tightly closed using parafilm paper for 12 h aging process at 45°C in the incubator shaker to form a solid hydrogel.

C. Surface modification and ambient pressure drying

After 12 h of aging, hydrogel was obtained. First, the hydrogel should be soaked with pure n-hexane solvent for 12 h inside the silicone mold to stimulate the formation of pore. The solvent exchange process was carried out 2 times. Then, the silylating agent (TMCS, HMDS, and PDMS) that had been dissolved in n-hexane with volume variations of 4:50 and 7:50 were mixed with hydrogel to be sonicated for 12 hours. The resulting gels were then dried with a gradual heating temperature of 60°C for 2 h followed by 100°C for the next 2 h.

D. Characterization

Tapped density measurements were performed using measuring glass. The transparency of silica aerogels was analyzed using Jasco V-750UV-Visible (UV-Vis) Spectrophotometer. Thermal stability was investigated using SDT650 TA Instruments Thermogravimetric analyzer (TGA). Yield of silica aerogels was calculated using the following equations:

$$\%\ yield\ silica\ aerogel = \frac{silica\ aerogel\ mass}{(sodium\ silicate\ mass + silylating\ agent\ mass)}\ x\ 100\% \quad (1)$$

3. Result and Discussion

The yield of silica aerogel at various synthesis conditions are shown in Table 1. The volume of silylating agent is directly proportional to the yield of silica aerogel. The yield of silica aerogel with TMCS 7:50 is higher than TMCS 4:50, which are 12.946 % and 14.306%. At the same ratio of silylating agent, HMDS has a higher yield (17.249%) compared to TMCS and PDMS due to the larger number of alkyl groups that can be substituted. The yield of silica aerogel is also directly proportional to the mass concentration of sodium silicate. However, without resin the yield drops because there are still sodium ions inside the solution during sol-gel process which hinder the formation of silica hydrogel.

Table 1. Yield of silica aerogel at various synthesis conditions

Silylating agent	Silylating agent to n-hexane ratio	Sodium silicate concentration	Yield
TMCS	4:50	6 %	12.946 %
TMCS	7:50	4%	3.060 %
TMCS	7:50	6 %	14.306%
TMCS	7:50	6 % without resin	6.379 %
TMCS	7:50	8%	23.720 %
HMDS	7:50	6 %	17.249%

PDMS	7:50	6 %	8.651%

Table 2. Density of silica aerogels at various synthesis conditions

Silylating agent	**Silylating agent to n-hexane ratio**	**Sodium silicate concentration**	**Density (g/cm^3)**
TMCS	4:50	6 %	0.4760±0.010
TMCS	7:50	4%	1.174±0.100
TMCS	7:50	6 %	0.7631±0.211
TMCS	7:50	6 % without resin	0.480±0.1
TMCS	7:50	8%	0.579±0.1
HMDS	7:50	6 %	0.5445±0.011
PDMS	7:50	6 %	0.4031±0.002

Silica aerogel is a solid with low density characteristics, between 0.032- 1.154 g/cm³ [1][2]. From Table 2, it can be concluded that silica aerogels with low density have successfully synthesized, except the one obtained from 4% sodium silicate concentration. At the same silylating agent ratio and sodium silicate concentration, PDMS produces the lowest density (0.4031±0.002 g/cm^3) compared to HMDS (0.5445±0.011 g/cm^3) and TMCS (0.7631±0.211 g/cm^3), although the values are not significantly different. Alkyl ($-CH_3$) groups in the silylating agents will modify the surface of aerogel to be superhydrophobic. Therefore, it will experience less shrinkage during ambient pressure drying which results in lower density.

Fig. 1 (a) shows the effect of silylating agent type and ratio on silica aerogel transmittance. The addition of silylating agent aims to maintain the integrity of pore structure when the drying process takes place. The more alkyl groups substituted, the less shrinkage happens. Thus, silica aerogel will be filled with air which makes it has a high transmittance [13]. The transmittance of aerogels in UV-Visible spectrum increases as the volume of the silylating agent increases. It can be proven by comparing the maximum transmittance value at 4:50 and 7:50 ratios which are 6.4531% and 13.8877% at a wavelength of 420 nm, respectively. HMDS and TMCS aerogels show better performance than PDMS. The transmittance of HMDS is higher due to its slow reaction rate with the silica surface which leads to the formation of aerogels with small pore size [14].

In terms of sodium silicate concentration, 6% with resin addition also gives better transmittance compared to 4% and 8% as can be seen in Fig. 1 (b). At the same concentration of 6%, silica aerogel without resin exchange has lower transmittance due to the presence of sodium ions which remain trapped in the structure. However, the transmittance of all aerogel samples is generally still low (<20%), therefore optimization in the synthesis parameters is needed if they are going to be applied as transparent insulation material.

p-ISSN: 2963-8577
e-ISSN: 2964-3511

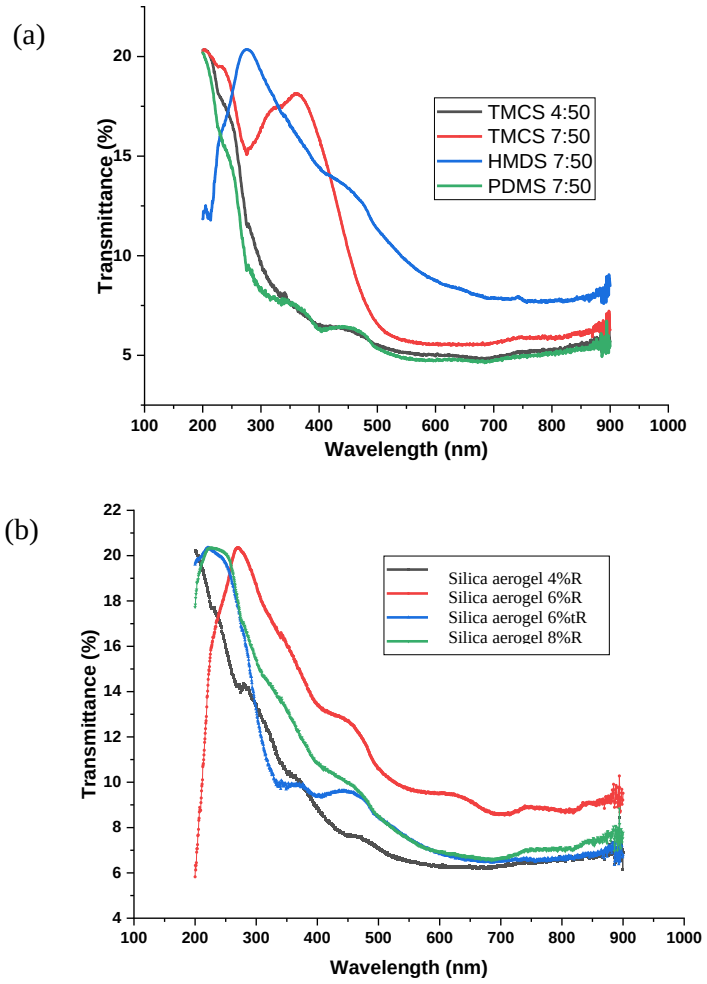

Figure 1. Transmittance of aerogels synthesized with (a) various silylating agents; (b) various sodium silicate mass concentration.

Fig. 2 shows the results of thermal stability measurement of aerogels at various synthesis condition. There are two steps of thermal degradation in the aerogel structure as indicated by the loss of mass. First, the evaporation of the remaining n-hexane solvent and water molecules below 100°C, followed by Si-CH_3 oxidation or the degradation of aerogel at higher temperature. The thermal stability of aerogel reflects its density (Table 2). Based on Fig. 2 (a), aerogel which was modified by TMCS at 4:50 performs better than 7:40 because it has lower density. In Fig. 2 (b), TMCS aerogel has more drastic loss of mass in the first step because there is still water or solvent inside the structure, as indicated by its higher density compared to HMDS and PDMS aerogels. HMDS aerogel is thermally stable up to 350°C. And although PDMS has some initial loss of mass due to solvent evaporation, it can be considered more stable for high temperature application, which is up to 400°C. From Fig. 2 (c), it can be concluded that resin exchange contributes significantly to the formation of aerogel. When the solvent exchange process occurs in hydrogels that still contain salt, n-hexane cannot replace water in the pores which results in poor thermal stability.

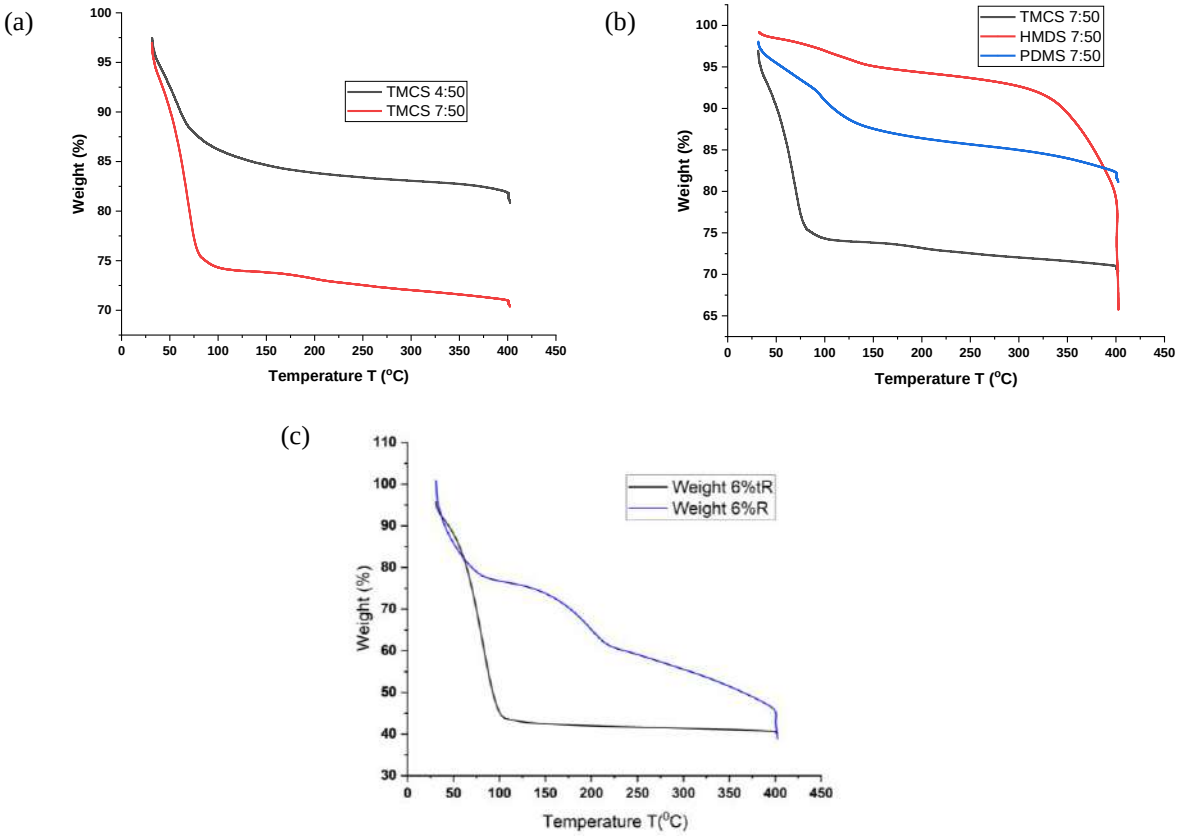

Figure 2. Thermal stability of the as-synthesized aerogels at (a) silylating agent volumetric ratio; (b) silylating agent type; (c) resin addition; and (d) sodium silicate mass ratio variations.

4. Conclusion

Silica aerogel with low density and high thermal stability are successfully synthesized from natrium silicate through sol-gel, surface modification, and ambient pressure drying. Overall, PDMS as silylating agent performs better than HMDS and TMCS in terms of thermal stability and density. Resin exchange is also proven as an important part to synthesize xerogel without impurities, However, the transparency of the aerogel still needs to be improved. Different synthesis conditions, silylating agents, or solvents should be considered in the future in order to produce transparent silica aerogel as thermal insulator.

References

[1]. N. Nazeran and J. Moghaddas, "Synthesis and characterization of silica aerogel reinforced rigid polyurethane foam for thermal insulation application," J Non Cryst Solids, vol. 461, pp. 1–11, Apr. 2017.
[2]. J. Wang, D. Petit, and S. Ren, "Transparent thermal insulation silica aerogels," *Nanoscale Advances*, vol. 2, no. 12. Royal Society of Chemistry, pp. 5504–5515, Dec. 01, 2020.
[3]. Y. L. He and T. Xie, "Advances of thermal conductivity models of nanoscale silica aerogel insulation material," *Applied Thermal Engineering*, vol. 81. Elsevier Ltd, pp. 28–50, Apr. 25, 2015.
[4]. E. Cuce, P. M. Cuce, C. J. Wood, and S. B. Riffat, "Toward aerogel based thermal superinsulation in buildings: A comprehensive review," *Renewable and Sustainable Energy Reviews*, vol. 34. Elsevier Ltd, pp. 273–299, 2014.
[5]. D. B. Mahadik, A. V. Rao, R. Kumar, S. V. Ingale, P. B. Wagh, and S. C. Gupta, "Reduction of processing time by mechanical shaking of the ambient pressure dried TEOS based silica aerogel granules," Journal of Porous Materials, vol. 19, no. 1, pp. 87–94, Feb. 2012.
[6]. S. W. Hwang, T. Y. Kim, and S. H. Hyun, "Optimization of instantaneous solvent exchange/surface modification process for ambient synthesis of monolithic silica aerogels," J Colloid Interface Sci, vol. 322, no. 1, pp. 224–230, Jun. 2008.

[7]. A. Soleimani Dorcheh and M. H. Abbasi, "Silica aerogel; synthesis, properties and characterization," *Journal of Materials Processing Technology*, vol. 199, no. 1. pp. 10–26, Apr. 01, 2008.
[8]. Z. A. Abdul Halim, M. A. Mat Yajid, and H. Hamdan, "Synthesis and characterization of rice husk ash derived - Silica aerogel beads prepared by ambient pressure drying," in *Key Engineering Materials*, 2016, vol. 694, pp. 106–110.
[9]. J. L. Gurav, I. K. Jung, H. H. Park, E. S. Kang, and D. Y. Nadargi, "Silica aerogel: Synthesis and applications," J Nanomater, vol. 2010, 2010.
[10]. Q. Feng *et al.*, "Synthesis of high specific surface area silica aerogel from rice husk ash via ambient pressure drying," Colloids Surf A Physicochem Eng Asp, vol. 539, pp. 399–406, Feb. 2018.
[11]. J.-H. Kim, J.-H. Ahn, J.-D. Kim, D.-H. Lee, S.-K. Kim, and J.-M. Lee, "Influence of Silica-Aerogel on Mechanical Characteristics of Polyurethane-Based Composites: Thermal Conductivity and Strength," Materials, vol. 14, no. 7, p. 1790, Apr. 2021.
[12]. H. Nguyen, P. Hoang, and N. Dinh, "Synthesis of Modified Silica Aerogel Nanoparticles for Remediation of Vietnamese Crude Oil Spilled on Water," J Braz Chem Soc, 2018.
[13]. T. Fu, J. Tang, K. Chen, and F. Zhang, "Visible, near-infrared and infrared optical properties of silica aerogels," Infrared Phys Technol, vol. 71, pp. 121–126, Jul. 2015.
[14]. P. M. Shewale, A. V. Rao, and A. P. Rao, "Effect of different trimethyl silylating agents on the hydrophobic and physical properties of silica aerogels," Appl Surf Sci, vol. 254, no. 21, pp. 6902–6907, Aug. 2008.

Biographies of Authors

Egiana Reshi Hardiane, S.T. received her Bachelor's degree in chemical engineering from Universitas Pertamina, Indonesia in 2023.

Gita Evi Monika Purba S.T. received her Bachelor's degree in chemical engineering from Universitas Pertamina, Indonesia in 2023.

Ayu Dahliyanti, M.Eng. is a lecturer in Chemical Engineering Department, Universitas Pertamina, Indonesia. She received her Master's degree from Tokyo Institute of Technology in 2015.

Vol. 2, No. 2, October 2023, pp. 131-144
p-ISSN: 2963-8577
e-ISSN: 2964-3511
DOI: 10.57102/jescee.v2i2.69

THE IMPLEMENTATION OF AHP AND WHALE OPTIMIZATION ALGORITHM IN THE SELECTION AND OPTIMIZATION OF BEST CLEAN ENERGY SOURCE

Niklas Parlindungan Simorangkir[1*], Aditya Tirta Pratama[2]
[1]Department of Industrial Engineering, Faculty of Engineering and Information Technology, Swiss German University
[2]Department of Industrial Engineering, Faculty of Engineering and Information Technology, Swiss German University

Abstract
Clean energy sources have become more and more important in the present time, especially with the goal to reduce the production of greenhouse gases. There are various clean energy sources available, and care must also be taken into which clean energy source is more prevalent in which location. Furthermore, with the multiple alternatives for such clean sources, a method has to be developed to choose the best one, and, if possible, have it optimized to produce the best performance. It is also good if the method developed only requires theories without any need of practical applications in real life (although this is strongly encouraged). This paper will show the utilization of a decision-making tool, namely the analytic hierarchy process, to decide the best energy source and which components are important and then conducts the optimization process through whale optimization algorithm. The research will then conclude with the best energy source chosen in its optimized state. It is hoped that this research will open a gateway into determining which energy sources to use digitally without any recourse to incurring costs on its way.

Keywords:
Decision analysis; optimization algorithm; clean energy

Article History:
Received: October 3rd, 2023
Revised: October 16th, 2023
Accepted: October 28th, 2023
Published: October 31st, 2023

Corresponding Author:
Niklas Parlindungan Simorangkir
Department of Industrial Engineering, Swiss German University, Indonesia
Email:
niklas.simorangkir@sgu.ac.id

1. Introduction

Renewable energy sources have become quite important today, as the world now moves to produce cleaner energy. This falls in line with some of the Sustainable Development Goals (SDG) set out by the United Nations (UN), which are (Osborn et al., n.d.):

- Goal 7: Ensure access to affordable, reliable, sustainable, and modern energy for all
- Goal 9: Build resilient infrastructure, promote inclusive and sustainable industrialization and foster innovation
- Goal 13: Take urgent action to combat climate change and its impacts

Note that there may be other SDGs that are applicable to this research. However, the three SDGs listed above are the most relevant ones.

There are various types of energy available to achieve the SDGs mentioned. These are hydro, solar, wind, biomass, nuclear, and geothermal. These sources are different to each other based on certain characteristics, which prove to be a challenge when determining which one is best to utilize. Moreover, it must also be considered where the renewable energy sources are going to be used, as each geographical area will have different parameters. In this paper, the country that these renewable energy sources will be based on is Indonesia.

Indonesia has already made strides to produce clean energy; this can be observed when the country joined the Clean Energy Demand Initiative (CEDI). It also has goals to achieve within specific timeframes:

- Nationally determined contribution (NDC) in 2030
- Net zero emissions (NZE) in 2060

- 23% renewable energy in primary energy mix in 2025

However, since energy is highly dependent upon for human survival, it is only natural that the most practical sources of energy are used based on the resources available in the country. This means that fossil fuels are still used (coal, oil and gases). In the year 2020, they constituted 88.7% of the primary energy supply, whereas all the renewable energy sources combined total at 11.3%. By looking at one of the goals that needs to be achieved, Indonesia needs 11.7% more renewable energy sources in the primary energy mix. The prediction whether it is possible to be achieved in a span of 5 years is outside the scope of this study and will not be discussed in-depth.

According to [2], there are nine types of fuels that are used for energy consumption in Indonesia: coal, oil, natural gas, hydro, geothermal, solar energy, wind energy, biofuel, biogases. However, nuclear power is not used as a source of energy yet. Even though it is clean and sustainable, considerable public opposition goes against the usage of this energy source. There are two major reasons for this opposition [3]:

- Multiple hazards and/or accidents may surface (nuclear accidents and weapons, radioactivity)
- The public was not active in the engagement of the decision-making of nuclear power which may lead to public mistrust

However, for this paper, nuclear energy will be included as one of the possible clean energy sources. This is since nuclear energy may be a key solution to energy sustainability in Indonesia, despite the apparently large public opposition against such source. With all these available clean energy sources, it must be known which source is the best one to be used.

This study is significant in two ways: the first is providing an alternative way of optimizing the available renewable sources and the second is developing a greater understanding as to how mathematical modelling and optimization algorithms have a role in such activity. Three research problems are also present: determining the best clean energy source, optimizing the best clean energy source and developing a suggested framework on such procedure. Lastly, three objectives must be met in this research: determining the key performance indicators (KPIs) to choose the best clean energy source, conducting decision-making process for best clean energy source and parameter prioritizations, utilizing Python for whale optimization algorithm application.

Therefore, to resolve the research problems and achieve the research objectives, a two-step method is implemented: the first step is to select the best clean energy source through analytic hierarchy process (AHP), a decision-making tool. The AHP components will be based on the input of two experts in the field of clean energy sources. After the best clean energy source has been chosen, then its parameters will be optimized through the whale optimization algorithm (WOA). The weighting of the parameters that need to be optimized is based on the input of one of the experts.

2. Methods

This chapter consists of the methods conducted to perform the research. It can be broken down into three phases: decision analysis, optimization, evaluation. The decision analysis consists of an explanation of how the AHP is performed. The optimization process explains the development of the energy cost model (along with its components' models) and its integration into the WOA, as well as its verification through Python. The integration of AHP and WOA is perfectly acceptable, as AHP could be "used in a particular case as a sole method or in combination with other notable systems or methods" [11]. The evaluation phase will indicate how the performance metrics are evaluated and how the suggested framework will be developed based on the findings.

A. Methodology Framework

Fig. 1 shows the framework of the research methods utilized in this work.

Figure 1. PDCA Framework

A strong structured framework is needed to ensure that the research will be conducted smoothly, outlining the activities clearly in each phase. Therefore, the Plan-Do-Check-Act (PDCA) framework is utilized. The explanations for the framework are as follows:

- Plan: this is where the problems of the research are stated, and the plan will be implemented.
- Do: the plan is implemented at a small scale, in this case Indonesia.
- Check: an evaluation of the results is conducted.
- Act: a suggested framework is developed which may indicate whether the process should be implemented at a larger scale.

B. Decision Analysis

The decision analysis conducted for this research is in the form of AHP. It is a type of multi-criteria decision-making method (MCDM), which is "a well-structured and multidimensional process developed to tackle decision-making problems in different fields and search for the most attractive alternative with consideration of all relevant criteria" [9]. AHP also has great availability in literature in its application. As such, this method will be used to select the best clean energy source. AHP is utilized as a decision-making tool because there are not many criteria and alternatives present in the decision system. As such, a sophisticated decision system (e.g., a combination of decision-making systems) is not needed for such decision processing: a simple and practical tool will suffice.

The process of AHP is developed by Thomas Saaty, which comprises of five steps [10]. First, the hierarchy model should be developed that will consist of goal (the objective), the alternatives (possible ways to achieve such objective), and the criteria (evaluations of the alternatives). Second, prioritizations will have to be set as weights for the criteria, which will then be used in pairwise comparisons. Third, the judgments will then be synthesized to produce a set of priorities for the hierarchy through combining the judgments of the criteria. Fourth, the judgments' consistency will be evaluated with inconsistency ratio. Fifth, the final decision will then need to be made based on the results received.

The building be simply denoted shown in Fig. 2.

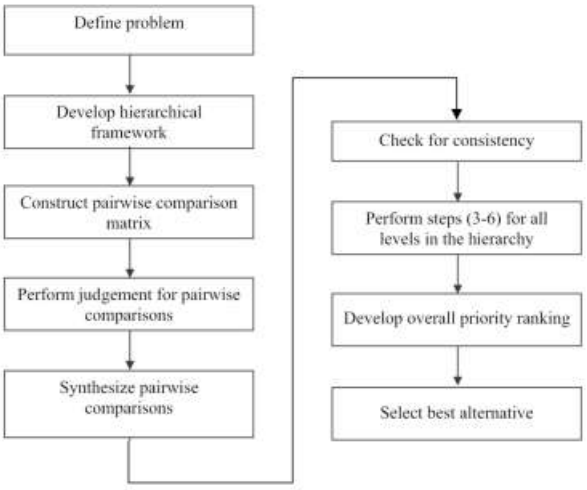

Figure 2. AHP Method Steps (Budiman & Pratama, 2022)

AHP has advantages that made it one of the common MCDM methods to use:

1. Only a pair of elements is needed in each instance of time, despite the numerous factors that may be involved in the situation.
2. Allows the inclusion of tangible variables and intangible variables (or, in other words, quantitative and qualitative).

Naturally, there are limitations to the AHP method. According to [7], there are two main issues:

1. Rank reversals: the method of rank reversals apparent in the AHP method means that if any alternative is added or deleted, then the relative rankings of the other alternatives will change.
2. Condition of order and preservation (COP): due to the priorities in AHP being derived from the eigenvector values, the COP is violated. As stated by Thomas Saaty: "For all alternatives x_1, x_2, x_3, x_4, such that x_1 dominates x_2 and x_3 dominates x_4, then the vector of priorities w should be such that not only $w(x_1) > w(x_2)$ and $w(x_3) > w(x_4)$ (preservation of order preference) but also that $w(x_1) / w(x_2) > w(x_3) / w(x_4)$ (preservation of order of intensity of preference)" (Saaty, 2013 as cited in [7]).

But even with the limitations listed above, AHP remains a powerful and common method in decision-making, showing that its limitations can be mitigated in various ways.

As mentioned before, criteria and alternatives are in an AHP system and so they need to be determined. The criteria for the AHP method are in the form of KPIs. There are various KPIs that characterize clean energy sources, which must be discussed later with an expert in this field.

As for the alternatives, there are different types of clean energy sources that are available to use. The purpose of the AHP method is to select one of these alternatives as the best clean energy source to use. There are six clean energy sources for consideration in this research:

- Hydro
- Solar
- Wind
- Biomass
- Nuclear
- Geothermal

After identifying the number of criteria as well as the details regarding the alternatives, the structure of the AHP can now be developed. It is shown in Fig. 3.

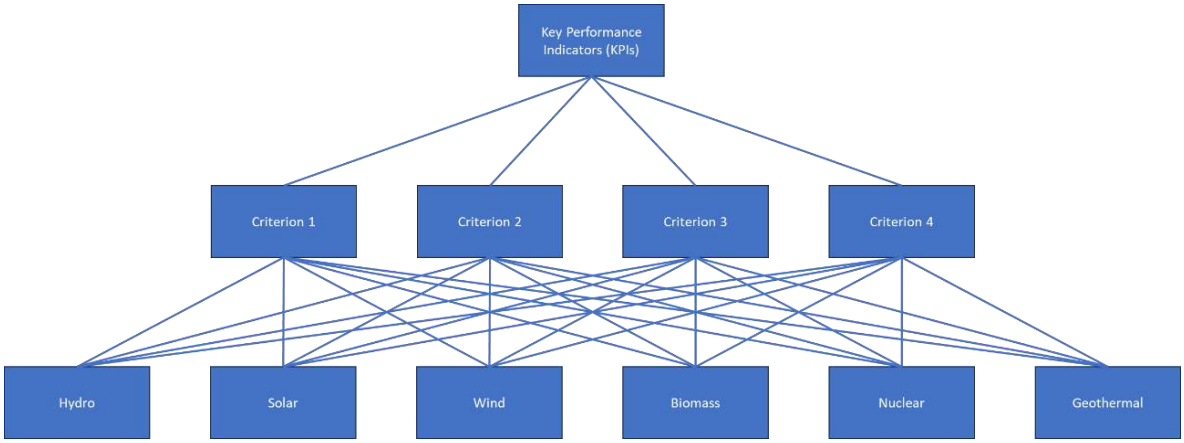

Figure 3. AHP Structure

AHP will be able to select the best alternatives using prioritizations. The criteria won't be equal in importance when compared to each other, and so prioritizations are needed, which are in the form of relative weights (relative since "the obtained criteria priorities are measured with respect to each other" [6]. These prioritizations are the results of pairwise comparisons, which mean that the judgments must be input for both criteria and alternatives. Pairwise comparisons can be understood using matrix, where a "pairwise comparison matrix A is a *m* x *m* real matrix, where *m* is the number of selected criteria." (Saaty, 1980 as cited in [4]). It also has several terms that needed to be understood. In the pairwise comparisons, "each entry a_{jk} of the matrix A represents the importance of the *jth* criterion relative to the *kth* criterion, where a_{jk} denotes the entry in the *jth* row and the *kth* column of A" (Saaty, 1980 as cited in [4]).

These judgments are given by two experts in this field. These experts act as decision-makers (or also known as domain experts), who will give judgment through a Google Form questionnaire, directly completing pairwise comparisons for the independent elements in the hierarchical structure. The judgments are made based on the comparison between multiple criteria and multiple alternatives. For example, geothermal will be compared with solar and the expert will judge which is more important than the other.

The levels of importance in the criteria and alternatives' comparisons that the expert will give are based on the Saaty scale. The judgment points and their explanations are shown below [10]:

- 1: equally important (the two variables have equal contribution to the objective)
- 3: moderately important (one element is moderately favored more than the other in terms of experience and judgment)
- 5: strongly important (one element is strongly favored more than the other in terms of experience and judgment)
- 7: very strongly important (one element is very strongly favored more than the other, where its dominance is clearly apparent)
- 9: extremely important (one element is favored more than the other in the highest possible order of affirmation)

In other papers, 2, 6, and 8 are also used as judgment points to represent intermediate values, but they are not used in this paper.

After gathering the judgments, the answers will be input into the SuperDecisions software. The reason why this software is chosen is because of the ease of use in conducting the pairwise comparison matrix methods; the experts' judgments can be input and then the decision results are immediately available. The outputs will be the prioritizations of the criteria and the alternatives. The prioritizations of the criteria come in the form of weights, which will then be used to determine the weight values of the variables in the energy cost model later. However, for the alternatives, the prioritizations themselves are the only information needed. Consideration of the inconsistency ratio of the answers must be considered, in which the recommended threshold is <10%. But this is another important limitation of AHP, in its consistency matrix. The AHP method "can only be sued for consistent decisions, and it is an important advantage if we want to avoid contradictions, but not all decisional problems can be consistent" [4]. Therefore, it is to be noted that even though consistency is important in

judgments, there are certain situations in which a higher inconsistency ratio (even up until 30%) may warrant acceptance. These situations are when accurate answers are more important than consistent ones.

According to [13], the formula for the consistency index (CI) calculation is:

$$CI = \frac{(\mu_{max} - n)}{(n-1)} \tag{1}$$

where μ_{max} is the biggest eigenvalue. The formula for the consistency ratio (CR) is as follows:

$$CR = \frac{CI}{RI} \tag{2}$$

where CI is consistency index and RI is random index, which is the "consistency index of a randomly generated pairwise evaluation matrix" [13].

C. Whale Optimization Algorithm

Whale optimization algorithm is a metaheuristic algorithm inspired by the hunting nature of the humpback whales. The hunting nature can also be termed as bubble-net feeding method, in which two maneuvers are involved: 'upward-spirals' and 'double-loops'. According to [8], they "dive around 12 m in the former maneuver and then start making bubble in a spiral shape around the prey and swim up toward the surface". As for the second maneuver, three stages are enacted: coral loop, lob-tail and capture loop. Fig. 4 shows the humpback whales' bubble-net feeding behavior.

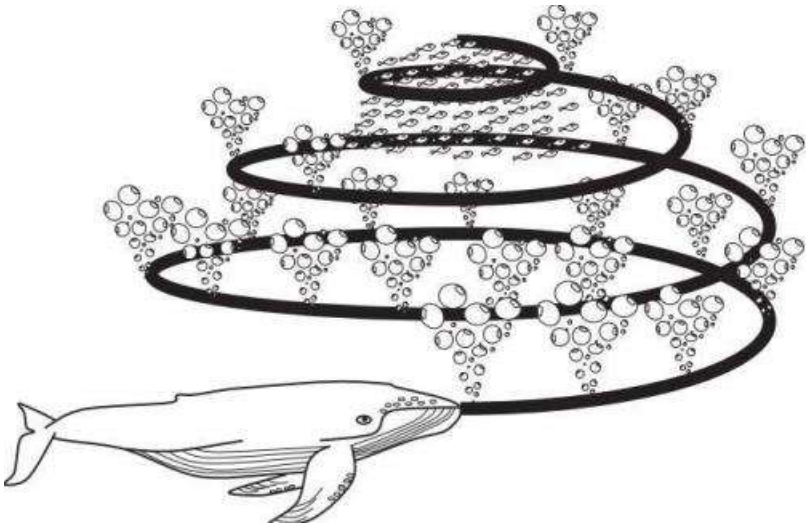

Figure 4. Humpback Whales' Bubble-Net Feeding Behavior [8]

It is one of the relatively simple algorithms to utilize and it has comparable better performance, which is why it has been chosen instead of its more famous counterparts, such as genetic algorithms. It was developed quite recently in 2016, but it already started being used increasingly throughout the years, as can be seen in Fig. 5.

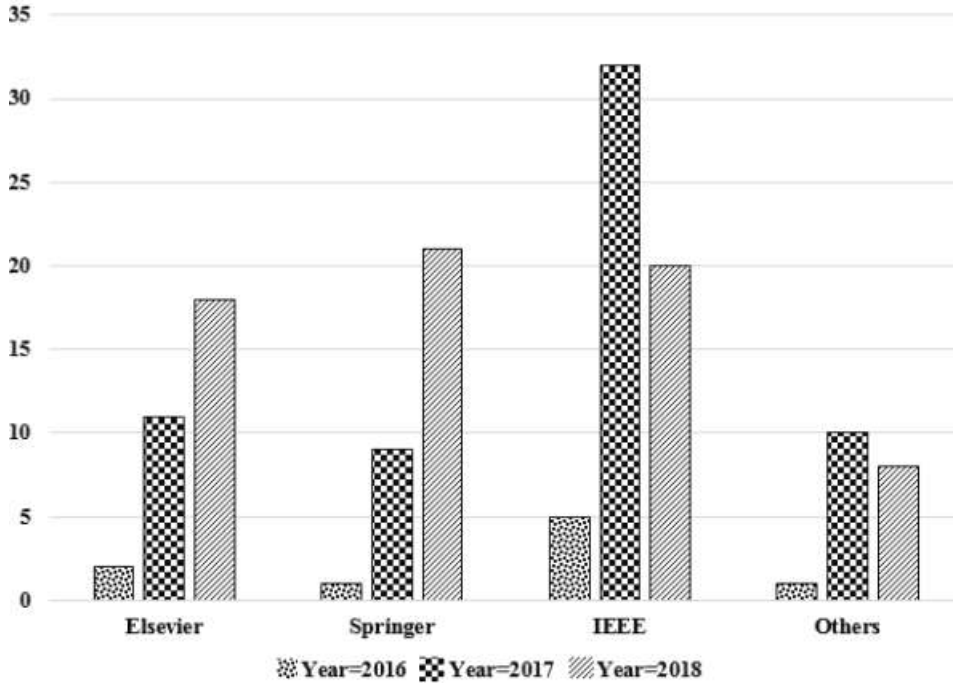

Figure 5. Trends of WOA Application [8]

There are three phases in whale optimization algorithm: exploration phase, encircling prey, and exploitation phase. The exploration phase means the diversification of the search space and the exploitation phase refers to the intensification of the best agent [12]. In this algorithm, the whales represent the solutions (note that the algorithm is composed of a set of solutions), and the main objective is for a whale to try to fill a new place in the search space that is considered the best in that current instance.

In the exploration phase, a whale globally searches for the best solution in a random manner. Its mathematical model is shown in (3).

$$V(k+1) = V_{random}(k) - Y * D \tag{3}$$

where V is position vector, k is current iteration, Y is coefficient vector, and D is distance. To calculate the coefficient vector, the formula is shown in (4).

$$Y = 2 * l * \beta - l \tag{4}$$

where Y is coefficient vector, l is decreasing linear value within the range [2, 0] and β is random value within the range [0, 1].

The exploration phase model also requires that the distance be calculated. Eq. (5) showcases how the distance can be calculated.

$$D = |X * V_{random}(k) - V(k)| \tag{5}$$

where D is distance, X is the coefficient vector, k is the current iteration. The formula also requires X to be determined, which is calculated using (6).

$$X = 2 * \beta \tag{6}$$

where X is coefficient vector and β is random value within the range [0, 1].

The second phase is the encircling prey. This is when the whale settles on a target as the best solution and informs other whales to focus on it. The mathematical modelling is the same as the one in the exploration phase mathematical model, however the random value of the position vector is replaced by the best position vector value. The formulation is shown in (7).

$$V(k+1) = V_{best}(k) - Y * D \tag{7}$$

where V is position vector, k is current iteration, Y is coefficient vector, D is distance. Calculating Y and D is the same as the one in the exploration phase mathematical model.

The final phase is the exploitation phase, in which there are two possible approaches: the shrinking circle and the spiral approach. This phase is used to produce the whales' bubble net behavior. The first part, the shrinking circle, determines the possible new positions of search agents that lie between the original position and the current best solution [14]. The spiral approach is slightly different, in that it does not focus on the new search agent positions between the original and the current best. Rather, this approach is to "mimic the helix-shaped movement of humpback whales" [14]. The formulation of the spiral approach is shown in Equation 8.

$$V(k+1) = \begin{cases} V_{best}(k) - Y * D \; if \; P < 0.5 \\ D * e^{mn} * \cos(2\pi h) + V_{best} \; if \; P \geq 0.5 \end{cases} \tag{8}$$

where m is a constant defining the logarithmic shape and n is the random number within the range [-1, 1].

With the information listed above, it can be surmised that WOA does have important advantages over its relatives. It has a high exploration ability as well as high exploitation and convergence, leading to its ability of avoiding high local optima and convergence speed during each iteration [5].

D. Energy Cost Model

The energy cost model is based on the KPIs that were going to be determined through a discussion with an expert. The energy cost model is shown in (9).

$$E = \alpha A + \rho B + \gamma C + \varphi D \tag{9}$$

where E is energy consumed, A is the first criterion, B is the second criterion, C is the third criterion, D is the fourth criterion. α, ρ, γ, φ are the weights used for the criteria, each used respectively. It is also important to note that this energy cost model seeks to optimize the energy cost through the minimization process.

The weights are determined through the decision analysis results. And since this model is utilized without any direct experimentation, each of the variables will be determined through probabilistic models.

The optimization process will be conducted through a programming language, namely Python. Python is software that allows users to be flexible in developing algorithms, such as whale optimization algorithm, which will be used for this research.

3. Result and Discussion

A. Decision Analysis

After a discussion with an expert, the four criteria for the selection of the best clean energy source have been determined. They are:

- Efficiency (%): this is based on the efficiency of the energy source in terms of producing energy. As it is desirable to have a highly efficient energy source, this leads to the belief that the higher the efficiency of the energy source, the more appealing it is.
- Levelized cost of energy ($/MWh): the levelized cost of energy refers to the how much energy should be sold for the break-even to occur at the end of its physical lifetime.
- Location site (km): this refers to the distance between the location site of the energy source and transportation lines/city. This is an important parameter regarding the maintenance of the energy source as well as the distribution of the energy to both urban and rural areas.
- Capital cost ($): the cost required to start the generating of the energy source. This is important due to the energy source needing capital for it to begin functioning (without the funds, no energy source can begin generating).

As the criteria are already identified, it is now possible for the AHP structure to be updated. Fig. 6 showcases the updated AHP structure.

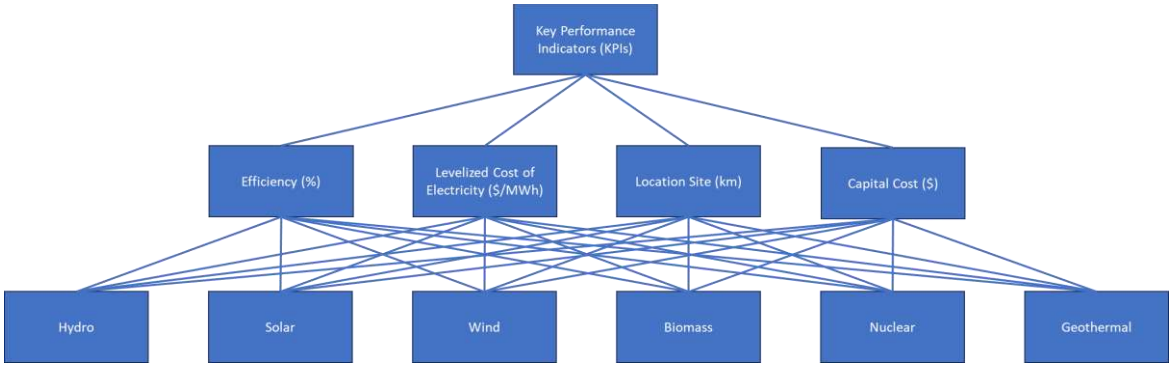

Figure 6. Updated AHP Structure

Since the AHP structure is already complete, now the AHP structure can be inserted into the SuperDecisions software. Fig. 7 shows the SuperDecisions layout for the AHP.

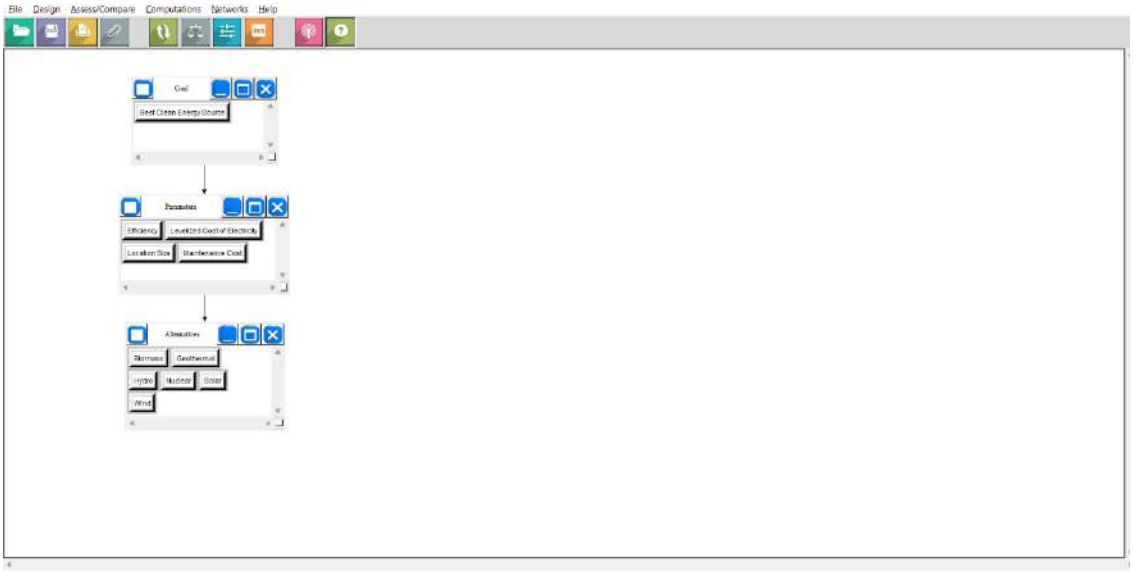

Figure 7. The AHP Layout in SuperDecisions

In SuperDecisions, the judgments that the experts gave (1, 3, 5, 7, and 9) are input into the pairwise comparisons window of the software (a sample is shown in Fig. 8). For the pairwise comparisons, two experts have given the judgments, which are then combined. The results of the priority weights for the alternatives are shown on Table 1.

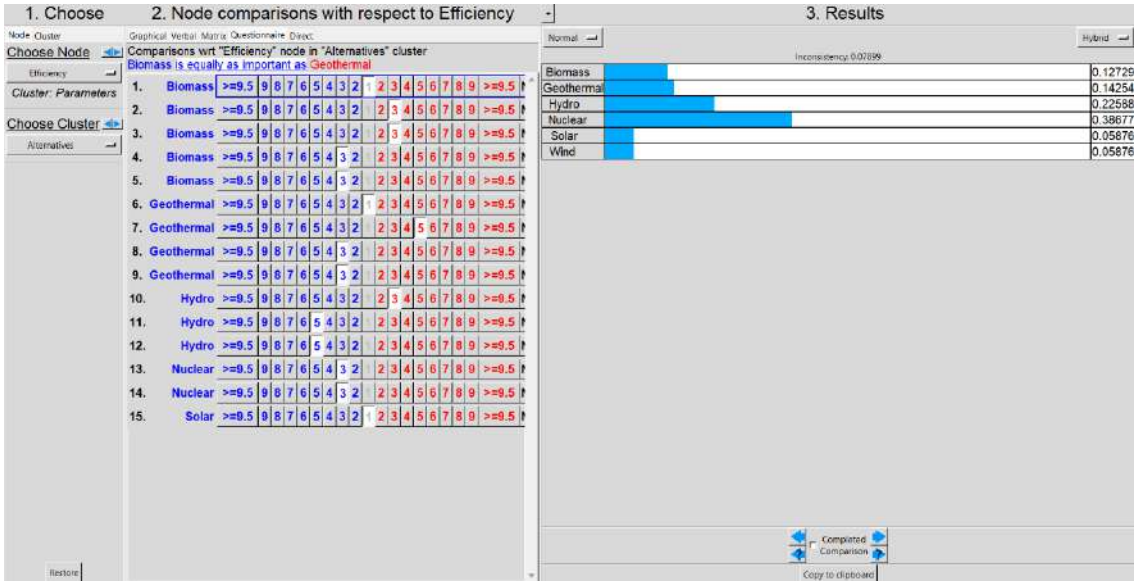

Figure 8. SuperDecisions Pairwise Comparisons Window Sample

Table 1. Priority Weights of the Alternatives

KPIs	**Priority Weights**
Hydro	0.23105
Solar	0.09960
Wind	0.11199
Biomass	0.14670
Nuclear	0.28041
Geothermal	0.13025

As can be seen on Table 1, nuclear has the highest priority weight as compared to the other alternatives, meaning that nuclear power is the best alternative (according to the judgments) and this energy source is the one that will proceed to the next stage: optimization.

It is also imperative that the inconsistency ratio is identified for all those involved in the decision-making process. It was previously mentioned that the recommended threshold is 10% or less. However, if the situations warrant so, the threshold can be enlarged to even 30%. According to the result of the AHP, the inconsistency ratio of Table 2 showcases the inconsistency ratios for the criteria.

Table 2. Inconsistency Ratios of the Criteria

KPIs	**Priority Weights**
Efficiency (%)	7.90%
Levelized cost of electricity ($/MWh)	3.32%
Location site (km)	18.0%
Capital cost ($)	9.77%

Efficiency, location site, and capital cost have inconsistency ratios below 10%, which meant that that answers remain consistent throughout. For the location site, the inconsistency ratio is over 10%, meaning that its inconsistency is concerning. It is acceptable, however, if consideration is taken on who gives the judgment in

that area: an expert with decades of experience in the field of energy. After considering the situation, the accuracy of the answers is more important than that of its consistency. Since the inconsistency is not quite significant from that of the threshold, it is therefore acceptable for the location site's results to be further processed.

Now, the priority weights for the key performance indicators (KPIs) of the energy sources are needed. Priority weights are important for updating the energy cost model and, later, the optimization itself. The values are shown on Table 3.

Table 3. Priority Weights of KPIs

KPIs	**Priority Weights**
Efficiency (%)	0.44191
Levelized cost of electricity ($/MWh)	0.14073
Location site (km)	0.23357
Capital cost ($)	0.18379

As shown on Table 3, efficiency has the highest priority weight and levelized cost of electricity has the lowest priority weight. These priority weights will then be incorporated into the energy cost model, which will be discussed in the next subchapter.

B. Energy Cost Model

The updated energy production model already has incorporated priority weights into it, which is shown in (10).

$$E = -0.44191A + 0.14073B + 0.23357C + 0.18379D \tag{10}$$

where A is efficiency (%), B is levelized cost of electricity ($/MWh), C is location site (km), and D is capital cost ($).

It is now important to determine the values of A, B, C, and D. Due to the different types of units that will be used in the energy consumption model, it is imperative that the values are 'standardized'. To do this, a logarithmic function will be used in each of the KPIs.

Because Indonesia did not yet have a nuclear power plant for generating energy for public demand, the data used are general data from trusted websites[1][2][3]. A range of values is used for each of the KPIs, and in the algorithm later, randomized values for each of the variables will be generated within that specific range. The data for the KPIs are on Table 4.

Table 4. Data for KPIs

KPIs	**Values**
Efficiency (%)	33 – 37
Levelized cost of electricity	39.39 – 126.37

[1] https://energyeducation.ca/encyclopedia/Nuclear_power_plant#:~:text=Typical%20nuclear%20power%20plants%20achieve,potentially%20reach%20above%2045%25%20efficiency.

[2] https://www.oecd-nea.org/upload/docs/application/pdf/2020-12/egc-2020_2020-12-09_18-26-46_781.pdf

[3] https://world-nuclear.org/information-library/economic-aspects/economics-of-nuclear-power.aspx

($/MWh)	
Location site (km)	8 – 30
Capital cost ($)	106 – 816

The energy cost model will then be utilized for the whale optimization algorithm, which will be discussed in the next subchapter.

C. Whale Optimization Algorithm

Fig. 9 shows the coding conducted to perform the whale optimization algorithm process.

```
# Required Libraries
import numpy as np
import random
import gc

# iWOA
from pyMetaheuristic.algorithm import improved_whale_optimization_algorithm
from pyMetaheuristic.utils import graphs

# Target Function - It can be any function that needs to be minimize, However it has to have only one argument: 'variables_values'. This Argument must be a list of variables.

# Target Function: Eason Function

def easom(variables_values = [0, 0, 0, 0]):
    A, B, C, D    = variables_values
    A = random.randrange(33, 37)
    B = random.randrange(40, 126)
    C = random.randrange(8, 30)
    D = random.randrange(106, 816)
    func_value = (-1*(0.44191 * (np.log(A))) + (0.14073 * (np.log(B))) + (0.23357 * (np.log(C))) + (0.18379 * (np.log(D))))
    return func_value

# iWOA - Parameters
parameters = {
    'hunting_party': 500,
    'min_values': (33, 40, 8, 106),
    'max_values': (37, 126, 30, 816),
    'iterations': 1000,
    'spiral_param': 0.5,
    'mu': 3,
    'verbose': True
}

# iWOA - Algorithm
iwoa = improved_whale_optimization_algorithm(target_function = easom, **parameters)

# iWOA - Solution
variables = iwoa[0][:-1]
minimum   = iwoa[0][ -1]
print('Variables: ', np.around(variables, 4) , ' Minimum Value Found: ', round(minimum, 4) )


gc.collect()
```

Figure 9. Whale Optimization Algorithm Coding

Shown in Fig. 9, there are some parameters in the WOA algorithm that require explanations and/or clarifications:

- The minimum values set in the algorithm are based on the minimum values of the parameters' range of values. For example, the minimum value set for efficiency is 33%, since in the range of possible efficiency values, 33% is the lowest value.
- The maximum values follow the same logic as that of the minimum values; they are based on the maximum values of the parameters' range of values.
- There are 1000 iterations utilized. This is to ensure that the global optimum is found instead of local optima (1000 iterations are more than enough to find the global optimum).

The whale optimization algorithm deals with data that are randomly generated. Therefore, it is highly important that numerous trials are conducted to produce multiple objective function values that can be compared. The comparisons will determine the lowest objective function value, in which the best parameter values are contained.

To ensure that the results achieved reduce the extreme probabilities, 50 trials will be conducted. However, there are some trials that have equal objective values. They are shown on Table 5.

Table 5. Objective Functions with Equal Value

Trials	**A**	**B**	**C**	**D**	**Objective**
1	37.00	41.86	30.00	137.5	0.2783
2	37.00	44.31	15.85	801.0	0.2783

3	37.00	126.0	24.1	816.0	0.2783
4	34.74	95.13	15.49	477.4	0.2783
5	33.00	40.00	8.000	106.0	0.2783

As there are five objective functions that have the lowest objective values that are equal, the values of the variables must now be considered. There cannot be multiple solutions; there can only be one. Therefore, two considerations are developed:

- The efficiency value must not be high.
- The costs' values must be low.

By looking at Table 5, it can be determined that the first objective function value is the best one. Therefore, the values to achieve the best solution are:

- Efficiency: 37%
- Levelized cost of electricity: $41.86/MWh
- Location site: 30 km
- Capital cost: $137.5

4. Conclusion

In conclusion, it can be gainsaid that the research is successful, in that it achieves the following three objectives:

- The KPIs for choosing the best clean energy source have been identified through consultation with experts within the energy field. The KPIs are also set as the parameters of the chosen clean energy source that must be optimized later.
- The decision-making process to choose the best clean energy source has been conducted successfully. AHP is used as the decision-making tool that proves to be sufficient to make decisions regarding this case.
- Python has been utilized for whale optimization algorithm application. The programming language has allowed good-quality results to be produced, which are then further processed to determine the optimized parameters.

There are, however, improvements to be made in this research. It is perhaps recommended that in the future, multiple optimization algorithms should be used instead of one, and the algorithm with the best result should be the one chosen. The second recommendation is that AHP should be integrated with another decision-making tool to produce better quality results (e.g., combining AHP with DEMATEL). Lastly, the research can be improved by conducting the research practically as well instead of just theoretically (this should be done with supervision from experts within the related field).

Acknowledgment

I would like to thank God for all the love and blessings that He gave me, which proved to be crucial in supporting me throughout the research and writing process. I extend my greatest gratitude to my family and friends, who provided me with their greatest care and support. I would like to thank Dr. Aditya Tirta Pratama, who was willing to become a corresponding author of this paper, guiding and leading me on how to resolve the obstacles that I have faced throughout my research.

References

[1] Osborn, D. et al., "Understanding the Transformational Challenge for Developed Countries," *Universal Sustainable Development Goals*. 2005. Available: https://sustainabledevelopment.un.org/content/documents/733FutureWeWant.pdf

[2] Pambudi, N. A. et al., "Renewable Energy in Indonesia: Current Status, Potential, and Future Development," *Sustainability (Switzerland)*, vol. 15, no. 3, 2023, doi: https://doi.org/10.3390/su15032342
[3] Sugiawan, Y., & Managi, S., "Public acceptance of nuclear power plants in Indonesia: Portraying the role of a multilevel governance system," *Energy Strategy Reviews*, vol. 26, 2019, doi: https://doi.org/10.1016/j.esr.2019.100427
[4] Petruni, A. et al., "Applying Analytic Hierarchy Process (AHP) to choose a human factors technique: Choosing the suitable Human Reliability Analysis technique for the automotive industry," *Safety Science*, vol. 119, p. 229 – 239, 2019 doi: https://doi.org/10.1016/j.ssci.2017.05.007
[5] Nasiri, J., & Khiyabani, F.M., "A whale optimization algorithm (WOA) approach for clustering," *Cogent Mathematics & Statistics*, vol. 5, 2018, doi: https://doi.org/10.1080/25742558.2018.1483565
[6] Mu, E., & Pereyra-Rojas, M., "Understanding the Analytic Hierarchy Process," *Practical Decision Making*, p. 7-22, 2017, doi: https://doi.org/10.1007/978-3-319-33861-3_2
[7] Ho, W., & Ma, X., "The state-of-the-art integrations and applications of the analytic hierarchy process"
[8] Gharehchopogh, F.S., & Gholizadeh, H., "A comprehensive survey: Whale Optimization Algorithm and its applications," *Swarm and Evolutionary Computation*, vol. 48, p. 1-24, 2019, doi: https://doi.org/10.1016/j.swevo.2019.03.004
[9] Febrianto, A. et al., "Training Material Decision Making for Mechanics Using Analytic Hierarchy Process (AHP): A Case Study of PT United Tractors Tbk.," *ACM International Conference Proceeding Series*, 2022, doi: https://doi.org/10.1145/3557738.3557739
[10] Emawan, D. et al., "Application of Analytic Hierarhcy Process (AHP) to Develop the Weighting of Key Performance Indicators on Gas Engine Power Plants," *Conference on Management and Engineering in Industry (CMEI)*
[11] Darko, A. et al., "Review of application of analytic hierarchy process (AHP) in construction," *International Journal of Construction Management*, vol. 19, p. 436-452, 2019, doi: https://doi.org/10.1080/15623599.2018.1452098
[12] Chen, H. et al., "A balanced whale optimization algorithm for constrained engineering design problems," *Applied Mathematical Modelling*, vol. 71, p. 45-59, 2019, doi: https://doi.org/10.1016/j.apm.2019.02.004
[13] Budiman, S.E., & Pratama, A.T., "Analytic Hierarchy Process (AHP) Method for Choosing The Best Secondhand Injection Machine for PT PLA," *ACM International Conference Proceeding Series*, 2022, doi: https://doi.org/10.1145/3557738.3557827
[14] Mirjalili, S., & Lewis, A., "The Whale Optimization Algorithm," *Advances in Engineering Software*, vol. 95, p. 51–67, 2016, doi: https://doi.org/10.1016/j.advengsoft.2016.01.008
[15] Russo, R. et al., "Criteria in AHP: A systematic review of literature," *Procedia Computer Science*, vol. 55, p. 1123-1132, 2015, doi: https://doi.org/10.1016/j.procs.2015.07.081

Biographies of Authors

Niklas Parlindungan Simorangkir
Niklas Parlindungan Simorangkir, S.T., B.Eng. obtained his bachelor's degree from Swiss German University and South Westphalia University of Applied Sciences.
He started his career as a member of the Faculty of Engineering and Information Technology at Swiss German University in September 2022 (as semi-fulltime teaching assistant), and (after a short break) has been assigned as full-time teaching assistant since August 2023. His recent activities include research in optimization, clean and sustainable energy source, and industrial automation.

Aditya Tirta Pratama
Dr. Eng. Aditya Tirta Pratama, S.Si, MT, obtained his bachelor's and master's degree from the University of Indonesia and earned his doctoral degree from the Department of System Cybernetics, Hiroshima University, Japan. He started his career as a member of the Faculty of Engineering and Information Technology at Swiss German University in 2005, and has been assigned as Head of the Department of Industrial Engineering since January 2022. His recent activities include research and community services in digital competence development and Industrial Internet of Things (IIoT).

Vol. 2, No. 2, October 2023, pp. 145-159
p-ISSN: 2963-8577
e-ISSN: 2964-3511
DOI: 10.57102/jescee.v2i2.70

JESCEE
Journal of Emerging Supply Chain, Clean Energy, and Process Engineering

ANALYSIS OF THE RELIABILITY OF THE 20KV DISTRIBUTION SYSTEM OF PT PLN (PERSERO) ULP TARAKAN USING ROOT CAUSE PROBLEM SOLVING METHODS

Sukmawati[1*], Achmad Budiman[2]
[1]Department of Electrical Engineering, Faculty of Industrial Engineering, Universitas Borneo Tarakan, North Kalimantan, Indonesia
[2]Department of Chemical Engineering, Faculty of Industrial Engineering, Universitas Borneo Tarakan, North Kalimantan, Indonesia

Abstract
The distribution system is one of the components of the power system that cannot be separated from the occurrence of interference or damage, which causes factors from within the equipment and factors from outside that can cause blackouts. In this final project, the reliability problems of SAIDI, SAIFI and CAIDI in 2021 at PT PLN (Persero) ULP Tarakan will be discussed using the RCPS (Root Cause Problem Solving) method. The parameters used to see the reliability of the distribution network are SAIDI (System Average Interruption Duration Index), SAIFI (System Average Interruption Frequency Index) and CAIDI (Customer Average Interruption Duration Index). By comparing the SAIDI, SAIFI and CAIDI reliability indices with the IEEE 1366-2003, SPLN 68-2: 1986 and WCS&WCC reliability indices. Where the comparison results of SPLN 68-2: 1986 and SAIDI = 21.09 j/p/t and 6.45 j/p/t (Meets Standard), SPLN 68-2: 1986 and SAIFI = 3.2 k/p/t and 7.38 k/p/t (Does Not Meet Standard), IEEE 1366-2003 and SAIDI = 2.3 j/p/t (Does Not Meet Standard), IEEE 1366-2003 and SAIFI = 1.45 k/p/t and 7.38 k/p/t (Does Not Meet Standard), IEEE 1366-2003 and CAIDI = 1.47 j/g/t and 9.89 j/g/t (Does Not Meet Standard), WCS&WCC and SAIDI = 3 j/p/t and 6.45 j/p/t (Does Not Meet Standard), WCS&WCC and SAIFI = 1.666 k/p/t and 7.38 k/p/t (Does Not Meet Standard). If it does not meet the predetermined standards, Root Cause Problem Solving analysis is carried out.

Keywords:
RCPS; reliability; distribution system; SAIDI; SAIFI; CAIDI

Article History:
Received: October 9th, 2023
Revised: October 16th, 2023
Accepted: October 27th, 2023
Published: October 31st, 2023

Corresponding Author:
Sukmawati
Department of Electrical Engineering, Universitas Borneo Tarakan, Indonesia
Email: sukma1435@gmail.com

1. Introduction

Distribution system is one of the components of the electric power system that cannot be separated from the occurrence of interference or damage, interference or damage that occurs in the distribution system either caused by factors from within the equipment itself or external factors will greatly affect the reliability of the distribution system in delivering electrical energy and will also result in disconnection of the network to the load resulting in blackouts [1].

There are several indices used to determine the level of service reliability based on how long an outage occurs during a year or known as the System Average Interruption Duration Index (SAIDI), how often an outage occurs during a year or known as the System Average Interruption Frequency Index (SAIFI), and how long the average outage felt by consumers for each interruption or known as the Customer Average Interruption Duration Index (CAIDI).

Reliability in distribution systems is a measure of the availability/level of service of providing electricity from the system to the user or customer. Reliability measures can be expressed as how often the system experiences outages, and how quickly it takes to restore conditions from outages that occur [2].

Blackouts result in losses both to customers and to PLN, so it is very necessary to analyze the reliability of the distribution system. One way to get to the root of the problem is to analyze using the Root Cause Problem Solving (RCPS) method.

2. Theory Foundation

A. Distribution System Faults

Disturbances in the distribution system are divided into two, namely:

1. Temporary Disturbance

Temporary disturbances are disturbances that occur for a short time and after that the system can return to normal work, but temporary disturbances that occur repeatedly can cause equipment damage.

2. Permanent Disturbance

Permanent disturbance is a disturbance that can be caused by damage to the equipment so that this disturbance only disappears after the damage is repaired, for example there is a branch that falls on the phase wire of the air duct so that this branch needs to be taken first so that the system can function normally again, in other words permanent disturbances can be overcome after the cause of the disturbance is eliminated.

B. Distribution System Faults

a. SAIFI (System Average Interruption Frequency Index)

SAIFI (System Average Interruption Frequency Index) is an index that informs about the average frequency of outages for each consumer within a year in an evaluated area.

Then SAIFI can be calculated by the formula:[3]

$$\text{SAIFI} = \frac{\text{number of customer outages}}{\text{number of customers served}} \text{ times/customers/year} \quad (1)$$

b. SAIDI (System Average Interruption Duration Index)

SAIDI (System Average Interruption Duration Index) is an index that informs about the average outage duration for each consumer within a year in an evaluated area.

Then SAIDI can be calculated by the formula:[3]

$$\text{SAIDI} = \frac{\text{Hours} \times \text{Customer Outage}}{\text{Number of Customers served}} \text{ Hours/customers/year} \quad (2)$$

c. CAIDI (Customer Average Interruption Duration Index)

CAIDI (Costumer Average Interruption Duration Index) is an index of the average duration or length of interruption for consumers affected by the interruption, formulated in (3):

$$\text{CAIDI} = \frac{\text{SAIDI}}{\text{SAIFI}} \text{ Hours/disturbance/year} \quad (3)$$

With:

SAIDI = Average outage duration index

SAIFI = Average outage frequency index

d. Standard Reliability index Value

This standard is intended to explain and determine the level of reliability of the power distribution system. The goal is to provide a directional guide in assessing the appearance and determining the level of reliability of the distribution system and also as a benchmark for progress or determine the projections that will be achieved by PT PLN (Persero) [3]. Reliability The SAIDI, SAIFI and CAIDI reliability index value standards based on SPLN, IEEE and WCS&WCC are shown in Table 1.

Table 1. Reliability Index Value Standards SAIDI, SAIFI and CAIDI

Reliability Index Standard	**Value Standard**		
	SAIDI j/p/t	**SAIFI k/p/t**	**CAIDI j/g/t**
SPLN 68-2 : 1986	21,09	3,2	-
IEEE std 1366-2003	2,3	1,45	1,47
WCS&WCC	3	1,666	-

Description:

j/p/t = hours/customer/year

k/p/t = times/customers/year

j/g/t = hours/disturbance/year

C. Root Cause Problem Solving Method

Steps to perform the RCPS method:

1. Problem Definition

Knowing what problems actually occur and knowing the impact that occurs from these problems.

2. Problem Structure

Steps in problem structuring:

a. Pareto data

Grouping disturbance data based on the type of disturbance and the cause of the disturbance so that by grouping the disturbance data it will make someone more focused on taking the right solution to handle the disturbance.

Pareto diagrams are used to see or identify the most dominant problems, defect types, or causes so that we can prioritize problem solving. To simplify the pareto diagram, we must first create a percentage of defects.

$$\text{Percentage} = \frac{\text{Number of distractions per item}}{\text{Total number of distractions}} \times 100\% \quad (4)$$

b. Problem tree

Creating a problem tree aims to ensure consistency in the application of problem solving is maintained to solve the problem from the root of the problem so that parts of the problem will not overlap.

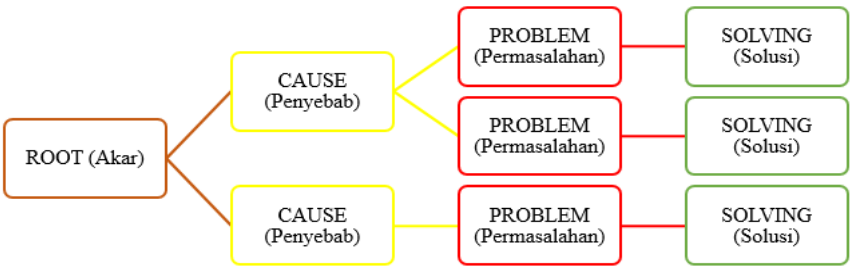

Figure 1. Problem Tree Diagram

3. Prioritize the Problem/Solution

Prioritizing issues can be done by creating a Priority Matrix.

a. Prioritization matrix

This is a comparison diagram between impact and ease of implementation as a stage of solution development.

3. Methods

A. Tools and Materials

The tools and materials used in analyzing and processing the research data consist of hardware and software, namely:

a. Hardware

The hardware used is 1 unit of computer/laptop, printer, stationery paper, cellphone and calculator.

b. Software

The software used is Microsoft Office 2013, including MS Word, MS Excel and MS Power Point and Google Web Browser.

B. Research Stage

The stages of research conducted by the author include:

a. Literature Study

Reading and collecting theories related to research including books, scientific journals, articles, internet services and others.

b. Data Retrieval,

The data that will be taken is the length of the disturbance, the number of times the disturbance, the total outage customers, and the total customers served.

c. SAIDI, SAIFI and CAIDI Calculation

From the data that has been collected, calculations are carried out to determine whether it meets the predetermined standards.

d. Analyzing using the RCPS Method
- Problem structure (pareto data, problem tree)
- Problem prioritization (pareto data analysis, priority matrix)

e. Making Conclusions & Suggestions

4. Results and Discussion

A. Monitoring Data for 2021

Recapitulation of PT PLN (Persero) ULP Tarakan Customer Monitoring Data in 2021 can be seen in Table 2.

Table 2. Customer Monitoring Data of PT PLN (Persero) ULP Tarakan in 2021

No	Month	Number of Customers	Number of Outage Customers	Outage Duration (Hour)	Hours x Number of Outage Customers
1	January	63.738	43.119	1,37	59.480,36
2	February	63.980	51.420	0,72	37.139,69
3	March	64.222	51.442	1,15	59.298,78
4	April	64.563	47.977	0,97	46.582,20
5	May	64.794	21.469	0,96	20.790,85
6	June	65.094	78.324	0,72	56.412,90
7	July	65.364	58.509	0,88	51.898,15
8	August	65.722	11.850	0,46	5.482,13
9	September	66.041	20.326	0,40	8.200,84
10	October	66.345	30.706	0,71	22.064,56
11	November	66.684	33.290	0,68	22.908,57
12	December	66.930	35.400	0,88	31.449,77

B. Calculation of SAIDI, SAIFI and CAIDI

The data used to find the system reliability index (SAIDI, SAIFI and CAIDI) is obtained from the 2021 Customer Monitoring Data Recapitulation data in Table 2.

1. SAIDI analysis can be calculated through the equation:
   - January Month

$$\text{SAIDI} = \frac{\text{Hours} \times \text{Customer Outage}}{\text{Number of Customers served}}$$
$$= \frac{59.480{,}36}{63.738}$$
$$= 0{,}93 \text{ Hours/customer/month}$$

- February Month

$$\text{SAIDI} = \frac{\text{Hours} \times \text{Customer Outage}}{\text{Number of Customers served}}$$
$$= \frac{37.139.69}{63.980}$$
$$= 0{,}58 \text{ Hours/customer/month}$$

2. SAIFI analysis can be calculated using the equation:
   - January Month

$$\text{SAIFI} = \frac{\text{Number of outages}}{\text{Number of customers served}}$$
$$= \frac{43.119}{63.738}$$
$$= 0{,}67 \text{ Times/customer/month}$$

   - February Month

$$\text{SAIFI} = \frac{\text{Number of outages}}{\text{Number of customers served}}$$
$$= \frac{51.420}{63.980}$$
$$= 0{,}80 \text{ Times/customer/month}$$

3. CAIDI analysis can be calculated using the equation:
   - January Month

$$\text{CAIDI} = \frac{\text{SAIDI}}{\text{SAIFI}}$$
$$= \frac{0{,}93}{0{,}67}$$
$$= 1{,}38 \text{ Hours/disturbance/month}$$

   - February Month

$$\text{CAIDI} = \frac{\text{SAIDI}}{\text{SAIFI}}$$
$$= \frac{0{,}58}{0{,}80}$$
$$= 0{,}72 \text{ Hours/disturbance/month}$$

The calculation results of SAIDI, SAIFI and CAIDI are summarized in Table 3.

Table 3. SAIDI, SAIFI and CAIDI Calculation Results

No	Month	SAIDI (j/p/b)	SAIFI (k/p/b)	CAIDI (j/g/b)
1	January	0,93	0,67	1,38
2	February	0,58	0,80	0,72
3	March	0,92	0,80	1,15
4	April	0,72	0,74	0,97

5	May	0,32	0,33	0,96
6	June	0,86	1,20	0,71
7	July	0,79	0,89	0,88
8	August	0,08	0,18	0,44
9	September	0,12	0,30	0,4
10	October	0,33	0,46	0,71
11	November	0,34	0,49	0,69
12	December	0,46	0,52	0,88
Total		6,45	7,38	9,89

Table 3 shows the results of the calculation of the reliability index of the 20kV distribution system. Where the data taken as research for the calculation there are 10 feeders. For the highest SAIDI = 0.93 j/p/b in January, the highest SAIFI = 1.20 k/p/b in June, and the highest CAIDI = 1.38 j/g/b in January.

C. Comparison Results

Table 4. SAIDI and SAIFI Comparison Results with SPLN 68-2: 1986 Standard

No	Standard SPLN 68-2: 1986	SAIDI	Description
1.	21,09 j/p/t	6,45 j/p/t	Meets Standard
No	Standard SPLN 68-2: 1986	SAIFI	Description
2.	3,2 k/p/t	7,38 k/p/t	Does not meet the standard

Table 5. SAIDI, SAIFI, and CAIDI Comparison Results with IEEE 1366-2003 Standards

No	Standard IEEE 1366-2003	SAIDI	Description
1.	2,3 j/p/t	6,45 j/p/t	Does not meet the standard
No	Standard IEEE 1366-2003	SAIFI	Description
2.	1,45 k/p/t	7,38 k/p/t	Does not meet the standard
No	Standard IEEE 1366-2003	CAIDI	Description
3.	1,47 j/g	9,89 j/g/t	Does not meet the standard

Table 6. SAIDI and SAIFI Comparison Results with WCS&WCC Standards

No	Standard WCS&WCC	SAIDI	Description
1.	3 j/p/t	6,45 j/p/t	Does not meet the standard
No	Standard WCS&WCC	SAIFI	Description
2.	1,666 k/p/t	7,38 k/p/t	Does not meet the standard

Based on Table 4 to Table 6 above, the reliability index that is categorized as reliable is only the SAIDI value in SPLN 68-2: 1986, and for other reliability index values it is categorized as less reliable.

D. Disturbance Analysis Using RCPS Method

1. Disruption Analysis with Pareto Data

Analysis of disturbances that occur at PT PLN (Persero) ULP Tarakan using pareto data as follows:

Table 7. Outage Disruption in 2021

Disorder	Causes of Disorder	Causes of Disorder
APP	In the investigation.	Loose connection/Loss of contact.
	Lifetime.	Overload.
	Insulation media leaks/fails.	Fire.
	Procedure error.	Failure of lightning protection equipment.
	Installation error.	
SR Cable	Lifetime.	Loose connection/Loss of contact.

	Vehicle.	Vandalism (Destruction by people).
	Foreign objects.	Third-party construction workers.
	Trees.	Landslides.
	In the investigation.	Fire.
	Insulation media leaks/fails	Animals.
	Overload.	Installation error.
PHBTR	Lifetime.	Animals.
	In the investigation	Fire.
	Overload.	Mechanical system malfunction.
JTR Cable	Trees.	Third-party construction workers.
	Overload.	Installation error.
	Lifetime.	Earthquake.
	Foreign objects.	Fire.
	In the investigation	Loose connection/Loss of contact.
	Vehicle.	Vandalism (Destruction by people).
	Animals.	
Conductor	Foreign objects.	Animals.
	Trees.	Kite/Wire.
	In the investigation	Lifetime.
Maintenance	Substation maintenance.	Repeater Maintenance.
	JTR maintenance.	Feeder maintenance.
	APP maintenance.	
Recloser	Foreign objects.	Trees.
	In the investigation	Animals.
DS/LBS	Foreign objects.	Animals.
	In the investigation	Trees.
Primary/Secondary Cable	Overload.	In the investigation
	Trees.	Loose connection/Loss of contact.
	Animals.	
MV Cell	In the investigation	Protection coordination.
	Corrosive/Salting.	Failure of lightning protection equipment.
	Overload.	
TR Pole	Trees.	In the investigation
	Corrosive/Salting.	Landslides.
Hardware M A	Lifetime.	Flashover.
	In the investigation	
Construction	Pole Replacement.	Cable construction.
Arrester	Lifetime.	Insulation media leaks/fails
	Foreign objects.	
Transformer	Insulation media leaks/fails	In the investigation
CO Branch	In the investigation	Lifetime.
Outgoing Cable to First Pole	-	-
Capacitor / AVR	-	-
Relay Outgoing Feeder	-	-
Pole	-	-
CT/PT kwh Meter Exim	-	-
Termination	-	-
Cable	-	-
Jointing	-	-
FCO Transformer	-	-

After making observations, the causes and frequency of interference are obtained as in Table 7 above. And for the percentage calculation, it is calculated using the following formula:

- APP

$$\text{Percentage} = \frac{\text{Total APP fault frequency}}{\text{Total fault frequency}} \times 100\%$$
$$= \frac{1435}{3002} \times 100\%$$
$$= 47{,}80\%$$

- SR Cable

$$\text{Percentage} = \frac{\text{Total frequency of SR Cable faults}}{\text{Total frequency of faults}} \times 100\%$$
$$= \frac{953}{3002} \times 100\%$$
$$= 31{,}75\%$$

From the above calculations, the percentage of disturbances are all still within reasonable limits because they are still below the percentage of 80%, the disturbance percentage table can be seen in Table 8.

Table 8. Frequency of Disturbance in 2021

NO	Disturbance	Frequency Disturbance	Percentage Disturbance	Cumulative Percentage
1	APP	1435	47,80%	47,8%
2	SR Cable	953	31,75%	79,5%
3	PHBTR	181	6,03%	85,6%
4	JTR Cable	94	3,13%	88,7%
5	Conductor	92	3,06%	91,8%
6	Maintenance	85	2,83%	94,6%
7	Recloser/PMCB	47	1,57%	96,2%
8	DS/LBS	32	1,07%	97,2%
9	Primary/Secondary Cable	25	0,83%	98,1%
10	MV Cell	14	0,47%	98,5%
11	TR Pole	13	0,43%	99,0%
12	Hardware Mounting Assembly	12	0,40%	99,4%
13	Construction	7	0,23%	99,6%
14	Arrester	6	0,20%	99,8%
15	Transformer	4	0,13%	99,9%
16	CO Branch	2	0,7%	100,0%
17	Outgoing Cable to First Pole	0	0,0%	100,0%
18	Capacitor / AVR	0	0,0%	100,0%
19	Relay Outgoing Feeder	0	0,0%	100,0%
20	Pole	0	0,0%	100,0%
21	CT/PT kwh Meter Exim	0	0,0%	100,0%
22	Termination	0	0,0%	100,0%
23	Cable	0	0,0%	100,0%
24	Jointing	0	0,0%	100,0%
25	FCO Transformer	0	0,0%	100,0%
Grand Total		**3002**	**100,0%**	

Because it calculates a reliability, a cumulative percentage is used to find out disturbances whose cumulative percentage is below 100.0%, it will be prioritized to be repaired using a problem tree.

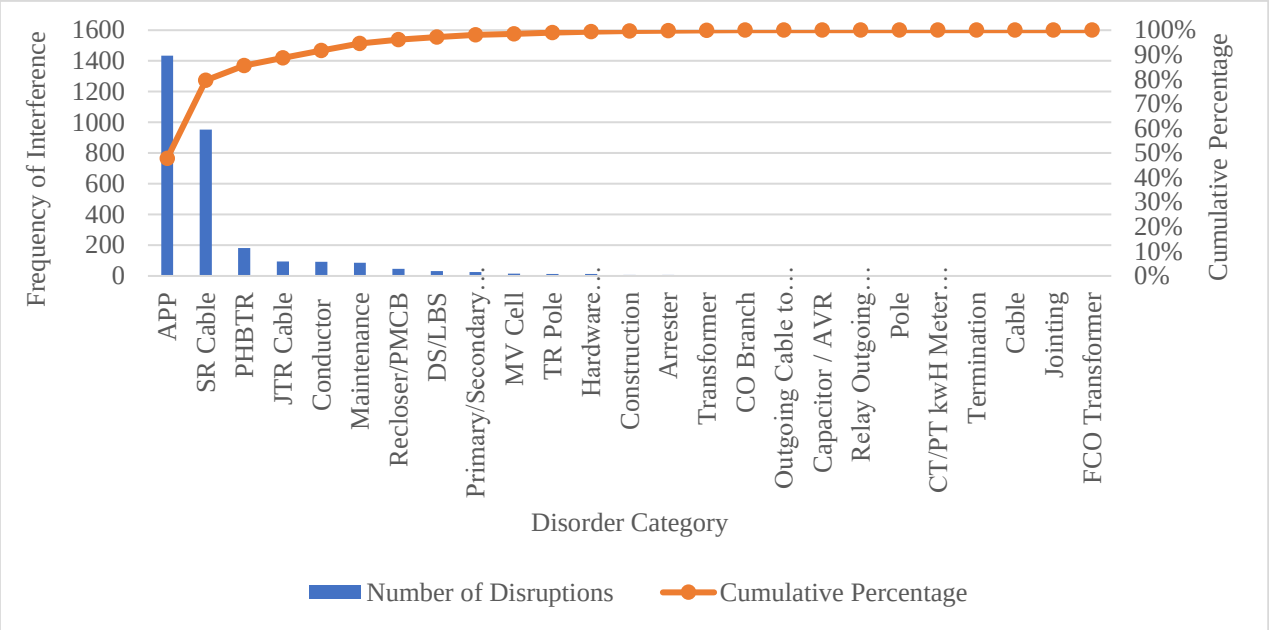

Figure 2. Pareto Diagram of the Causes of Outage Disorders in 2021

2. Disturbance Analysis with Problem Tree and Prioritization Matrix
   a. Problem Tree

   Figs. 3 to 6 below are the mapping of the problems causing the Tarakan city disorder depicted in the RCPS diagram (Problem Tree). To facilitate reading, the following colors are used Brown as Root, Yellow as Cause, Red as Problem, Green as Solving.

p-ISSN: 2963-8577
e-ISSN: 2964-3511

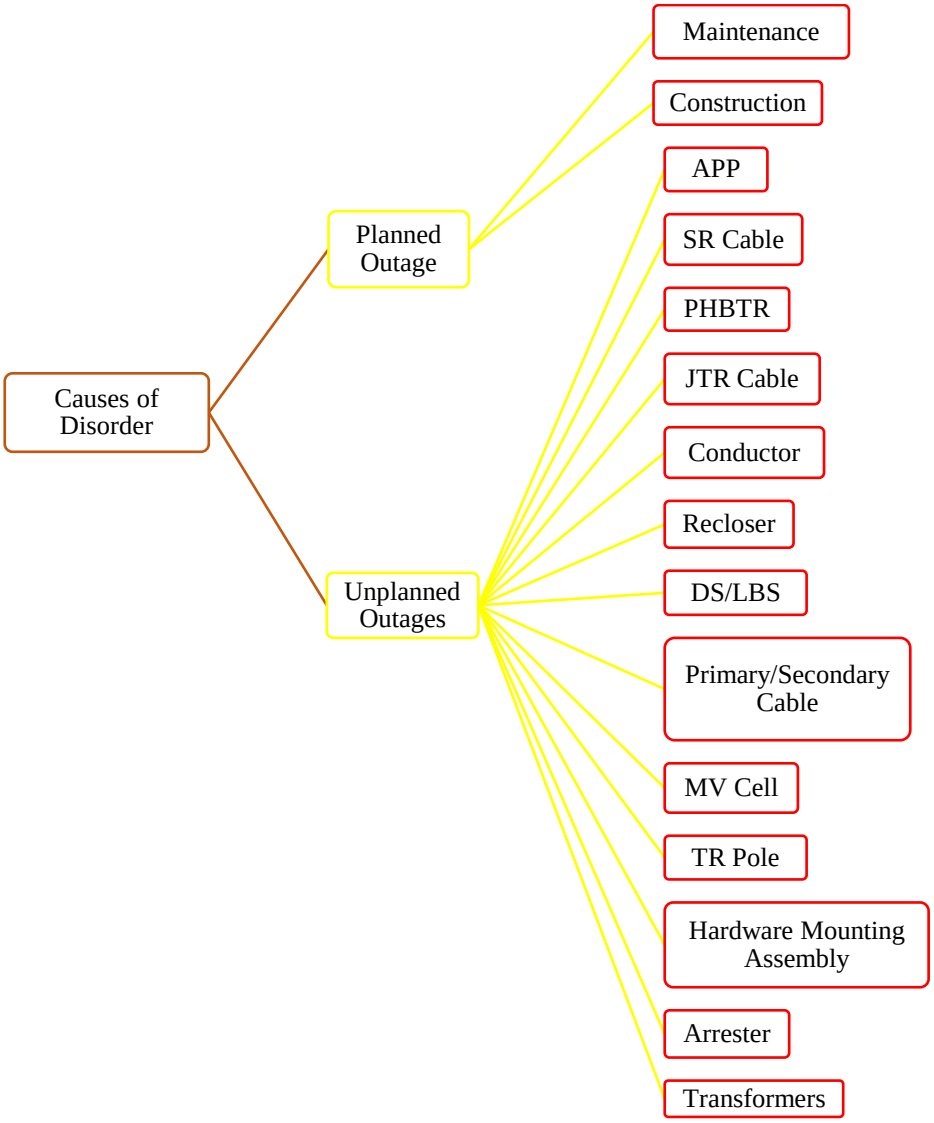

Figure 3. Root Cause of the Problem

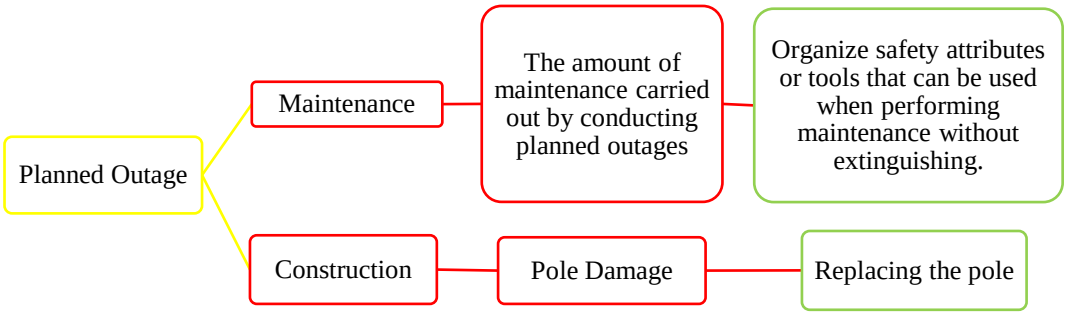

Figure 4. Cause Problem Solving

p-ISSN: 2963-8577
e-ISSN: 2964-3511

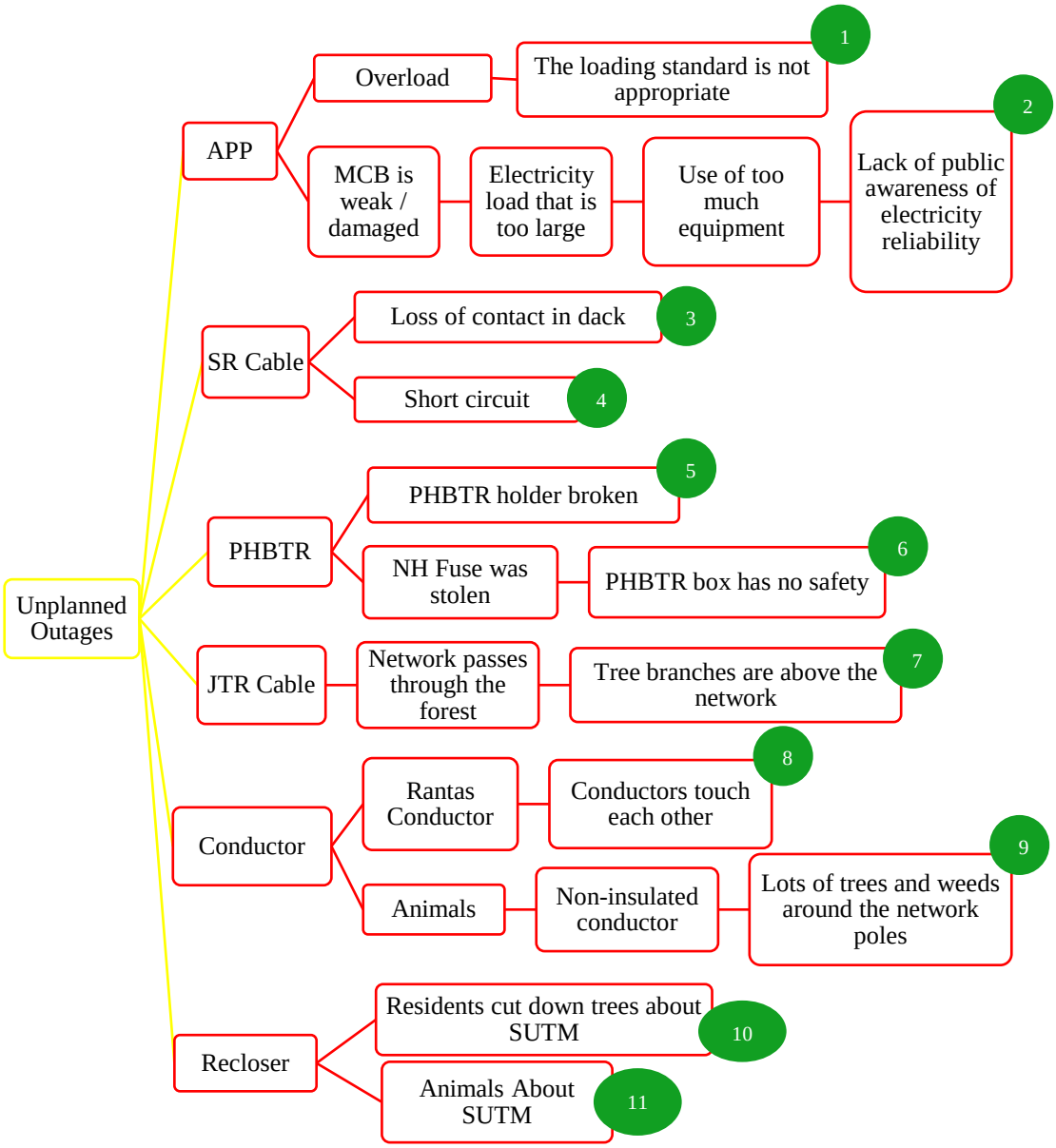

Figure 5. Cause Problem 1

p-ISSN: 2963-8577
e-ISSN: 2964-3511

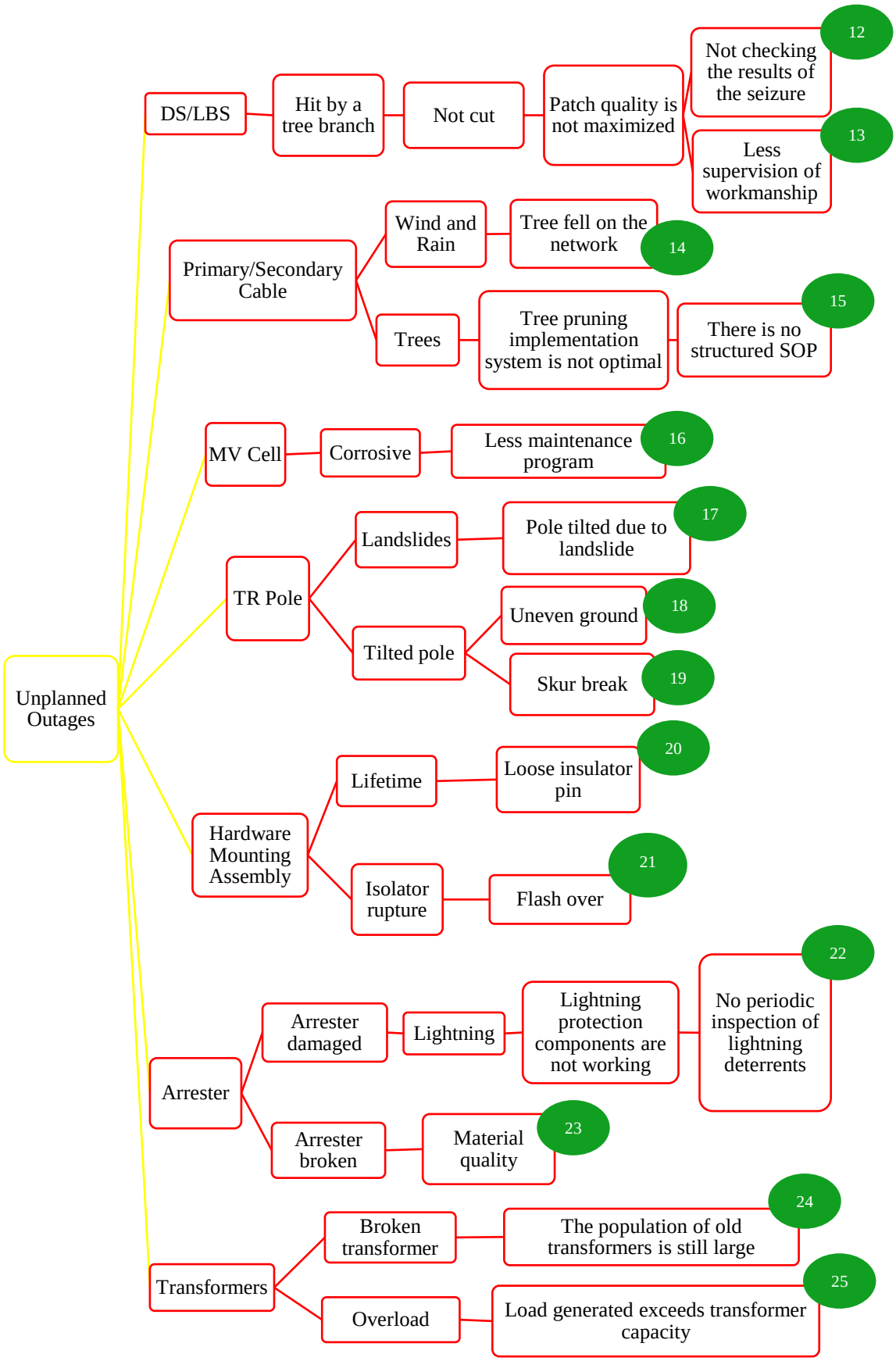

Figure 6. Cause Problem 2

b. Improvement Initiatives and Prioritization

After creating the problem tree, the existing problems can be identified. From these problems will be obtained improvement ideas that can be done to overcome the problem of the number of disturbances that occur in the feeder in the city of Tarakan.

The following problem solving to solve the problem of interference in the repeater in the city of Tarakan

Table 9. Problem Solving

No	Problem	Solving
1	The loading standard is not appropriate	Re-installation by paying attention to the standards that have been set again
2	Lack of public awareness of electricity reliability	Socialization and installation of safety signs
3	Loss of contact in dack	Repairing and replacing cables that have lost contact
4	SR cable emits sparks	Repairing or replacing cables that are short-circuited
5	PHBTR holder broken	Inspect components and replace components that are not suitable for use.
6	PHBTR box has no safety	Installing security such as a padlock on the PHBTR box.
7	Tree branches are above the network	Pruning or removing trees.
8	Conductors touch each other	Repairing or replacing damaged wires.
9	Large number of trees and weeds around network poles.	Pruning or removing trees and clearing weeds around network poles.
10	Residents cut down trees about SUTM	Socialization
11	Animals about SUTM	Installing alkaduri or animal guards
12	Less supervision of work	Appoint a daily supervisor or make a daily supervisor schedule
13	Not checking the results of the seizure	Inspecting and evaluating the results of the demolition
14	Tree fell on the network	Replace broken network cables caused by fallen trees
15	There is no structured SOP	Make SOP
16	Lack of maintenance program	Conduct thorough inspections and follow up on inspection results
17	The pole is tilted because it is prone to landslides	Straighten poles, and conduct checks
18	Uneven ground	Perform casting on poles that are prone to collapse
19	Skur broke	Installing skur
20	Loose insulator pin	Replacing insulator pins
21	Flash over	Replacing the insulator
22	No periodic inspection related to lightning deterrence	Make a regular inspection schedule related to lightning deterrence
23	Low material quality	Replace damaged equipment, use and buy quality materials
24	The population of old transformers is still very large	Conduct a distribution transformer assessment (transformer condition assessment)
25	The load generated exceeds the transformer capacity	Adding transformer power

From these improvement initiatives, it is necessary to prioritize initiatives based on the level of convenience and impact that will be obtained if the initiative is carried out. The following is a priority matrix for reducing outage interference based on the results of the analysis:

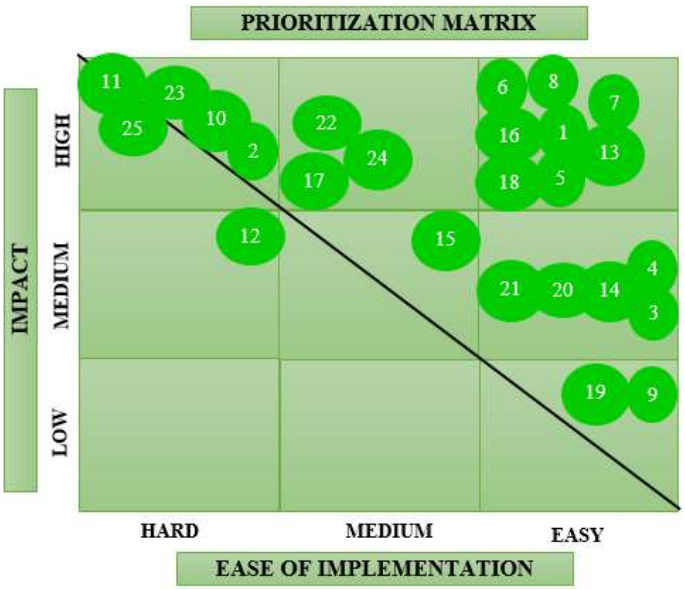

Figure 7. Prioritization Matrix

5. Conclusion

From the results of analysis and calculation, it can be concluded:

a. Based on the data on blackout disturbances in 2021, the most disturbances are disturbances of Limiting and Measuring Devices (APP) with a total number of 1435 disturbances and a duration of 587.1 hours.
b. Based on the 2021 fault frequency data, there are 15 faults out of 25 that are prioritized for repair, namely APP, SR Cable, PHBTR, JTR Cable, Conductor, Maintenance, Recloser/PMCB, DS/LBS, Primary/Secondary Cable, MV Cell, TR Pole, Hardware Mounting Assembly, Construction, Arrester, and Transformer.
c. Based on the reliability of SPLN 68-2: 1986, IEEE, and WCS&WCC, the reliability index of PT PLN (Persero) ULP Tarakan is categorized as reliable and less reliable because the SAIDI, SAIFI and CAIDI values meet the standards and some do not meet the standards, which meet the standards are SPLN 68-2: 1986 with a value of 21.09 j/p/t and SAIDI with a value of 6.45 j/p/t. And those that do not meet the standard are SPLN 68-2: 1986 and SAIFI with values of 3.2 k/p/t and 7.38 k/p/t, IEEE and SAIDI with values of 2.3 j/p/t and 6.45 j/p/t, IEEE and SAIFI with values of 1.45 k/p/t and 7.38 k/p/t, IEEE and CAIDI with values of 1.47 j/g/t and 9.89 j/g/t, WCS&WCC and SAIDI with values of 3 j/p/t and 6.45 j/p/t, WCS&WCC and SAIFI with values of 1.666 k/p/t and 7.38 k/p/t.
d. The highest SAIDI value in January was 0.93 j/p/b, the lowest SAIDI value in August was 0.08 j/p/b. And for the annual SAIDI value of 6.45 j/p/t.
e. The highest SAIFI value in June was 1.20 k/p/b, the lowest SAIFI value in August was 0.18 k/p/b. And the annual SAIFI value is 7.38 k/p/t.
f. The highest CAIDI value in January was 1.38 j/g/b, the lowest CAIDI value in September was 0.4 j/g/b. And the annual CAIDI value is 9.89 j/g/t.

References

[1]. M. R. Harjian, S. T. Supriyatna, and A. B. Muljono, “Analisis Keandalan Sistem Distribusi 20 KV Pada Gardu Induk Kuta PT. PLN Unit Layanan Pelanggan Praya Menggunakan Metode Section Technique Dan FMEA (Failure Model and Effect Analysis),” 2021.
[2]. A. M. Syafar, Penentuan indeks keandalan sistem distribusi 20 kv dengan metode FMEA (Failure Mode Efect Analysis). 2019.
[3]. D. Wahyudi, “Evaluasi Keandalan Sistem Distribusi Tenaga Listrik Berdasarkan SAIDI Dan SAIFI Pada PT. PLN (Persero) Rayon Kakap,” J. Tek. Elektro, vol. 1, no. 8, pp. 1–7, 2016.

Biographies of Authors

Sukmawati is an undergraduate student of Electrical Engineering Department of Borneo University Tarakan. she was born in Bulukumba on January 12, 2000. she was a member of the Electrical Engineering Student Association Organization for the 2019-2022 period.

Achmad Budiman is a Lecturer in Electrical Engineering since 2002. He obtained a Bachelor's degree in electrical engineering from Universitas Gadjah Mada, Yogyakarta. He graduated with a Master's degree in electrical engineering from ITS Surabaya. Currently, He is the Head of the Electrical Engineering Department, at Universitas Borneo Tarakan. He is interested in the field of stability in the power distribution and transmission system.

Vol. 2, No. 2, October 2023, pp. 161-169
p-ISSN: 2963-8577
e-ISSN: 2964-3511
DOI: 10.57102/jescee.v2i2.71

JESCEE
Journal of Emerging Supply Chain, Clean Energy, and Process Engineering

THE QUEUING SYSTEM ANALYSIS FOR PATIENT REGISTRATION COUNTERS AT A HOSPITAL

Ferdinan Ramadhan[1], Resista Vikaliana[2*]
[1]Department of Logistics Management, Sciences Institute of Social and Management Studies STIAMI
[2*]Department of Logistics Engineering, Faculty of Industrial Engineering, Universitas Pertamina

Abstract
Hospitals are vital for healthcare and must continually enhance service quality to boost patient satisfaction. Lengthy outpatient service times, particularly during peak demand, can detrimentally affect service quality. This study investigates the application of queuing theory to the registration service facilities at PKK Hospital. The goal is to identify an appropriate queuing model to describe the outpatient registration counters' conditions and assess the model's performance. The research employs a quantitative approach, using data from observations and literature review, with purposive sampling. The study concludes that the Multiple Channel – Single Phase queuing model is most suitable for describing the outpatient registration counters at PKK Hospital. According to the findings, this queuing model offers optimal performance, with an average service time of 4.076 minutes per patient and a corresponding waiting time of approximately 3-8 minutes.

Keywords:
Queuing system; services; hospitals; multiple channels-single phase

Article History:
Received: October 12nd, 2023
Revised: October 21st, 2023
Accepted: October 29th, 2023
Published: October 31st, 2023

Corresponding Author:
Resista Vikaliana
Department of Logistics Engineering,
Universitas Pertamina
Indonesia
resista.vikaliana@universitaspertamina.ac.id

1. Introduction

The increasingly rapid development of the era must be balanced with the need to be able to keep up with the flow of current developments in the field of goods or services which are currently occurring rapidly. Like providing fast service in the hospital service industry. Hospitals are important institutions of the system service health that provides complex medical services, emergency services, knowledge and technology transfer centers and acts as a referral center. Hospital need always improving quality service to use increase satisfaction user services where this is appropriate Decree of the Minister of Health of the Republic of Indonesia No.983/SK/MENKES/XI/92 which states that the hospital's mission is to provide quality and affordable health services to the community to improve the level of public health.

The minimum time standard for outpatient service based on the Ministry of Health Number 129/Menkes/SK/II/2008 is less or equal to 60 minutes. Queues that occur in hospitals can have an impact on this function if the waiting time is too long, that matter can reduce the quality of service perceived by the community. Very long queues and taking too long to get a turn for service are very annoying, which is detrimental to those who need service because time is wasted just waiting [1], [2]. The provider also experiences indirect losses because it will lower work efficiency, profit, even giving rise to an image that bad for the patient [3].

Queuing theory is the science of queue formation [4]. Queuing is the activity of waiting for your turn to be served due to the arrival of customers and unbalanced service times. The difference between the number of requests for service facilities and the facility's ability to serve gives rise to two logical consequences [5], [6]. Therefore, queuing theory is the right method to solve the problem of long queues in a facility.

According to previous research, queuing theory used to compare manual counters (with serving staff) and the use of self-service counters (THB). The results show that the use of self-service counters reduces queues for ticket purchases [7]. Several other studies show an increase in customer satisfaction after improving the queuing system [8]–[11]. This research examines patient registration queues at hospitals, which has not been studied much by previous research.

To see the application of this queuing theory to registration service facilities, the author chose the PKK hospital as the research object. PKK Hospital is one of the hospital centers located in Bekasi which provides various community needs with complete and adequate facilities so as to attract people's interest in coming for treatment. Currently there are 2 registration counters which are used to serve patients seeking treatment. At certain times, many visitors come to the PKK hospital, resulting in busy service and queue problems. When providing services to patients, events occur in the system queue no can avoided and becomes a problem that must be addressed immediately find a solution. Facilities and services, including queue management, are factors that influence customer satisfaction [12]–[15]. Good service, including queue management, will increase customer satisfaction, including hospital patients [3], [16]. Long queues make patients feel disturbed,because it considers their waiting time spend it wasted free for queue forserved. Queue waiting time will be a determining factor in choosing hospital services. So this research was carried out with the aim of determining an appropriate queuing model to describe the conditions at the outpatient registration counter at PKK Hospital and to determine the performance of the queuing model at the outpatient service registration counter at PKK Hospital.

2. Method

In this research the author uses a quantitative approach with descriptive research type [17] states that "the quantitative approach is the measurement of quantitative data and objective statistics through scientific calculations derived from samples of people or residents who are asked to answer a number of questions about a survey to determine the frequency and percentage of their responses.

Queuing theory is considered appropriate in solving queuing problems [5], [6], [18]. The descriptive research in this study explains how the queuing theory is applied to the queuing system in outpatient registration based on the results of the queuing formula calculation for model B (M/M/S). The research was carried out in December 2021 with data collection carried out over 14 random days. Based on initial discussions with management, this research was carried out at the outpatient registration facility in the poly department from 9 am to 4 pm.

This research involves a dependent variable and an independent variable. Identification of variables in this research is used to assist in determining the data collection tools and data analysis techniques used. The variable grid can be seen in the table below.

Table 1. Variable Grille

Variables	Variable dimensions	Indicator	No. Items
Outpatient registration counter queuing system (Haizer & Render, 2005)	Operational	1. The outpatient registration counter is open from 7 am to 9 pm 2. The hospital opens poly clinic services from 8 am to 8 pm	1 2
	Queue	3. Using a queuing theory system to register 4. Reduces the occurrence of complications during registration	3 4
	Registration process	5. Provide information and education to patients 6. Entering and checking patient personal data and asking for collateral used	5 6
	Number of counters registration	7. Counters are opened according to the number of queues 8. If there is a buildup at one counter, the counter will be opened again	7 8
	Average arrivals	9. View the number of arrivals on the previous day 10. Analyzing the number of arrivals to meet the number of counters that will be opened,	9 10
	Performance	11. Have accuracy, speed, responsiveness and provide clear information in serving patients 12. Hospital employees provide performance in accordance with company SOPs	11 12
	Optimal service	13. Able to provide effective communication to patients 14. Service officers provide accurate information regarding the doctor's arrival schedule	13 14

To obtain data in this study, the author used primary and secondary data obtained from direct observation in the field. In this study, the researcher observed directly at the registration counter, what had to be observed was service time, patients waiting and patients who were undergoing the registration process. And the results of studying various libraries and other literature that are relevant to research objectives such as online media and textbooks. The sampling technique used in this research is purposive sampling. Purposive sampling is a data collection technique with certain considerations. Sampling technique with certain criteria. In this study, the sample used is data from the queue at the registration counter for outpatient registration at the PKK hospital for the period January 2022.

The steps that must be taken in implementing and analyzing data are as follows:

1. Input research data, namely data on the number of arrivals and number of services divided into 60 minutes, and calculate the average number,
2. The average number of arrivals and the number of services must meet steady state conditions ($\rho = < 1\frac{\lambda}{c\mu}$) Where λ is the average number of arrivals. μ is the average number of services and c is the number of officers. If it has not met the steady state then the number of service facilities must be increased.
3. Test the suitability of the Poisson distribution on the number of arrivals and exponential data on service levels using the chi square test.

$$x^2 = \Sigma_{i=1}^{b}\Sigma_{j=1}^{k}\frac{\left(O_{lj} - E_{lj}\right)^2}{E_{lj}} \quad (1)$$

   If the hypothesis is accepted then the distribution follows Poisson and exponential, if the hypothesis is rejected then the distribution is general.

4. Determine the queue model

   Determining the performance measure of the service system, namely (Ls) the number of customers estimated in the system (Lq) the number of customers estimated in the queue (Ws) the estimated waiting time in the system (Wq) the estimated waiting time in the queue.

5. Make conclusions and make decisions based on the value of the analysis obtained to optimize services.

3. Result and Discussion

A. Research Result

In this study, arrivals at the outpatient registration counter at PKK Hospital had a Poisson distribution and service time was assumed to have an exponential distribution. To test the truth, a chi square test was carried out.

Table 2. Data on The Average Number of Service Times at The Outpatient Service Patient Registration Counter at PKK Hospital

Day	Observation time				Number of patients	Amount of time
	09.00-10.00		13.00-14.00			
	Number of patients	Amount of time	Number of patients	Amount of time		
Monday	26	3.92	20	4.15	46	8,073
Tuesday	21	3.95	18	4.22	39	8,175
Wednesday	18	4.17	24	3.88	42	8,042
Thursday	22	4.23	18	3.89	40	8,116
Friday	20	4.25	23	3.91	43	8,163
Monday	20	4.20	19	4.37	39	8,568
Tuesday	20	4.15	25	3.84	45	7,990
Wednesday	19	4.16	20	3.85	39	8,008

Day	Observation time				Number of patients	Amount of time
	09.00-10.00		13.00-14.00			
	Number of patients	Amount of time	Number of patients	Amount of time		
Thursday	21	4.29	19	4.00	40	8,286
Friday	24	4.04	21	4.24	45	8,280
Total	**211**	**41.35**	**207**	**40.35**	**418**	**81,700**

Matrix form for the number of patients from 09.00 - 10.00

1. Matrix A is a matrix that contains the number of patients every day from 09.00-10.00
2. Matrix B is a matrix that contains the total number of patients every day

$$A = \begin{bmatrix} 13 \\ : \\ 11 \end{bmatrix} \qquad B = \begin{bmatrix} 12 \\ : \\ 8 \end{bmatrix}$$

The properties of matrix multiplication are:

If the column and row have the same number then they can be added:

So, $C = A + B = \begin{bmatrix} 25 \\ : \\ 19 \end{bmatrix}$

Calculation Results Based on Analysis Using Queuing Theory

Based on the results of the queuing system regarding arrival rates and service time levels, the outpatient service queuing system model at PKK Hospital is a queuing system model with a Poisson arrival pattern and exponential service time.

a. Average patient arrival

$\lambda = \frac{patient\ count}{duration\ of\ observation}$

$\lambda = \frac{418}{20\ jam}$

λ = 20.90 patients every hour

λ = 0.348 patient every minute

It can be seen that in 1 minute there are 0.348 patients who come or 1 patient comes every 2.874 minutes.

b. Average patient service time

To find the eaverage service time obtained from:

$$x = \frac{cumulative\ service\ time}{patient\ count}$$

$$x = \frac{1704}{418}$$

$x =$ 4.076 minutes per patient

It can be seen that, 1 patient is served for 4,076 minutes, so:

$$\mu = \frac{1}{average\ service\ time}$$

$$\mu = \frac{1}{4.076}$$

$\mu = 0.245$ patients per minute

By obtaining the values of λ and μ where λ > μ, to calculate the performance of the queuing system, it is necessary to know whether the steady state condition is met or not. Steady state is a condition where the level of utility or service facility is less than 1 or the average patient arrival time is smaller. of the average patient service time required. Can be searched as follows:

1. Probability of busy times

$$\rho = \frac{\lambda}{c\mu}$$

$$\rho = \frac{0.348}{2\ (0.245)} = 0.710 = 71\%$$

The value of the service facility usability level obtained is less than 1, meaning that the average patient arrival time does not exceed the average patient service time provided so that it meets steady state conditions.

2. The probability that all officers are unemployed

$$P_0 = \frac{1}{\left[\sum_{n=0}^{C-1} \frac{1}{n!}\left(\frac{\lambda}{\mu}\right) n\right] + \frac{1}{c!}\left(\frac{\lambda}{\mu}\right) C \frac{c\mu}{c\mu - \lambda}}$$

$$P_0 = \frac{1}{\frac{1}{0!}\left(\frac{0..348}{0.245}\right)^0 + \frac{1}{1!}\left(\frac{0.348}{0.245}\right)^1 + \left[\frac{1}{2!}\left(\frac{0.348}{0.245}\right)^2 \frac{2(0.245)}{2(0.245) - 0.348}\right]}$$

$$P_0 = 0.169 = 16.9\%$$

It can be seen that the probability that there are no patients or staff who are unemployed is 16.9%.

3. Average number of patients in the system

$$L_s = \frac{\lambda\mu\left(\frac{\lambda}{\mu}\right)^c}{(C-1)!\ (C\mu - \lambda)^2} P_0 + \frac{\lambda}{\mu}$$

$$L_s = \frac{(0.348\ \times 0.245)\left(\frac{0.348}{0.245}\right)^2}{(2-1)!\ \times ((1 \times 0.245) - 0.348)^2} \times 0.169 + \frac{0.348}{0.245}$$

$L_s = 2.862$ patient every minute

4. Average number of patients in queu

$$L_q = L_s - \frac{\lambda}{\mu}$$

$$L_q = 2.862 - \frac{0.348}{0.245}$$

$$L_q = 1.411$$

It can be seen that, in 1 minute on average there are 1,441 patients in the queue or there is 1 patient in the queue every 0.693 minutes.

5. Average waiting time in the system

$$W_s = \frac{L_s}{\lambda}$$

$W_s = \frac{2.862}{0.348} = 7.706$ minutes per patient

This means that an average of 1 patient waits in the system for 7,706 minutes.

6. Average wait in queue

$$W_q = \frac{L_q}{\lambda}$$

$$W_q = \frac{1.411}{0.348} = 4.14$$

It can be seen that, on average, 1 patient waits in the queue for 4.14 minutes.

At PKK Hospital the number of outpatient visits that come every day varies as can be seen in the graph below.

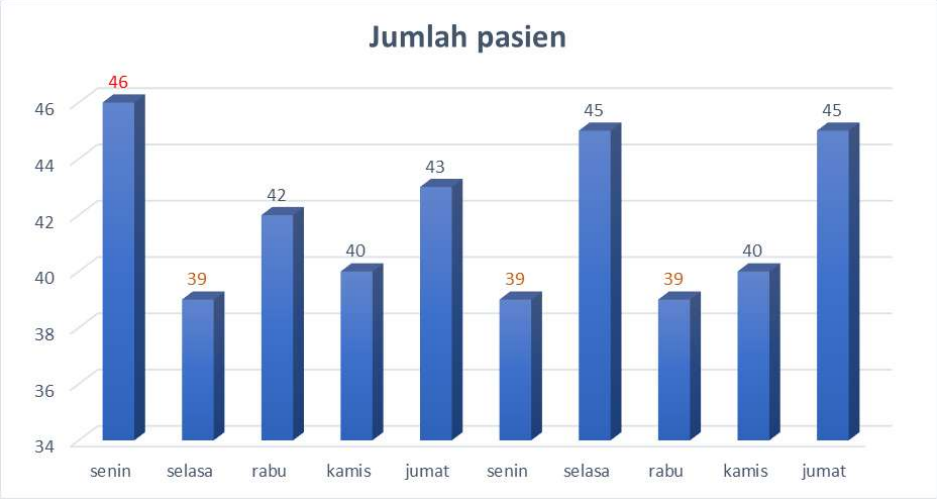

Figure 1. Data on The Number of Outpatients at PKK Hospitals

Based on Fig. 1. the research carried out for 14 days at the PKK hospital had the highest number of outpatients, namely on Monday in the first week, there were 46 patients, while the lowest number of outpatients at the PKK hospital was 39 patients. on Tuesday in week I, Monday in week II and Wednesday in week II.

Queuing System Model

Based on the results of the analysis of the average size of patient arrivals (0.348) and the suitability test is fulfilled, so when determining the performance size of the queuing system at inter-arrival times using a general model.

System Performance Measures

Based on the results of observations of the queuing system process at the outpatient service patient registration counter at PKK Hospital, the queuing performance will be calculated using the queue model (M/M/c): (GD /∞/∞).

The arrival rate and queue service level are known, namely:

$\lambda = 0.348$

$\mu = 0.245$

$C = 2$ officer

So, the queuing system utilization ratio is 71%, which means that the queuing system with 2 officers working is very good. If you test the performance of the queuing system by adding 3 and 4 officers, then the calculation results are presented in Table 3 as follows:

Table 3. Queuing System Utilization Ratio

	λ	μ	Utilization ratio
	Patients/min	Patients/min	%
1	0.348	0.245	71%
2	0.348	0.245	47.30%

	λ	μ	Utilization ratio
	Patients/min	**Patients/min**	**%**
3	0.348	0.245	35.50%

Based on the calculation results in Table 3, it shows that with the addition of counter officers to 3 and 4 officers, the queuing system utilization ratio decreases from 71% to 47.3% and 35.5%. This shows that the queuing system is working well if there are only 2 officers in the service and if there are additional officers, it will be even worse if there are 3 and 4 officers. Therefore it is recommended to maintain with 2 service officers which is quite efficient seen from the utilization ratio.

B. Discussion

Referring to the results of research conducted by the author, it shows that there is an analysis that influences the service at the registration counter. Looking at the results of this research and linking it with research that has been carried out previously by previous researchers regarding the application of queuing theory to BPJS patient services specifically for internal medicine at the Bunda Thamrin general hospital in Medan (Ade Kumalasari, 2018), it can be concluded that queuing theory uses the method according to (Heizer and Render, 2016) (M/M/2): (FCFS /∞/∞) has a role in knowing that service at the PKK hospital registration counter has been achieved with 2 counter staff and the result is 1 patient arrives every 2,874 minutes, and 1 patient waits for 4.1 minutes in the queue, 7,706 minutes of patient waiting in the system with a probability of busy periods of 71%,

This is in line with research (Ade Kumalasari, 2018) entitled "Application of queuing theory to BPJS patient services specifically for internal medicine at Bunda Thamrin Medan general hospital" which states (M/M/2): (FCFS /∞/∞). That patient arrival times have a Poisson distribution, and patient service times have an exponential distribution with the number of services of 2 officers with the result that 1 patient arrives every 2,899 minutes and 1 patient waits for 2.5 minutes in a queue of 12.3 minutes. With the stipulated time at Bunda Thamrin Medan General Hospital of 5-10 minutes.

Thus, the results above indicate that the faster the service provided by the registration officer, the more the patient's waiting time will be reduced. Queuing theory model using methodsaccording to Heizer and Render (2016) (M/M/2) : (FCFS /∞/∞). It is in accordance with previous research on the application of queuing theory in BPJS patient services specifically for internal medicine at the Bunda Thamrin general hospital in Medan (Ade Kumalasari, 2018) and can know that the waiting time for services is optimal according to the hospital's provisions for service times.

4. Conclusion

Referring to the research results and discussion of the previous chapter, the author concludes the application of queuing theory in PKK hospitals as follows:

1. The appropriate queue model to describe the conditions at the outpatient registration counter at PKK Hospital is the Multiple Chanel - Single Phase queue model because there is one queue line and has 2 outpatient registration counter service facilities at PKK Hospital. helps in anticipating queue build-up at outpatient registration counter services. The queuing discipline model used at PKK hospitals is First Come First Serve (FCFS), that is, the first patient to arrive will be served first and the arrival and service capacity is unlimited.
2. The performance of the queuing model for the outpatient registration service system at PKK Hospital is optimal because it has a level of use of registration facilities that is in accordance with the results obtained, namely an average of 1 patient served for 4,076 minutes per patient, this time is in accordance with the waiting time for services at the hospital. The optimal PKK is around 3-8 minutes.

5. Suggestion

Based on the research results and conclusions that have been presented, maintaining 2 service officers is quite efficient, seen from the utilization ratio of 71%. It is hoped that the results of this research can be used as guidance material for further research. The author suggests that future researchers who will research PKK hospitals conduct research using different variables and examine more sources and references.

References

[1] A. P. Singh, "Lean Manufacturing: An Approach for Waste Elimination." [Online]. Available: www.ijert.org
[2] I. Leksic, N. Stefanic, and I. Veza, "The impact of using different lean manufacturing tools on waste reduction," *Advances in Production Engineering And Management*, vol. 15, no. 1, pp. 81–92, Mar. 2020, doi: 10.14743/APEM2020.1.351.
[3] B. S. Sabarguna, *Quality Assurance Pelayanan Rumah Sakit*, 2nd ed. Yogyakarta, Indonesia: Konsorsium Rumah Sakit Islam Jateng-DIY, 2004.
[4] J. Heizer, B. Render, and C. Munson, *Principles of Operations Management with MyOMLab*.
[5] E. Herjanto, *Manajemen Operasi*, 3rd ed. Jakarta: Grasindo, 2008.
[6] N. D. Satmoko *et al.*, *Manajemen Operasi*. Bandung, Indonesia: Widina, 2020.
[7] R. Vikaliana, "Resista Vikaliana: Analysis of Commuter Line Ticket Purchase Queuing System in Bogor Station ANALYSIS OF COMMUTER LINE TICKET PURCHASE QUEUING SYSTEM IN BOGOR STATION," 2017. [Online]. Available: https://megapolitan.antaranews.com
[8] B. I. Lucyantoro and M. R. Rachmansyah, "PENERAPAN STRATEGI DIGITAL MARKETING , TEORI ANTRIAN TERHADAP TINGKAT KEPUASAN PELANGGAN (Studi Kasus di MyBCA Ciputra World Surabaya)," 2017.
[9] B. A. B. Iii, M. Penelitian, and O. Penelitian, "Dani Prabowo, 2012 Analisis Model Antrian Bank Central Asia (BCA) Kantor Cabang Pembantu Cimahi Universitas Pendidikan Indonesia | repository.upi.edu".
[10] R. D. W. I. Puspitasari, "Sistem antrian pada pelayanan tiket kereta api di stasiun solo balapan," 2016.
[11] D. I. Stasiun, B. Cirebon, D. A. N. Stasiun, and C. Prujakan, "Analisis Sistem Antrian … (Sugito)".
[12] B. Imran and A. H. Ramli, "Kepuasan pasien, citra rumah sakit dan kepercayaan pasien di provinsi sulawesi barat," *Buku 2: Sosial dan Humaniora*, vol. ISSN (P) :, pp. 1–7, 2019.
[13] S. Kurnia, W. Hastuti, A. A. Mudayana, and A. P. Nurdhila, "Hubungan Mutu Pelayanan dengan Kepuasan Pasien Peserta BPJS di Rumah Sakit Umum Daerah Yogyakarta," vol. 11, no. 2, 2017.
[14] F. Ahmad, Irmayani, and A. Kadir, "Pengaruh Sarana Prasarana, Prosedur Penerimaan Pasien, Pelayanan Perawat Terhadap Tingkat Kepuasan Pasien Di Ruang Rawat Inap Rumah Sakit Umum Daerah (Rsud) Daya Makassar," *e-Journal STIKES Nani Hasanuddin Makassar*, vol. 2, no. 1, pp. 1–8, 2013, [Online]. Available: http://ejournal.stikesnh.ac.id
[15] A. J. Djohan, "Faktor-Faktor yang Mempengaruhi Kepuasan dan Kepercayaan untuk Mencapai Loyalitas Pasien Rawat Inap pada Rumah Sakit Swasta di Kota Banjarmasin," *Jurnal Aplikasi Manajemen*, vol. 13, no. 2, pp. 257–271, 2015.
[16] J. Harfika and N. Abdullah, "PENGARUH KUALITAS PELAYANAN DAN FASILITAS TERHADAP KEPUASAN PASIEN PADA RUMAH SAKIT UMUM KABUPATEN ACEH BARAT DAYA," *Balance*, vol. XIV, no. 1, 2017.
[17] J. W. Creswell, *Research design : qualitative, quantitative, and mixed methods*, 4th ed. California, USA: Sage Publications, Inc., 2014.
[18] J. Heizer and B. Render, *Manajemen Operasi*, 11th ed. Salemba Empat, 2016.

Biographies of Authors

Ferdinan Ramadhan is a graduate of Logistics Management, Institut Ilmu Sosial dan Manajemen in Jakarta, Indonesia. Currently, he is working in the procurement section in the Nutrition division of a private hospital in Jakarta.

Resista Vikaliana is a lecturer in Logistics Engineering, Faculty of Industrial Technology at Universitas Pertamina Jakarta. Her research interest is in operation management, global supply chain including traceability in supply chain, and logistics halal.

Vol. 2, No. 2, October 2023, pp. 171-177
p-ISSN: 2963-8577
e-ISSN: 2964-3511
DOI: 10.57102/jescee.v2i2.72

JESCEE
Journal of Emerging Supply Chain, Clean Energy, and Process Engineering

SIMULATION STUDY OF A SINGLE-PHASE INDUCTION MACHINE AS A WATER PUMP SYSTEM UTILIZING PHOTOVOLTAIC

Elfin Faturiansyah[1], Syukriyadin Syukriyadin[1*], Hafid Hafid[1]
[1]Department of Electrical and Computer Engineering, Faculty of Engineering, Universitas Syiah Kuala

Abstract
This paper presents a simulation study of using a single-phase induction machine as a solar PV powered water pump system equipped with Maximum Power Point Tracking (MPPT) on the boost converter. Inverters are used to convert DC voltage stored in batteries to drive single-phase induction machines. The simulation was carried out to analyze the system's performance in generating electrical power from solar panels and using it to operate the water pump. This research also considers variables such as fluctuations in sunlight intensity, as well as the dynamic response of induction machines and MPPT converters. From the simulation test results, it was found that the system as a whole will work well if it uses a radiation input that is more significant than 750 W/m^2. The load in the form of a single-phase induction motor, which is inductive, influences variations in the output power produced by the solar PV at the boost converter.

Keywords:
Simulation; solar PV; boost converter; inverter; induction machine

Article History:
Received: October 2nd, 2023
Revised: October 12th, 2023
Accepted: October 21st, 2023
Published: October 31st, 2023

Corresponding Author:
Syukriyadin Syukriyadin
Department of Electrical and Computer Engineering, Universitas Syiah Kuala, Indonesia
Email: syukriyadin@usk.ac.id

1. Introduction

Water use is an obligation that must be fulfilled for human life; in daily needs, water is used for drinking, cooking, washing, and sanitation purposes, as well as agricultural needs [1]. To make it easier for people to regulate the amount of water needed, they can use a water pump machine to provide clean water needs. The problems faced by some people in water pumps, especially those in inland areas, are the need for fuel oil (BBM) supply and the distance of the village from the reach of the PLN electricity network.

Solar power generation (PLTS) is an alternative generator that can be used to overcome this problem. PLTS is also one of the renewable energy generators that is widely used in Indonesia, and this is because Indonesia is a tropical country that has relatively high solar radiation, namely 1677 kWh/m^2 per year. Its use is quite flexible [2].

A solar panel is a *p-n* junction semiconductor that can absorb photons in light to produce electrical power or what can be called the PV effect. The power produced by the panel depends on the radiation value of sunlight, temperature, and the terminal voltage of the solar panel. Several types of materials are used to make solar panels, which provide different characteristics from one another. Various kinds of research have been carried out to implement a mathematical equation for solar panels or PV cells. One of the equivalent circuit models and the mathematical equation model for solar PV can be seen in [3].

Photovoltaics or solar panels are semiconductors that produce output in the form of DC electricity, which is converted from sunlight. The power produced by photovoltaics is greatly influenced by the intensity of solar radiation and the surrounding air temperature, where these two factors are directly proportional to producing the maximum power point [4].

The output produced by photovoltaics is limited by voltage, current, and power. In conditions of stable solar radiation and panel temperature, there is an operating point that can produce voltage and current output with maximum values. In the literature, maximum power point (MPP) conditions are usually called peak power point (PPP) or optimal operating point (OOP).

Using PLTS or Photovoltaic power plant requires the MPPT control method to obtain maximum power output and high efficiency on solar panels. There are two methods or algorithms that are widely used to implement MPPT, namely the Perturb and Observe (P&O) and Incremental Conductance (IC) methods; both methods are more manageable and require lower costs [5].

The P&O method can cause oscillations in the power produced if solar radiation varies, so this method is more suitable for constant solar radiation conditions. Then, to overcome the shortcomings of the P&O method, the Incremental Conductance method can be used because the IC method has a high level of efficiency, as well as good accuracy and power control [6].

The MPPT algorithm is used in DC-DC converters to extract maximum power output from photovoltaics. The converter input is mostly an uncontrolled DC voltage. Switched-mode DC-DC converters are used to change uncontrolled DC input into controlled DC output at the desired voltage level [7]. A boost converter is used because it is able to transfer maximum energy from the PV panel to the load regardless of the varying solar radiation that occurs. The amount of output voltage produced can be regulated by determining the size of the duty cycle (*D*) using a switching component [7][8].

In this research, a single-phase induction machine as a water pump system utilizing a photovoltaic and boost converter controlled by an incremental conductance algorithm and an inverter will be simulated using MATLAB/Simulink.

2. Experimental Section

A. System Modelling

The block diagram shows the system parts used in this research, as shown in Fig. 1.

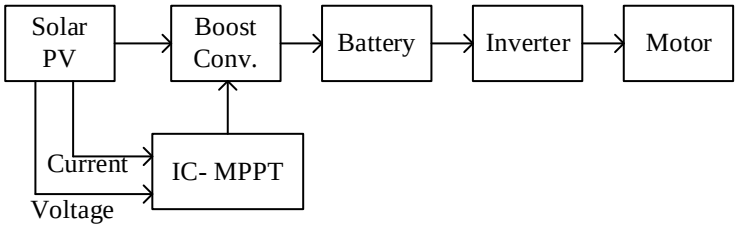

Figure 1. Block Diagram of System Modeling

This research uses Monocrystalline solar panels, the Kyocera KC200GT type, with a capacity of 200 Watts. The solar PV data is shown in Table 1.

Table 1. Specification of Solar PV

Maximum power (Pmax)	200 *W*
Maximum power voltage (Vmp)	26.3 *V*
Maximum power current (Imp)	7.61 *A*
Open circuit voltage (Voc)	32.9 *V*
Shor circuit current (Isc)	8.21 *A*
Series Connected Modules (per String)	12
Strings	2

This research uses induction motor specifications, as shown in Table 2.

Table 2. Specification of Induction Machine

Model	YC90S4
Voltage, Frequency	220V~50Hz
Current	7.7 A
Power	750 Watt
Speed	1500 rpm
Stator impendance	2.02 Ω
Rotor impedance	4.12 Ω
Mutual inductance of the primary winding	0.177 H

B. Simulation Modeling of Solar PV, MPPT with Boost Converter

In this research, it was explained previously that an MPPT system and boost converter will be used, which function to regulate the PV output optimally and according to what is needed. The boost converter will work by

following the IC-MPPT algorithm, where the algorithm will provide a reference voltage to the boost converter, which will then be adjusted to the voltage produced by the solar PV so that the output voltage will be maintained at a specific value. The simulation circuit model is shown in Fig .2.

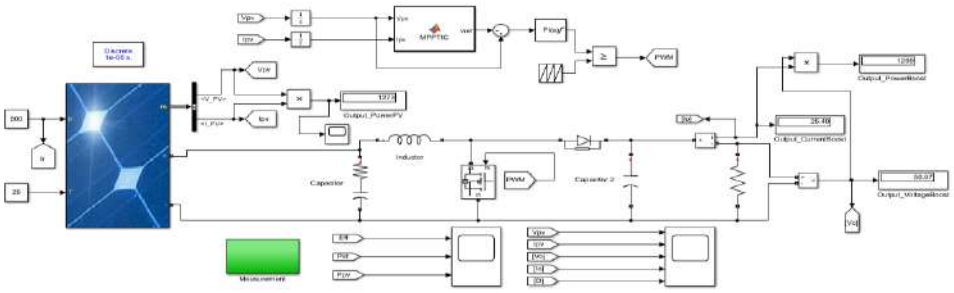

Figure 2. Equivalent Circuit Model of Solar PV, MPPT with Boost Converter

Batteries are used in this research as electrical energy storage, where the stored energy is then fed into the inverter. The inverter used in this research is a single-phase full bridge type with a MOSFET switching component, while the induction motor used is a single-phase induction motor, which functions as the load for the system, as shown in Fig .3.

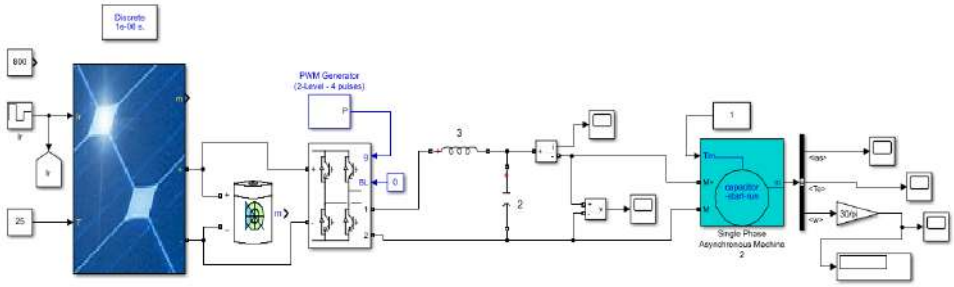

Figure 3. Equivalent Circuit Model of Solar PV, Battery, Inverter and Induction Machine

3. Result and Discussion

The simulation uses a solar radiation value of 800 W/m^2, which is a stable condition because it is considered difficult for solar irradiation to be in STC conditions or a value of 1000 W/m^2. Meanwhile, the temperature has a value of 25°C because this temperature value is still possible to obtain when in the field. Meanwhile, the load used in this simulation circuit is a resistor load with a value of R = 25 Ω, with a time duration of t = 0.75 sec, as shown in Fig .4.

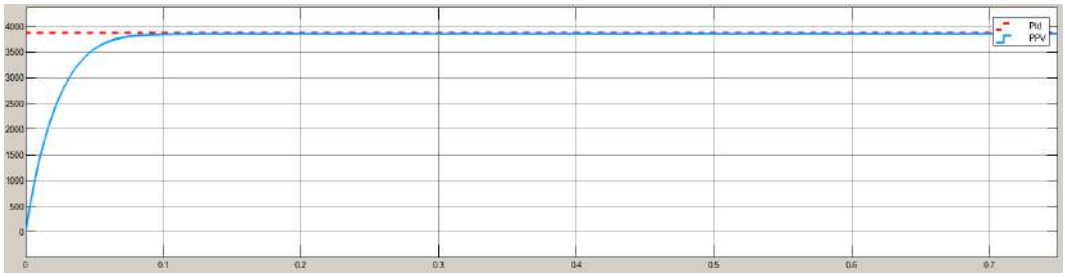

Figure 4. Simulation output power curve under changing environmental conditions

Based on Fig. 4 above, it can be seen that the graph shows the ideal output power Pid as the maximum power that can be produced by the panel (Pmp) according to the datasheet. P_{PV} is as power extracted using a boost converter. The Pid value in Fig. 4 above is 3853 Watts, and this value is obtained through the PV array plot on SIMULINK, which can display the P-V characteristics of the module with an input irradiation value that can be adjusted.

Analytically, the Pid value with irradiation of 800 W/m^2 can be calculated as follows:
Based on the datasheet, it is known as:

V_{oc} = 32.9 V, I_{sc} = 8.21 A, V_{mp} = 26.3 V, I_{mp} = 7.61 A, panel efficiency = 14.19%, and PV STC Area = 1425 mm^2 x 990 mm^2 = 1, 41 m^2.
if $P_{id} = P_{mp}$, Then P_{id} = Efficiency x Solar Irradiation x PV STC area
Pid = 14.19% x 800 W/m^2 x 1.41 m^2
Pid = 160 W
With a total of 24 modules, then
Pid = 160 W x 24
Pid = 3840 W

The power produced by PV takes time to reach the steady state point (rise time); this happens because the MPPT is tracking the maximum power point, where it will adjust the input voltage provided by the PV with the reference voltage set by the MPPT. The reference voltage Vref on the MPPT is compared with the voltage produced by the PV so that an error value is obtained. The error value will then be entered into the PI controller, which regulates the magnitude of the duty ratio, which will be compared again with the carrier signal so that it can finally be given as input to the IGBT gate driver in the boost converter. This method with a PI controller can provide better tracking results than others because it uses a closed-loop system. From the results obtained, the PI controller has succeeded in providing a duty ratio value that can reduce the rise time required by the circuit for a steady state or that the existing rise time process only takes less than 0.1 sec.

Table 3. Output Power for Changing Irradiation Conditions

Irradiance (W/m^2)	P_{pv} (Watt)	P_{id} (Watt)	Extracted Power (%)
800	3853	3876	99
700	3129	3403	92
600	2333	2923	78

For other irradiance conditions, it is shown in Table 3. Based on Table 3, the higher the simulation input irradiation value given, the greater the output power P_{PV} will be and closer to the maximum power P_{mp} so that the resulting extraction power will be greater. The irradiation value of 800 W/m^2 is the best irradiation value to be used in the next system, and this is because the steady state error difference is slight, making the extraction power used also higher.

To see the response of electromagnetic torque and motor speed when the system is loaded with an induction machine, a simulation test has been carried out, as shown in Fig .5 and Fig. 6, respectively.

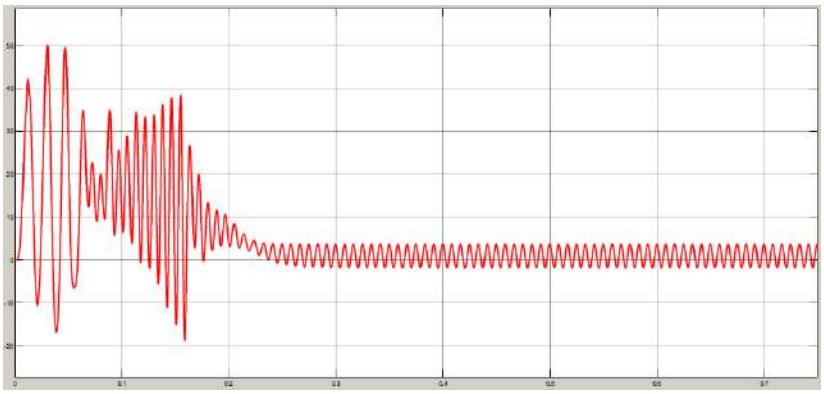

Figure 5. Electromagnetic Torque of Induction Machine

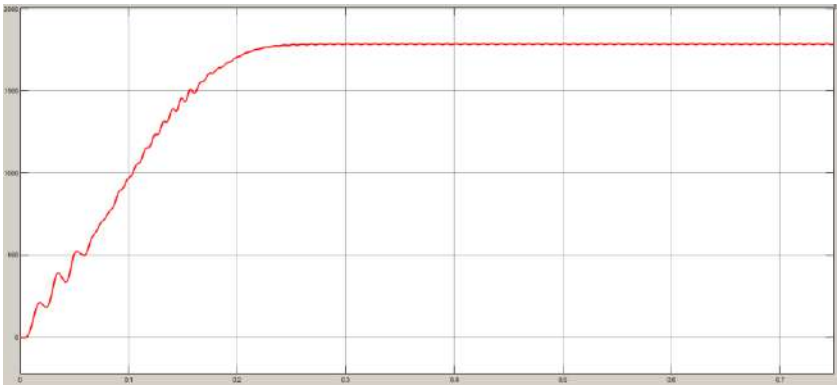

Figure 6. Rotor Speed of Induction Machine

Based on Figure 5, it can be seen that the electromagnetic torque produced by the motor is around 3.7 N.m. Based on Figure 6, the induction machine speed produced by the system is above the synchronous speed of around 1750 rpm; this proves that the induction machine is running at speeds of more than 1500 rpm, so the system has successfully carried the induction machine load.

When the motor is run at irradiance-changing conditions, namely at irradiation conditions of 800 W/m^2 at 0 – 3.5 sec, 600 W/m^2 at 3.51-7 sec, and 700 W/m^2 at 7.1-10.5 sec, the voltage and current responses of induction machine are obtained as shown in Fig .7 and Fig .8, respectively.

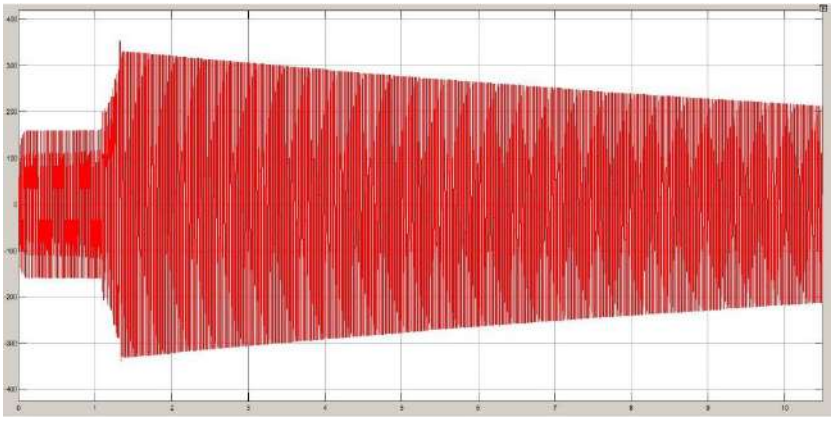

Figure 7. Induction Machine Voltage Response under Variable Irradiance Conditions

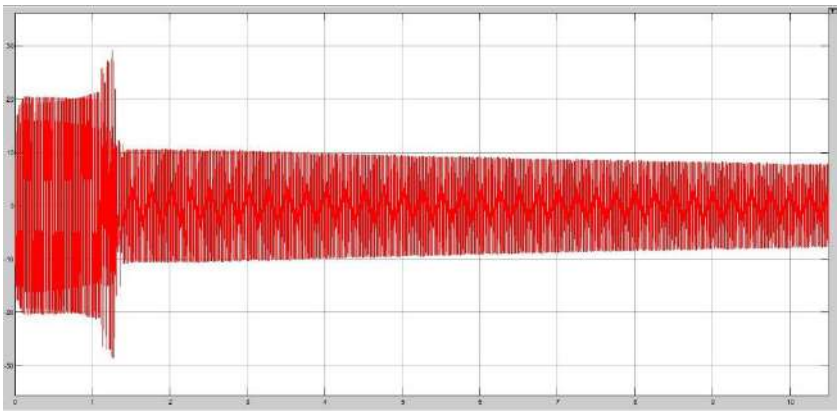

Figure 8. Induction Current Response under Variable Irradiance Conditions

Based on Fig. 7, the voltage produced by the system appears to have decreased quite significantly even though it can produce a maximum voltage at t = 1.25 sec with a value of 320 V; this is due to changes and a decrease in irradiation not being able to provide a stable voltage to the motor load which is an inductive load. Then, the maximum current shown in Fig. 8 above is stable at a value of 10.5 A. The current does not experience significant changes or decreases caused by changes in irradiation, which experience decreases or increases, so the current value will continue to be stable and steady state even though there is a slight decrease.

4. Conclusion

From the simulation results that have been produced, it can be concluded that the system design using the MATLAB/Simulink application has been successfully carried out; this is because the load in the form of a single-phase induction machine has been successfully carried out with a rotor speed of 1750 rpm, which has proven that the system has met load requirements so that the load can produce speeds above the synchronous value.

References

[1] B. Hartono and P. Purwanto, “Perancangan Pompa Air Tenaga Surya Guna Memindahkan Air Bersih Ke Tangki Penampung,” SINTEK J. J. Ilm. Tek. Mesin, vol. 9, no. 1, 2015.
[2] I. D. Sara, “Analisis Potensi Kondisi Suhu dan Radiasi Sinar Matahari di Kota Banda Aceh untuk Pengembangan Pembangkit Listrik Tenaga Surya,” in Seminar Nasional dan Expo Teknik Elektro, 2014, pp. 142–145.
[3] I. Yahyaoui, "Advances in Renewable Energies and Power Technologies: Volume 1: Solar and Wind Energies," Elsevier, 2018.
[4] A. Parastiwi, R. I. Putri, S. Adhisuwignjo, and M. Rifa, "Photovoltaic Terapan: Photovoltaic Terapan," vol. 1. UPT Percetakan dan Penerbitan Polinema, 2018.
[5] M. M. Rana, M. R. Ali, A. K. Ajad, and M. Moznuzzaman, “Analysis of P&O and INC MPPT Techniques for PV Array Using MATLAB,” IOSR J. Electr. Electron. Eng., vol. 11, no. 04, pp. 80–86, 2016.
[6] S. Qin, M. Wang, T. Chen, and X. Yao, “Comparative Analysis of Incremental Conductance and Perturb-and-Observation Methods to Implement MPPT in Photovoltaic System,” in 2011 International Conference on Electrical and Control Engineering, 2011, pp. 5792–5795.
[7] M. K. Kazimierczuk, "Pulse-Width Modulated DC-DC Power Converters," John Wiley & Sons, 2015.
[8] Muhammad Farhan Rozi, Syukiryadin Syukiryadin, Suriadi Suriadi, "Pengaturan Maximum Power Point Tracking (MPPT) Menggunakan Artificial Neural Network (ANN) Berbasis Simulasi," KITEKRO, Vol.5, No.1, 2022.

Biographies of Authors

Elfin Faturiansyah (1998) graduated from Electrical Engineering at Syiah Kuala University in 2023 with a specialization in electrical energy engineering. His research interests are renewable energy, power generation systems, and electric machines.

Syukriyadin (1971) has been working as the academic staff in the Department of Electrical Engineering, University of Syiah Kuala since 1999. His research interests are Renewable Energy Technology, Electric Energy Management, Electric Vehicle Transportation Engineering, Microgrids, Intelligent Electric Power Systems, and Electronic Power Applications in Power Systems.

Hafidh (1972) has been working as the academic staff in the Department of Electrical Engineering, University of Syiah Kuala since 1999. His research interests are focused on power electronics, renewable energy technology and its integration to power grid or isolated grid. His works on renewable energy have been mainly centered in two type of renewable sources; wind and solar. Currently he is preparing some programs related to the integration studies of small scale hybrid renewable power plant and its impact on the distribution networks in a particular area in Aceh, Indonesia.

Vol. 2, No. 2, October 2023, pp. 179-186
p-ISSN: 2963-8577
e-ISSN: 2964-3511
DOI: 10.57102/jescee.v2i2.73

JESCEE
Journal of Emerging Supply Chain, Clean Energy, and Process Engineering

EXTRACTION OF FLAVONOID CONTENT FROM BANANA PEEL (MUSA PARADISIACA L.) BY ULTRASOUND – ASSISTED EXTRACTION METHOD AND ITS SPF VALUE

Hasna Nabila Putri[1], Eduardus Budi Nursanto [1,2,*], Dita Floresyona [1,2], Muhammad Ayoub[3], Mohd Hizami Mohd Yusouf [3]

[1]Chemical Engineering Department-Universitas Pertamina, Jalan Teuku Nyak Arief,, Jakarta Selatan 12220, Indonesia
[2]Center of Downstream Chemical Industry-Universitas Pertamina, Jalan Teuku Nyak Arief, Jakarta Selatan 12220, Indonesia
[3]HICOE—Center for Biofuel and Biochemical Research, Institute of Self-Sustainable Building, Department of Chemical Engineering, Universiti Teknologi PETRONAS, Seri Iskandar 32610, Perak, Malaysia

Abstract
In this study, banana peel was used as a natural sunscreen compound because of its natural antioxidants, such as flavonoids, tannins, triterpenoids, and phenols. Extraction is carried out using Ultrasound-Assisted Extraction method with variations in ethanol solvent concentration and material to solvent ratio at 45°C for 45 minutes. The ethanol concentrations used are 96%, 70%, and 50% and the material to solvent ratio 1/10, 1/20, and 1/30. From the results of the study, the highest yield and SPF value were obtained at ethanol concentration of 50% and material to solvent ratio 1/30. The yield in this variation is 15.2646%, and the SPF value is 8.9874 with the maximum protection category. The highest Total Flavonoid Content (TFC) results was obtained at 70% ethanol concentration and the ratio of material to solvent 1/30, namely 1.6559 mg QE/g. From the variation with the best TFC value, the mass transfer coefficient is 0.0151 mL/µg QE.min.

Keywords:
Kepok banana peel; total flavonoid content; sun protecting factor; ultrasound-assisted extraction

Article History:
Received: August 31st, 2023
Revised: September 30th, 2023
Accepted: October 21st, 2023
Published: October 31st, 2023

Corresponding Author:
Eduardus Budi Nursanto
Department of Chemical Engineering, Universitas Pertamina, Indonesia
Email:
eduardus.bn@universitaspertamina.ac.id

1. Introduction

Ultraviolet radiation, one of which is, will be very dangerous to human skin. Exposure to ultraviolet radiation will damage cells in the skin and can be at risk of becoming a cancer. One example of a disease caused by ultraviolet radiation is burning skin. One way to protect the skin from ultraviolet radiation is by using sunscreen. Sunscreen has an active ingredient that can protect the skin from UV radiation. The active ingredient consists of ultraviolet absorbent and ultraviolet reflector. Because sunscreen is only a protector, there will be a small amount of ultraviolet light absorbed into the skin. Therefore, the sunscreen used must contain a certain amount of SPF or Sun Protecting Factor [1].

Banana peel contains quite a lot of flavonoid compounds because of the high antioxidant content in bananas. Flavonoid compounds can be used as constituent compounds sunscreen. Flavonoid compounds are obtained by extraction, one of the extraction methods that can be used is Ultrasound-Assisted Extraction (UAE). In Indonesia, it is very rare to find the extraction of flavonoids using UAE. Whereas when compared to other extraction methods, such as maceration or soxhlet, UAE has advantages that can reduce extraction time and the use of solvents [2-5].

2. Experimental Section

A. Banana Peel Preparation

Banana peels are washed thoroughly using running water, then dried in an open room overnight. Then, the dry skin is blended until it goes into pieces.

B. Extraction Of Flavonoid Content in Banana Peel

Banana peels are weighed and put into an Erlenmeyer flask containing solvent. The solvent used, namely ethanol, was varied in concentration 96%, 70%, and 50% with each amount based on the raw material/solvent ratio that had been determined, i.e. 1/10 (g/mL), 1/20 (g/mL), 1/30 (g/mL).

Extraction was carried out using an ultrasonic water bath at atmospheric pressure with a temperature of 45°C for 45 minutes. The extract obtained was then filtered using a vacuum filter and then the filtrate was separated from the solvent by a vacuum oven at a temperature of 40-50 °C and a pressure of 0.2 bar. The yield of the extract for each variation was calculated as % (wt/wt) using the equation:

$$\%yield = \frac{dried\ banana\ peel\ extract\ mass}{raw\ banana\ peel\ mass} \times 100\% \quad (1)$$

C. Phytochemical Screening

Flavonoid Test. 1 mL of banana peel extract was mixed with 1 mL of 96% ethanol, 0.1 gram of Mg powder, and 10 drops of concentrated HCl. If the extract contains flavonoids, it will form red, yellow or orange colour.

Triterpenoid Test. 2 mL of banana peel extract was mixed with 10 drops of CH_3COOH and 2 drops of concentrated H_2SO_4. Then shake gently and leave for a while. If the extract contains triterpenoids, it will form red colour.

Tannin Test. 2 mL of banana peel extract was mixed with 2 mL of aquadest and few drops of 1% $FeCl_3$. If the extract contains tannins, it will form blackish green colour.

Phenolic Compound Test. 1 mL of banana peel extract was mixed with 3 drops of 1% $FeCl_3$. If the extract contains polyphenol, it will form red, green, blue, purple or black colour.

Alkaloid Test. 10 mL of banana peel extract was mixed with 1.5 mL of 2 M HCl then heated for 5 minutes and added 5 drops of Dragendorff's reagents. If the extract contains alkaloid, it will form orange color and precipitate.

Saponin Test. 2 mL of banana peel extract was mixed with 10 mL hot aquadest, shake for 15 minutes then added a few drops of 2 M HCl. If the extract contains saponins, it will form a stable foam for a while.

D. Determination Of Total Flavonoid Content (TFC) Using $AlCl_3$ Method

Determination TFC of banana peel extract was carried out using the colorimetric method with quercetin was used to make a calibration curve. The results were expressed as μg quercetin (μg.QE)/gr banana peel.

25 mg of quercetin was weighed and put into a 25 mL volumetric flask, then added ethanol of all concentrations up to 25 mL as the main solution of 1000 μg/mL. Then diluted to standard solutions of 40 μg/mL, 60 μg/mL, 80 μg/mL, 100 μg/mL, and 120 μg/mL. Then, 0.5 mL of the standard solution and 0.5 mL of each extract solution were separated into several vials and added with 1.5 mL of 96% ethanol, 0.1 mL of 10% $AlCl_3$, 0.1 mL of 1 M potassium acetate and 2.8 mL of aquadest. These solutions were incubated for 30 minutes at 25°C then the absorbance of each solution was measured at a wavelength of 438 nm using a UV-Vis spectrophotometer. The absorbance data of each standard solution then made into a calibration curve by connecting absorbance as coordinate (Y) and concentration of standard solution as abscissa (X), while the absorbance data of each extract solution was used to calculate the TFC using the equation:

$$TFC = \frac{c \times V \times f}{m} \quad (2)$$

where TFC is the total flavonoid content (μg.QE/mg dry weight), c is quercetin equivalent (μg/ml), V is total product volume (mL), f is dilution factor (1), and m is raw banana peel mass (mg).

E. Determination Of Mass Transfer Coefficient

The mass transfer coefficient was calculated for the extract which had the highest TFC. Extraction was carried out with time variations of 5, 15, 30, 45 and 60 minutes. The calculation of the mass transfer coefficient is carried out by the following equation:

$$\frac{t}{C_t} = \frac{1}{k(C_e)^2} + \frac{t}{C_e} \quad (3)$$

where k is second-order mass transfer coefficient (mL/μg.min), t is time (minutes), C_e is concentration of solute in solution at equilibrium (ppm QE), C_t is concentration of solute in solution at a certain time t (ppm QE).

The mass transfer coefficient value is obtained by plotting the graph between t/C_t as the Y axis and t (time) as the X axis. Then $1/C_e$ will be obtained as the slope and used to calculate the mass transfer coefficient (k) from the intercept.

F. Determination Of SPF Values

Dried banana peel extract of 96%, 70%, and 50% ethanol was dissolved in each ethanol concentration to the concentration of 300 ppm. SPF value was determined with firstly calculated the area under curve (AUC) of absorbances at 280-400 nm with 5 nm interval using the equation:

$$[AUC] = \frac{A_a + A_b}{2} \times (dP_{ab}) \quad (4)$$

with A_a is absorbance at wavelength a nm, A_b is absorbance at wavelength b nm, and dP_{ab} is difference in wavelength a and b. AUC of each wavelength segment is summed up to calculate the SPF value using the equation:

$$log\ S\ PF = \frac{\sum AUC}{(\lambda_n - \lambda_1)} \quad (5)$$

with λ_n is the longest wavelength (400 nm), and λ_1 is the shortest wavelength (290 nm).

3. Result and Discussion

Based on Fig. 1 and Table 1, it can be concluded that there is an increase in the amount of yield along with the increasing amount of solvent used. This is in accordance with the principle of the gradient concentration that increase following the greater volume of solvent [1]. In addition, the greater the volume of solvent, the faster the diffusion process occurs and facilitate the mass transfer process [2].

Table 1. Extraction Yield Result

Yield (%)			
Material/Solvent Ratio (gr/mL)	**Ethanol Concentration (%)**		
	96	**70**	**50**
1/30	10.4065	11.9175	15.2646
1/20	8.8401	9.9564	13.5078
1/10	5.7167	6.6717	11.3103

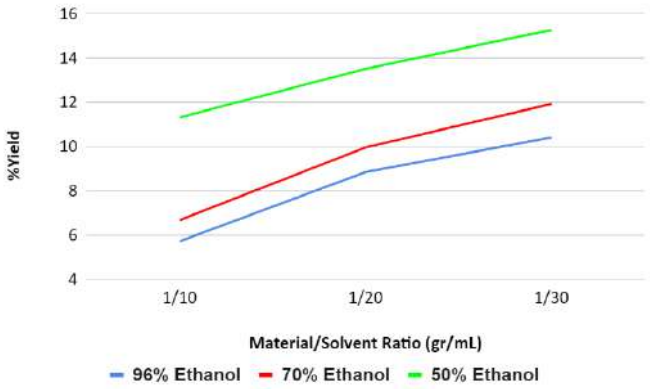

Figure 1. Effect of ethanol concentration and material/solvent ratio on extraction yield of banana peel

Meanwhile, the smaller concentration of solvent used, the greater the extract yield produced. According to previous studies, with variations in ethanol concentrations of 0% (100% water), 50%, and 100%, the highest yield was obtained at a concentration of 50% and the lowest at a concentration of 100% [3]. This result shows correlation between increasing polarity of ethanol with the addition of water volume, so that more polyphenolic compounds (not only flavonoids) are extracted [3]. In addition, the viscosity value of water is higher than ethanol, so ethanol has lower barrier mass transfer [3].

Based on the Table 2, in this study banana peel extract contained several types of compounds, such as flavonoids, triterpenoids, tannins, phenolic compounds, alkaloids, and saponins. This is due to the ability of these compounds to dissolve in polar solvents. These compounds are included in the antioxidant compounds that have many benefits. One of the benefit is for a sunscreen constituent, because of high photoprotective ability of these compounds.

Table 2. Phytochemical Test of Extract Sample

Phytochemical	Result	Examples of Compounds
Flavonoid	Red (+)	Quercetin, catechin, gallocatechin [4]
Triterpenoid	Red (+)	Lupenone [5]
Tannin	Blackish green (+)	Tannin **Error! Reference source not found.**
Phenolic Compound	Black (+)	Chyrsin, caffiec acid, cinnamic acid [7]
Alkaloid	Orange (+)	Phenylalanine [8]

Saponin	Stable foam (+)	Saponin **Error! Reference source not found.**

The TFC value can be calculated using a standard calibration curve and the results are expressed in mg.QE (Quercetin Equivalent)/gr banana peel. The standard curves were made for 96%, 70%, and 50% ethanol concentrations respectively and the equations can be seen in Table 3 below.

Table 3. Standard Calibration Curve of Quercetin

Ethanol Concentration	Equation	R^2
96%	y = 0.004x – 0.0103	0.9915
70%	y = 0.0048x – 0.0184	0.9932
50%	y = 0.005x – 0.0183	0.9935

Based on Fig. 2 and Table 4, there is strong correlation between extract yield with the increasing amount of solvent during extraction. This is in accordance with the principle of the concentration gradient which gets bigger following increase of solvent amount [1]. In addition, the greater the volume of solvent, the faster the diffusion process occurs [2]. The amount of solvent volume will also affect the contact area between the material and the solvent. The more amount of solvent led to wider contact area and the distribution of the solvent [9]. Even distribution of solvent can increase yield and the amount of solvent will reduce the level of saturation of the solvent so that the components will be extracted perfectly [9].

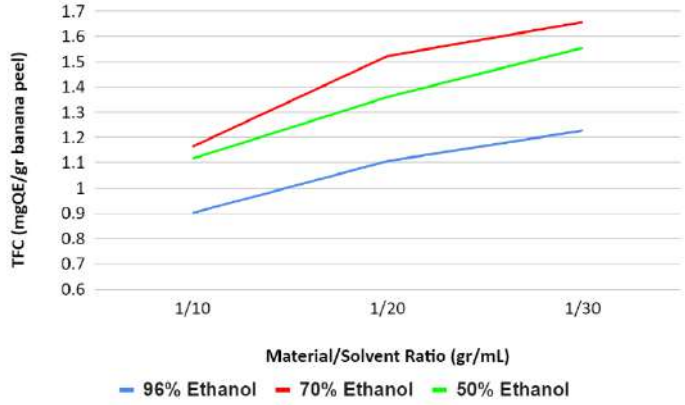

Figure 2. Effect of ethanol concentration and material/solvent ratio on TFC banana peel extract

Table 4. Total Flavonoid Content (TFC) on Banana Peel Extract

TFC (mgQE/gr banana peel)			
Material/Solvent Ratio (gr/mL)	Ethanol Concentration (%)		
	96	70	50
1/30	1.2273	1.6559	1.5548
1/20	1.1068	1.5222	1.3604
1/10	0.9014	1.1639	1.1166

In addition, an increasing number of solvents will also increase the ability of the solvent to extract and increase the contact time that lasts between the material and the solvent [9]. Since the UAE uses cavitation principle for mass transfer, an increase in total volume led to higher extraction efficiency [10].

Based on Fig. 2, it is also known that the TFC value of 70% ethanol has the highest yield, followed by 50% ethanol and 96% ethanol. Quercetin solubility should increase with increasing ethanol concentration [11]. However, in this study, the lowest TFC value at 96% ethanol. Based on the phytochemical screening and from reference, it was found that the type of flavonoid in banana peel is catechin. Catechin is a flavonoid that belongs to the flavanol group, while the $AlCl_3$ method cannot detect flavonoids other than the flavone and flavonol groups [12].

The equation used to determine the value of the mass transfer coefficient (k) is a second-order reaction rate equation, with previous fittings and the highest R^2 value is obtained when the second-order equation is used.

In addition, the determination of the mass transfer coefficient with the first order cannot be used to describe all processes and can only describe processes that have a single mechanism [13]. There are two main mechanisms involved in extraction with UAE in plant samples. The first mechanism involves changes in plant

cell walls due to ultrasonic waves from the UAE. During this process, water molecules from the solvent are used assisted with ultrasonic energy which makes the plant matrix swell and then destroys it which makes the components of bioactive compounds extracted out. The second mechanism is the process of dissolving flavonoids in organic compounds with the help of ultrasonic waves, so that ethanol can extract the desired flavonoid compounds.

From (3), we get a graph plot between t/C_t vs. time (minutes) as follows.

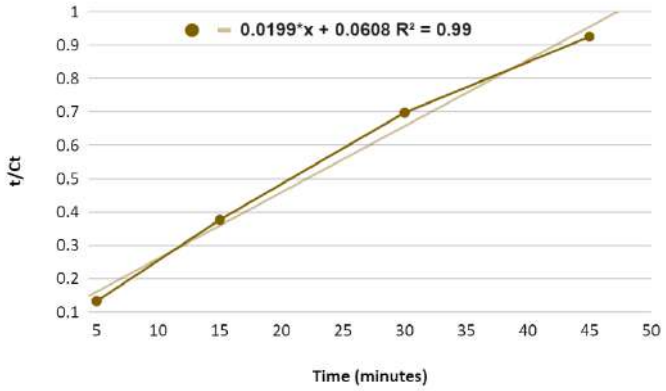

Figure 3. Mass transfer kinetic model of flavonoid extraction from banana peel

.

Fig. 3 shows the equation obtained from plotting t vs. t/C_t is $y = 0.0199x + 0.0608$ with $R^2 = 0.9901$. Through the calculation of the intercept value, the mass transfer coefficient value of 0.0151 mL/μgQE.min was obtained. This number means that in 1 minute of extraction, to extract 1 μg quercetin is required 0.0151 mL 70% ethanol.

Table 5. SPF Value Results from Extracted Banana Peels

Ethanol Concentration (%)	SPF Value
96	7.6138
70	7.6566
50	8.9874

Based on the Table 5, Sun Protection Factor (SPF) value from extracts of 96%, 70% and 50% are 7.6138, 7.6566, and 8.9874. The SPF value of banana peel extract from solvent concentrations of 96% and 70% can be categorized as having extra protection and 50% solvent concentration can be categorized as having maximum protection based on the classification by Wilkinson & Moore [15].

Table 5 shows that the highest SPF value was obtained at 50% ethanol extract and the lowest SPF value was obtained at 96% ethanol extract. The SPF value obtained is comparable to the yield which also has the highest yield on 50% ethanol extract and the lowest on 96% ethanol extract. However, this result is not match with the TFC value where, the highest TFC value is in the 70% ethanol extract. There is possibility of other bioactive compounds besides flavonoids, which are more soluble in 50% ethanol resulting in high yield value. Thus, it can be said that the more bioactive compounds extracted, the higher the SPF value obtained.

Bioactive compounds that have a photoprotective role are generally soluble in polar solvents because they are included in the class of antioxidant compounds, especially phenolic compounds. Based on previous research, the highest SPF value of hazelnut peel ethanol extract was obtained in the ethanol extract which had the highest Total Phenolic Content (TPC) value, not in the extract with the highest TFC value [14]. This proves that the SPF value is not only depend on TFC, but also by the TPC value. Several photoprotective phenolic compounds in addition to the flavonoid group contained in the ethanolic extract of banana peels are p-coumaric acid, β-tocopherol [16]; ferulic acid [18]; chlorogenic acid [19]; carotenoids, coumarin [20].

The SPF value produced by natural ingredients often does not meet the standards commonly sold in the market. However, the incorporation of natural ingredients with synthetic ingredients as a constituent of sunscreens has been shown to increase the SPF value of the sunscreen. This is evidenced by previous research, the combination of 0.1% rutin (a type of flavonoid) with 6% benzophenone resulted in an increase in the SPF value from 24.3±1.53 to 33.3±2.89 when flavonoids were added [16].

The banana peel extracts were analysed using FTIR for identifying the chemical bond in the component. The FTIR result of chemical bond shows the possibility component. The analysis was carried out on all variations of

ethanol concentration (96%, 70%, and 50%) with a material/solvent ratio of 1/30 gr/mL and used quercetin as the standard.

Table 6. FTIR Results of Banana Peel

Bond	Wavelength Frequency (cm^{-1})	Banana Peel Extract Wave Number (cm^{-1})			Identification Result
		96% Ethanol	70% Ethanol	50% Ethanol	
O-H	3500-3200	3367.1030	3353.6040	3415.3140	Flavonoids, Saponins
C-H	3200-2800	2946.6970	2952.4820	2954.4110	Phenols
C=O	1800-1600	1658.4810	1650.7670	1646.9110	Flavonoids
N-H	1680-1550	1658.4810	1650.7670	1646.9110	Alkaloids
CH_2	1480-1440	1452.1350	1454.0640	1457.9210	Triterpenoids
CH_3	1480-1440	1452.1350	1454.0640	1457.9210	Triterpenoids
C=C aromatic	1465-1430	1452.1350	1454.0640	1457.9210	Flavonoids
C-O	1300-800	1112.7250	1110.7970	1108.8680	Flavonoids, Phenols, Tannins
C-O-H	1050-1000	1027.8730	1022.0870	1018.2300	Tannins
C-H aromatic	800-500	638.3225	673.0349	613.2524	Flavonoids
Fingerprint Region of Flavonoid	1300-900	1027.8730	1022.0870	1018.2300	Flavonoids

From Table 6, the three extracts have the main functional groups present in flavonoid compounds, namely O-H, C=O, C=C aromatic, and C-H aromatic [21]. In addition, there are also supporting functional groups that represent other compounds, namely triterpenoids, alkaloids, tannins, phenols, and saponins according to the results of phytochemical screening in this study.

4. Conclusion

Extraction of flavonoids from banana peels using Ultrasound-Assisted Extraction (UAE) method was carried out with variations in ethanol concentration and material/solvent ratio. The greater amount of solvent resulting in higher extract yield and Total Flavonoid Content (TFC). The highest yield and TFC was found at the ratio of material to solvent 1/30 gr/mL. And the smaller the solvent concentration, the greater the yield obtained which is at 50% ethanol. While the highest TFC value obtained at 70% ethanol and the lowest at 96% ethanol. The highest TFC in banana peels was obtained at 70% ethanol with a material/solvent ratio of 1/30 gr/mL, which was 1.6559 mg.QE/gr. The highest Sun Protecting Factor (SPF) value of banana peel extract was obtained at 50% ethanol, which was 8.9874 with maximum protection category. The mass transfer coefficient value of banana peel extraction was calculated on the variation with the highest TFC, and the mass transfer coefficient value was 0.0151 mL/μg.QE.min

Acknowledgment

This work was supported by Universitas Pertamina – Universiti Teknologi Petronas Research Grant

References

[1] M. D. Esclapez, J. V. Garcia-Perez, A. Mulet and J. A. Carcel, "Ultrasound-Assisted Extraction of Natural Products," *Ca´rcel,* pp. 108-120, 2011.
[2] N. Medina-Torres, T. Ayora-Talavera, H. Espinosa-Andrews, A. Sánchez-Contreras and N. Pacheco, "Ultrasound Assisted Extraction for the Recovery of Phenolic Compounds from Vegetable Sources," *Agronomy,* pp. 1-19, 2017.
[3] S. Sahin and R. Samli, "Optimization of olive leaf extract obtained by ultrasound-assisted extraction with response surface methodology," *Ultrasonics Sonochemistry,* pp. 595-602, 2013.
[4] C. Dong, H. Hu, Y. Hu and J. Xie, "Metabolism of Flavonoids in Novel Banana Germplasm during Fruit Development," *Frontiers in Plant Science,* pp. 1-10, 2016.

[5] F. Xu, X. Huang, H. Wu and X. Wang, "Beneficial health effects of lupenone triterpene: A review," *Biomedicine & Pharmacotherapy,* pp. 198-203, 2018.
[6] Hasma and Winda, "Identifikasi senyawa metabolit sekunder ekstrak kulit pisang kepok (musa paradisiaca l) dengan metode KLT," *Jurnal Kesehatan Manarang,* pp. 125-131, 2019.
[7] A. M. Aboul-Enein, Z. A. Salama, A. A. Gaafar, H. F. Aly, F. Abou-Elella and H. A. Ahmed, "Identification of phenolic compounds from banana peel (Musa paradaisica L.) as antioxidant and antimicrobial agents," *Journal of Chemical and Pharmaceutical Research,* pp. 46-55, 2016.
[8] B. A. Ahmad, U. A. Zakariyya, M. Abubakar, M. M. Sani and M. A. Ahmad, "Pharmacological Activities of," in *Banana Nutrition - Function and Processing Kinetics*, IntechOpen, pp. 1-20, 2019.
[9] F. Mas'ud, Fajar, H. Bangngalino, S. Indriati, A. Todingbua, Suhardi and M. Sayuti, "Model development to enhance the solvent extraction of rice bran oil," *OCL,* pp. 1-9, 2019.
[10] I. F. Olawuyi, J. J. Park and W. Y. Lee, "Effect of extraction conditions on ultrasonic-assisted extraction of polyphenolic compounds from okra (Abelmoschus esculentus L.) leaves," *The Korean Society of Food Preservation,* pp. 476-486, 2020.
[11] R. S. Razmara, A. Daneshfar and R. Sahraei, "Solubility of Quercetin in Water + Methanol and Water + Ethanol from (292.8 to 333.8) K," *Journal of Chemical & Engineering Data,* pp. 3934-3936, 2010.
[12] Y. Desmiaty, J. Ratnawati and P. Andini, "Penentuan jumlah flavonoid total ekstrak etanol daun buah merah (pandanus conoideus lamk.) secara kolorimetri komplementer," *Jurusan Farmasi Universitas Jend. Achmad Yani,* pp. 1-8, 2009.
[13] O. R. Alara and N. H. Abdurahman, "Kinetics studies on effects of extraction techniques on bioactive compounds from Vernonia cinerea leaf," *Journal Food Science Technology,* pp. 580-588, 2019.
[14] S. Ivanovic, N. Avramovic, B. Dojcinovic, S. Trifunovic, M. Novakovic, V. Teševic and B. Mandic, "Chemical Composition, Total Phenols and Flavonoids Contents and Antioxidant Activity as Nutritive Potential of Roasted Hazelnut Skins (Corylus avellana L.)," *Foods,* pp. 1-14, 2020.
[15] M. Sharma and A. Sharma 2023, "A review on Nature Based Sunscreen Agent". *IOP Conf. Ser.: Earth Environ. Sci*.,1110, 012047, 2023
[16] A. R. Nunes, Í. G. P. Vieira, D. B. Queiroz, A. L. A. B. Leal, S. M. Morais, D. F. Muniz, J. T. Calixto-Junior and H. D. M. Coutinho, "Use of Flavonoids and Cinnamates, the Main Photoprotectors with Natural Origin," *Hindawi,* pp. 1-9, 2018.
[17] J. S. Waghmare and A. H. Kurhade, "GC-MS analysis of bioactive components from banana peel (Musa sapientumpeel)," *European Journal of Experimental Biology,* pp. 10-15, 2014.
[18] J. W. Zhang, J. H. Wang, G. H. Wang, C. C. Wang and R. Q. Huang, "Extraction and characterization of phenolic compounds and dietary fibres from banana peel," *Acta Alimentaria,* pp. 525-537, 2019.
[19] N.-S. M. Yazid, M. F. Zulkifli, W. I. W. Ismail and R. Siva, "Chlorogenic acid from banana and papaya peels inhibit lipid accumulation in 3T3-L1 cells," *Malaysian Journal of Fundamental and Applied Sciences,* pp. 561-565, 2019.
[20] B. O. Oyeyinka and A. J. Afolayan, "Potentials of Musa Species Fruits against Oxidative Stress-Induced and Diet-Linked Chronic Diseases: In Vitro and In Vivo Implications of Micronutritional Factors and Dietary Secondary Metabolite Compounds," *Molecules,* pp. 1-30, 2020.
[21] S. J. Gustia, I. Septiawan and Iriany, "Ekstraksi flavonoid dari bayam merah (alternanthera amoena voss)," *jurnal integrasi proses,* pp. 162-167, 2017.

Biographies of Authors

Hasna Nabila Putri. Hasna graduated her bachelor's degree from Chemical Engineering Department, Universitas Pertamina, Indonesia.

Eduardus Budi Nursanto. Eduardus graduated his doctoral degree education majoring in clean energy and chemical engineering from Korea University of Science and Technology, South Korea. Currently, he is active faculty member at Chemical Engineering Department, Universitas Pertamina, Indonesia.

Dita Floresyona: Dita graduated her doctoral degree majoring in chemistry from Université Paris sud-Université Paris saclay, France. Currently, she is active faculty member at Chemical Engineering Department, Universitas Pertamina, Indonesia

Muhammad Ayoub: Ayoub is associate professor at Chemical Engineering Department, Universiti Teknologi Petronas, Malaysia.

Mohd Hizami Mohd Yusouf. Yusouf is faculty member at Chemical Engineering Department, Universiti Teknologi Petronas, Malaysia.

ISSN 2963-8577
ISSN 2964-3511

Faculty of
Industrial Technology
Universitas Pertamina
Jl. Teuku Nyak Arief, RT.7/RW.8, Simprug, Kec. Kby. Lama, Kota Jakarta Selatan, Daerah Khusus Ibukota Jakarta 12220